



UNIVERSITÀ DEGLI STUDI DELLA BASILICATA
SAFE - Scuola di Scienze Agrarie, Forestali, Alimentari ed Ambientali

Università degli Studi della Basilicata

Dottorato di Ricerca in
Scienze Agrarie, Forestali e degli Alimenti

TITOLO DELLA TESI

“Vulnerability of Mediterranean forests to climate change, innovative methodologies for remote and in field monitoring of their health status and resilience to extreme events”

Settore Scientifico-Disciplinare
“AGR-05”

Coordinatore del Dottorato
Prof.ssa Teresa ZOTTA

Dottorando
Dott. Santain Settimio Pino ITALIANO

Relatore
Prof. Francesco RIPULLONE

Ciclo: XXXVI



UNIVERSITÀ DEGLI STUDI DELLA BASILICATA
SAFE - Scuola di Scienze Agrarie, Forestali, Alimentari ed Ambientali

Università degli Studi della Basilicata

PhD in
Agricultural, Forest and Food Sciences

TITLE

“Vulnerability of Mediterranean forests to climate change, innovative methodologies for remote and in field monitoring of their health status and resilience to extreme events”

Scientific Area (SSD)
“AGR-05”

Coordinator
Prof.ssa Teresa ZOTTA

PhD Student
Dott. Santain Settimio Pino ITALIANO

Tutor
Prof. Francesco RIPULLONE

Cycle XXXVI

Index

Riassunto.....	7
Abstract.....	13
1. Introduction.....	18
1.1 <i>The climate is changing</i>	18
1.2 <i>Drivers of forest dieback and mortality</i>	20
1.3 <i>Forest dieback around the world and the Mediterranean basin</i>	24
1.4 <i>Monitoring forest health</i>	26
1.5 <i>Resistance, recovery and resilience of forests</i>	28
1.6 <i>Future scenarios and possible actions</i>	30
1.7 <i>Purposes and aims</i>	32
1.8 <i>References</i>	32
2. <i>ASSESSING FOREST VULNERABILITY TO CLIMATE CHANGE COMBINING REMOTE SENSING AND TREE-RING DATA: ISSUES, NEEDS AND AVENUES</i>	42
2.1 <i>Abstract</i>	42
2.2 <i>Introduction</i>	43
2.3 <i>Resilience Indexes to Assess the Vulnerability of Forests</i>	48
2.4 <i>Methods for Monitoring and Studying Forest Vulnerability</i>	49
2.4.1 <i>Tree Crown Evaluations</i>	49
2.4.2 <i>Dendroecology</i>	50
2.4.3 <i>Remote Sensing</i>	51
2.5 <i>Decoupling of NDVI–Growth Relationship</i>	52

2.6	<i>Low Spatial Resolution and Remote Sensing Signal Anomalies</i>	54
2.7	<i>Conclusions</i>	56
2.8	<i>References</i>	57
3.	DROUGHT LEGACIES IN MIXED MEDITERRANEAN FORESTS: EFFECTS OF OVERSHOOT DROUGHTS, SPECIES CHARACTERISTICS AND SITE CONDITIONS	68
3.1	<i>Abstract</i>	68
3.2	<i>Introduction</i>	69
3.3	<i>Materials and methods</i>	72
3.3.1	<i>Study sites</i>	72
3.3.2	<i>Climate data, soil moisture and drought index</i>	74
3.3.3	<i>Tree-ring width data and field sampling</i>	75
3.3.4	<i>Characterizing impacts of the drought using remote sensing data</i>	77
3.3.5	<i>Correlations between growth, climate variables, soil moisture and drought</i>	77
3.3.6	<i>Resilience indices</i>	78
3.3.7	<i>Statistical analyses</i>	79
3.4	<i>Results</i>	80
3.4.1	<i>Climate trends and drought severity</i>	80
3.4.2	<i>Growth patterns</i>	80
3.4.3	<i>Growth responses to climate</i>	82
3.4.4	<i>Growth responses to drought and soil moisture</i>	83
3.4.5	<i>Growth resilience indices</i>	85
3.4.6	<i>Modeling post-drought recovery and legacies</i>	86

3.5	<i>Discussion</i>	88
3.6	<i>Conclusions</i>	92
3.7	<i>Tables</i>	94
3.8	<i>Supporting Information</i>	99
3.9	<i>References</i>	118
4.	RADIAL GROWTH, WOOD ANATOMICAL TRAITS AND REMOTE SENSING INDEXES REFLECT DIFFERENT IMPACTS OF DROUGHT ON MEDITERRANEAN FORESTS	127
4.1	<i>Abstract</i>	127
4.2	<i>Introduction</i>	128
4.3	<i>Material and methods</i>	130
4.3.1	<i>Study area</i>	130
4.3.2	<i>Climate data and drought index</i>	132
4.3.3	<i>Field sampling</i>	133
4.3.4	<i>Tree-ring width data</i>	133
4.3.5	<i>Quantitative earlywood anatomy</i>	134
4.3.6	<i>Remote sensing data</i>	135
4.3.7	<i>Statistical analyses</i>	135
4.4	<i>Results</i>	136
4.4.1	<i>The 2017 drought and stand structure</i>	136
4.4.2	<i>Growth and EW anatomy responses to the 2017 drought</i>	136
4.4.3	<i>Relationships between growth, wood anatomy and remote-sensing indices</i>	140

4.4.4 Relationships between climate, growth, earlywood anatomy and remote-sensing indices.....	141
4.5 Discussion.....	141
4.5.1 Management implications.....	144
4.6 Conclusions.....	144
4.7 Tables.....	146
4.8 Supporting Information.....	151
4.9 References.....	160
5. Conclusion.....	168
6. Funding and Acnowledgments.....	171
6.1 Funding.....	171
6.2 Acnowledgments.....	172

Riassunto

Gli studi condotti negli ultimi decenni hanno dimostrato che le alterazioni climatiche, come siccità e ondate di calore, sempre più frequenti, stanno causando fenomeni di stress e deperimento forestale, influenzando cambiamenti della composizione, struttura e distribuzione biogeografica delle foreste. I fenomeni di deperimento sono stati osservati in tutto il mondo ed in particolar modo stanno interessando il bacino del Mediterraneo considerato un hotspot dei cambiamenti climatici. Dunque, questi fenomeni possono rendere le nostre foreste vulnerabili, ovvero incapaci di tollerare i fattori di stress nel tempo e nello spazio. Tutto ciò si manifesta con la riduzione/assenza di risposta delle foreste a tali eventi climatici estremi, con perdita di resilienza o della capacità di recupero fino a provocare fenomeni di deperimento e morte delle piante. Dunque, è necessario capire come le foreste rispondono agli eventi climatici estremi e in che modo è possibile analizzare tali fenomeni.

Il presente lavoro mira ad esporre l'attività di ricerca svolta sulla vulnerabilità delle foreste agli attuali eventi meteorici nell'ambito dei cambiamenti climatici, con lo scopo di migliorare le conoscenze sulla tematica e comprendere le dinamiche forestali che potrebbero guidare verso scenari futuri. È stato eseguito un attento lavoro di "review" che ha permesso non solo analizzare l'attuale stato dell'arte sulla vulnerabilità delle foreste ma anche individuare eventuali incertezze e criticità. Infatti, la valutazione della vulnerabilità delle foreste è molto complessa, a causa dei molteplici fattori che influenzano la risposta delle foreste ai cambiamenti climatici e dei diversi metodi impiegati per analizzare lo stato di salute delle stesse. Dunque, attraverso la sopracitata "review" abbiamo argomentato ed evidenziato i principali metodi di studio, le problematiche, le esigenze e le possibili soluzioni che potrebbero essere adottate per superare alcune criticità che la ricerca sta affrontando.

Le attività di ricerca hanno interessato lo studio di sei siti forestali localizzati nella regione Basilicata (Sud-Italia). I popolamenti analizzati sono stati interessati dalla severa siccità del 2017 manifestando sintomi di deperimento (ingiallimenti fogliari,

rarefazione delle chiome e morte); dunque risultano essere adeguati per investigare e valutare la risposta delle foreste a eventi climatici estremi, come siccità e ondate di calore. In queste aree abbiamo tentato di comprendere se precedenti condizioni climatiche favorevoli potrebbero aver stimolato la crescita rendendo le foreste più vulnerabili a successivi stress da siccità. Ovvero abbiamo indagato su eventuali fenomeni di overshoot strutturale che potrebbero contribuire al deperimento delle foreste. Questo fenomeno ha attratto la nostra attenzione perché gli studi e le dinamiche che guidano i fenomeni di overshoot strutturale sono ancora poco note. I sei siti forestali analizzati ricadono nei comuni di: Savoia di Lucania “sito di Orto Siderio” (di seguito OS) e “sito Grotta dell’Angelo” (di seguito GA), Accettura “sito di Accettura Palazzo” (di seguito AP), Vietri di Potenza (di seguito VP), Castelmezzano (di seguito CM) e Pietrapertosa (di seguito PI). Sono tutti boschi misti in cui vegetano diverse specie mediterranee come, *Quercus pubescens Willd.*, *Fraxinus ornus L.*, *Acer monspessulanum L.* e *Pinus pinaster Aiton.*

Per ciascun sito è stata individuata un’area rappresentativa dell’intero popolamento (5000 m²) in cui sono stati eseguiti rilievi strutturali (diametro a petto d’uomo 1,30 m, altezza delle piante) e qualitativi (% di defogliazione delle chiome). In ogni sito sono stati selezionati a caso 15 individui maturi per ciascuna delle due specie arboree più abbondanti e sono state estratte da ciascun albero dei campioni legnosi utili per lo studio dendrocronologico. Dunque, il campionamento complessivamente ha interessato 180 alberi e sono stati misurati 8531 anelli annuali di crescita.

Oltre alla descrizione di ciascun sito (esposizione, suolo, quota ecc) e la valutazione qualitativa della trasparenza delle chiome (percentuale di defogliazione) abbiamo utilizzato anche dati telerilevati, in particolare l’indice NDVI (collezioni Sentinel-2, risoluzione spaziale 10 mX10 m) per caratterizzare ulteriormente lo stato delle chiome in seguito all’impatto del 2017. Inoltre, considerando gli incrementi di crescita degli alberi “Basal Area Increment” (BAI) prima, durante e dopo un disturbo è stato possibile comprendere se e come i popolamenti stanno rispondendo a tali eventi, calcolando per ciascuna specie in ciascun sito, gli indici di resilienza (resistenza, recupero, resilienza, resilienza relativa e impatto). Per avere una

panoramica più ampia degli eventi siccitosi avvenuti nell'area di studio sono stati calcolati gli indici di resilienza considerando anche precedenti annate siccitose (2003 e 2012). Inoltre, sono stati evidenziati gli effetti legacy della siccità sottraendo l'incremento dell'area basale (BAI) osservato da quello previsto.

Il calcolo degli indici di resilienza ha consentito di osservare che la resilienza e la resilienza relativa dopo il 2017 erano inferiori rispetto a quelle degli eventi siccitosi del 2003 e del 2012, mentre l'impatto tendeva ad aumentare. Il *F. ornus* ha presentato un elevato recupero dopo la siccità del 2017 nella maggior parte dei siti, mentre la quercia mostra maggiore resistenza all'evento siccitoso. L'*A. monspessulanum* ha risposto alla siccità in maniera simile alla *Q. pubescens*. Complessivamente tutte le latifoglie studiate hanno mostrato una risposta migliore al disturbo rispetto al *P. pinaster* (originato da impianto artificiale).

Per la maggior parte dei siti e delle specie la riduzione della crescita, dovuta alla siccità, è stata seguita da una rapida ripresa e da effetti legacy positivi, in particolare nel caso di *F. ornus*. Abbiamo riscontrato eredità negative di siccità della durata di due anni soprattutto per il sito di VP (*Q. pubescens* e *A. monspessulanum*) e GA (solo in *P. pinaster*). Un leggero effetto legacy negativo si osserva anche per il sito di OS (solo *Q. pubescens*) probabilmente causato da danni strutturali e da una diffusa mortalità che hanno influito sulla ripresa della quercia in quest'area. Viceversa, si osserva un leggero lascito positivo da siccità su *F. ornus* nel sito OS probabilmente dovuto al rilascio post-siccità della competizione (diffusa mortalità delle querce). Nei siti di GA e VP, dove si osserva maggiormente un effetto legacy negativo, gli elevati tassi di crescita dei popolamenti forestali prima della siccità (cioè, lo structural overshoot) in risposta alle precedenti condizioni umide dell'inverno-primavera possono aver predisposto gli alberi ai danni da siccità e al conseguente effetto legacy negativo.

Nel complesso, la risposta dei popolamenti forestali alla siccità del 2017 è dipesa certamente dalle condizioni del sito e dalle caratteristiche delle specie studiate. Infatti non solo gli indici di resilienza, ma anche i valori NDVI hanno mostrato

risposte sito specifiche. Inoltre gli effetti legacy osservati hanno consentito di trovare prove della nostra ipotesi di overshoot strutturale in alcuni siti sperimentali, evidenziando che le condizioni pre-siccità possono influenzare ed esacerbare i danni da siccità nei popolamenti sovradimensionati (ovvero caratterizzati da una notevole crescita della vegetazione pre-siccità probabilmente oltre la normale capacità di carico dell'ecosistema sito-specifico).

Per ottenere maggiori informazioni sulle dinamiche forestali, in risposta ai cambiamenti climatici, abbiamo ritenuto opportuno approfondire lo studio, impiegando l'anatomia del legno e il telerilevamento, ma focalizzando l'analisi su quattro siti (AP, OS, CM, PI) in cui coesistono le stesse specie, quercia e frassino, ovvero le specie più diffuse nei boschi misti mediterranei di latifoglie termofile. In tal modo, abbiamo potuto ottenere elementi di anatomia quantitativa, utili per analizzare nel dettaglio i tratti xilematici, e informazioni telerilevate attraverso l'utilizzo di indici vegetazionali (NDVI, EVI, NDWI) a risoluzione moderata (collezioni Landsat, risoluzione spaziale 30m X 30m). Tutto ciò con lo scopo di osservare in che modo e se gli incrementi radiali e l'anatomia del legno correlano con le informazioni telerilevate. Per eseguire le analisi anatomiche dell'earlywood (di seguito EW) abbiamo selezionato 6 campioni legnosi, con più alta intercorrelazione, per ciascuna delle due specie analizzate per ogni sito (quercia e frassino). Per ciascuno di questi è stata eseguita un'analisi dei tratti anatomici del legno dal periodo 2001 al 2021. Gli studi dendro-anatomici sono molto laboriosi e richiedono molto tempo ma riescono a restituire informazioni dettagliate infatti le variabili anatomiche (dimensione del lume dei vasi, numero dei vasi xilematici ecc) sono considerati importanti proxy per studiare la risposta delle foreste ai cambiamenti ambientali. L'analisi anatomica ha interessato 48 campioni legnosi, 1008 anelli di crescita e con un totale di 17028 vasi xilematici misurati. Abbiamo quantificato tratti anatomici come: area dell'anello, aree dell'EW e del legno tardivo (LW), area (%) occupate dai vasi nell'EW, area del lume dei vasi e densità dei vasi. Queste misure hanno consentito di calcolare, il diametro idraulico (Dh) e conducibilità idraulica potenziale (Kh). I dati telerilevati sono stati ottenuti per il periodo 2001-2021, utilizzando le collezioni Landsat (L5, L7, L8 e L9). Gli indici vegetazionali stimati sono: NDVI, EVI, utilizzati per caratterizzare la copertura

della chioma e attività fotosintetica, e l'NDWI utilizzato per esaminare il contenuto idrico della chioma. Il risultato è stato il calcolo di 960 valori (mensili) per ciascun indice con un totale di 2880 valori analizzati. Inoltre, utilizzando le bande dell'infrarosso termico (TIRS 1 e TIRS 2) delle collezioni Landsat abbiamo valutato l'emissività termica del suolo per validare ulteriormente l'impatto della siccità del 2017.

In generale, l'accrescimento è diminuito durante l'anno di siccità (2017), in particolare per *Q. pubescens*, che ha mostrato notevole defogliazione. Entrambe le specie (quercia e frassino) hanno mostrato un calo di Dh nel 2018 dopo la siccità. Relazioni positive sono state osservate tra area degli anelli di crescita, Dh e dati di telerilevamento (NDVI, EVI, NDWI) per *Q. pubescens*, risultando una specie molto reattiva. In siti molto colpiti, come OS, è stata osservata covariazione tra Dh e crescita (ovvero tendenze positive significative), tali relazioni possono essere ulteriori conferme di condizioni di forte stress. Complessivamente i risultati hanno mostrato una un'elevata variabilità della risposta alla siccità tra le specie e i siti analizzati, ma il frassino sembra mostrare un minore declino della crescita rispetto alla quercia.

Pertanto, analizzando le variabili anatomiche, sembrerebbe che il *F. ornus* mostri una migliore risposta a fenomeni di stress idrico e minore mortalità rispetto a *Q. pubescens*. Ciò consente anche di confermare i risultati restituiti dagli indici di resilienza, ovvero in generale un migliore recupero post-siccità del frassino rispetto alla quercia.

Dunque, la dendrocronologia e lo studio degli indici di resilienza sembrerebbero indicare anomalie che sono state ulteriormente confermate grazie all'utilizzo dell'anatomia del legno e del telerilevamento. Questo tipo di approccio è importante, dal momento che esistono pochissimi studi che impiegano un'analisi multiscala di questo tipo. Inoltre questo studio contribuisce a documentare le conseguenze ecologiche della siccità, ovvero probabili modifiche della composizione delle foreste mediterranee in risposta ai cambiamenti climatici, con la formazione di comunità dominate da specie meglio adattate a eventi siccitosi. Le

informazioni ottenute potrebbero, oltre che implementare l'attuale stato dell'arte sulla vulnerabilità delle foreste mediterranee e sui fenomeni di overshoot strutturale, aiutare a chiarire le relazioni tra dendrocronologia, anatomia del legno e telerilevamento, evidenziando l'opportunità di lavorare a diverse scale multi-temporali utilizzando tecniche diverse.

Inoltre, il nostro lavoro fornisce informazioni su specie mediterranee diffuse ma poco studiate come *A. monspessulanum* e *il F. ornus*; in particolare quest'ultima specie sembrerebbe avere ottime possibilità di occupare siti forestali notevolmente impattati dalla siccità. Per avere informazioni più dettagliate e comprendere quale potrebbe essere l'evoluzione delle foreste mediterranee e quindi quali potrebbero essere gli scenari futuri, saranno necessarie analisi multi-proxy e studi di lungo termine atti a monitorare lo stato delle foreste e le dinamiche di competizione tra le diverse specie mediterranee.

Abstract

Studies conducted over the past decades have shown that climate alterations, such as droughts and heat waves, are increasingly causing forest stress and dieback, affecting changes in the composition, structure and biogeographic distribution of forests. Dieback phenomena have been observed worldwide and are particularly affecting the Mediterranean basin, which is considered a climate change hotspot. Therefore, these phenomena can make our forests vulnerable, i.e. unable to tolerate stressors in time and space. This manifests itself in the reduction/absence of forest response to such climatic events, such as loss of resilience or the ability to recover, even to the dieback and death of entire forests. Thus, it is necessary to understand how forests respond to extreme climatic events and how such phenomena can be analysed.

This report intends to present the research work carried out to investigate the vulnerability of forests to climate change, with the aim of improving current knowledge on the subject and understanding forest dynamics that could lead to future scenarios. Careful “review” work was carried out, which not only made it possible to analyse the current state of the art on forest vulnerability, but also to identify any uncertainties and critical issues. The assessment of forest vulnerability is very complex due to the many factors influencing the response of forests to climate change and the different methods used to analyse forest health. Through the review, we have highlighted the problems, needs and possible solutions that could be adopted to overcome some of the critical issues that research is facing.

Specifically, the research activities involved the study of six forest sites located in Basilicata region (Southern Italy). The stands analysed were affected by the severe drought of 2017, showing symptoms of dieback (leaf yellowing, crown thinning and death), and thus appear to be suitable for investigating and assessing the response of forests to extreme climatic events, such as droughts and heat waves. In these areas, we attempted to understand whether previous favourable climatic conditions might have stimulated growth by making forests more vulnerable to subsequent drought stress. That is, we investigated possible structural overshoot

phenomena that could contribute to forest dieback. This phenomenon attracted our attention because the studies and dynamics driving structural overshoot phenomena are still poorly understood. The six forest sites analysed fall within the municipalities of: Savoia di Lucania 'Orto Siderio site' (hereafter OS) and 'Grotta dell'Angelo site' (hereafter GA), Accettura 'Accettura Palazzo site' (hereafter AP), Vietri di Potenza (hereafter VP), Castelmezzano (hereafter CM) and Pietrapertosa (hereafter PI). These are mixed woods in which various Mediterranean species vegetate, such as *Quercus pubescens* Willd., *Fraxinus ornus* L., *Acer monspessulanum* L. and *Pinus pinaster* Aiton.

For each site, an area representative of the entire stand (5000 m²) was identified, in which structural (diameter at breast height 1.30 m, plant height) and qualitative (to assess the state of defoliation of the crowns) surveys were carried out. At each site, 15 mature individuals of each of the two most abundant tree species were randomly selected and wood samples useful for the dendrochronological study were extracted from each tree. A total of 180 trees were sampled and 8531 annual growth rings were measured.

In addition to the description of each site (exposure, soil, elevation, etc.) and the qualitative assessment of canopy transparency (percentage of defoliation), we also used remotely sensed data in particular the NDVI index (Sentinel-2 collections, spatial resolution 10 mX10 m) to further characterise the status of the canopies following the 2017 impact. Furthermore, by considering the Basal Area Increment (BAI) of trees before, during and after droughts, it was possible to understand whether and how stands respond to such events, by calculating the resilience indices (resistance, recovery, resilience, relative resilience and impact) for each species at each site. In order to have a broader overview of the drought events that occurred in the study area, resilience indices were also calculated considering previous drought years 2003 and 2012. In addition, the legacy effects of drought were highlighted by subtracting the observed increase in basal area (BAI) from that expected.

The calculation of resilience indices showed that resilience and relative resilience after 2017 tended to be lower than during the droughts of 2003 and 2012, while impact tended to increase. *F. ornus* showed a high recovery after the 2017 drought at most sites, while oak shows greater resistance to the drought event. *A. monspessulanum* responded to drought similarly to *Q. pubescens*. Overall, all broadleaves studied showed a better response to the disturbance than *P. pinaster* (originated by artificial planting).

For most sites and species, the reduction in growth due to drought was followed by a rapid recovery and positive legacy effects, particularly in the case of *F. ornus*. We found negative two-year drought legacies mainly in VP site (*Q. pubescens* and *A. monspessulanum*) and GA site (only in *P. pinaster*). A slight negative legacy effect is also observed in OS site (*Q. pubescens* only) probably caused by structural damage and widespread mortality affecting oak recovery in this area. Conversely, a slight positive drought legacy is observed on *F. ornus* at the OS site probably due to post-drought release in the competition (widespread oak mortality). At GA and VP sites, where a negative legacy effect is most observed, the high growth rates of forest stands prior to drought (i.e. structural overshoot) in response to previous wet winter-spring conditions may have predisposed trees to drought damage and the resulting negative legacy effect.

Overall, the response of forest stands to the 2017 drought certainly depended on site conditions and the characteristics of the species studied. Indeed, not only the resilience indices, but also the NDVI values showed site-specific responses. Furthermore, the observed legacy effects allowed us to find evidence for our structural overshoot hypothesis at some experimental sites, highlighting that pre-drought conditions can influence and exacerbate drought damage in overbuilt stands (i.e. characterised by significant pre-drought vegetation growth probably beyond the normal carrying capacity of the site-specific ecosystem).

In order to obtain more information on forest dynamics in response to climate change, we considered it appropriate to deepen the study, using wood anatomy and

remote sensing, but focusing the analysis on four sites (AP, OS, CM, PI) where the same species, oak and ash, coexist, i.e. the most widespread species in Mediterranean thermophilic mixed deciduous forests. In this way, we were able to obtain quantitative anatomy elements, useful for analysing xylem traits in detail, and remote sensing information through the use of vegetation indices (NDVI, EVI, NDWI) with moderate resolution (Landsat collections, spatial resolution 30m X 30m). The aim was to observe how and whether radial increments and wood anatomy correlate with the remote sensing information. To perform the earlywood anatomical analyses (hereafter EW) we selected 6 wood samples, with the highest intercorrelation, for each of the two species analysed for each site (oak and ash). An analysis of the anatomical traits of the wood from 2001 to 2021 was performed for each of these. Dendro-anatomical studies are very laborious and time-consuming to develop, but they are able to return detailed information, in fact anatomical variables (lumen size, number of xylem vessels, etc.) are considered important proxies for studying the response of forests to environmental changes. The anatomical analysis involved 48 woody samples, 1008 growth rings and a total of 17028 xylem vessels measured. We quantified anatomical traits such as: ring area, areas of the EW and late wood (LW), area (%) occupied by vessels in the EW, vessel lumen area and vessel density. These measurements allowed the calculation of hydraulic diameter (Dh) and potential hydraulic conductivity (Kh). The remotely sensed data were obtained for the period 2001-2021, using the Landsat collections (L5, L7, L8 and L9). The vegetation indices estimated are NDVI and EVI used to characterise canopy cover and photosynthetic activity and NDWI used to examine canopy water content. The result was the calculation of 960 (monthly) values for each index with a total of 2880 values analysed. In addition, using the thermal infrared bands (TIRS 1 and TIRS 2) from the Landsat collections, we assessed the thermal emissivity of the soil to further validate the impact of the 2017 drought.

In general, growth decreased during the drought year (2017), especially for *Q. pubescens*, which showed considerable defoliation. Both species (oak and ash) showed a decrease in Dh in 2018 after the drought. Positive relationships were observed between the area of growth rings, Dh and remote sensing data (NDVI,

EVI, NDWI) for *Q. pubescens*, confirming it as a very reactive species. At highly affected sites, such as the OS site, a covariation between Dh and growth (i.e. significant positive trends) was observed, such relations may be further confirmation of highly stressed conditions. Overall, even in this case, the results showed a high variability in drought response between the species and sites analysed, but ash seems to show less growth decline than oak.

Therefore, analysing the anatomical variables, it would appear that *F. ornus* shows a better response to water stress phenomena and lower mortality than *Q. pubescens*. This also further confirms the results returned by the resilience indices, i.e. in general a better post-drought recovery of ash than oak.

Thus, the use of dendrochronology and the study of resilience indices seem to indicate anomalies that have been further confirmed through the use of wood anatomy and remote sensing. This type of approach is relevant, as there are very few studies that employ a multiscale analysis of this type. Furthermore, this study contributes to documenting the ecological consequences of drought, i.e. probable changes in the composition of Mediterranean forests in response to climate change with the formation of communities dominated by species better adapted to drought events.

The information obtained could, in addition to implementing the current state of the art on Mediterranean forest vulnerability and structural overshoot phenomena, help clarify the relationships between dendrochronology, wood anatomy and remote sensing, highlighting the opportunity to work at different multi-temporal scales using different techniques.

Furthermore, our work provides information on widespread but little-studied Mediterranean species such as *A. monspessulanum* and *F. ornus*, and in particular the latter would seem to have a good chance of occupying forest sites significantly impacted by drought. In order to have more detailed information and to understand what the evolution of Mediterranean forests might be and thus what the future scenarios might be, multi-proxy analyses and long-term studies will be needed to

monitor the state of forests and the dynamics of competition between different Mediterranean species.

1. Introduction

The topic addressed by this thesis represents one of the most important challenges researchers have been facing in recent years, as extreme weather events are increasing in duration and intensity (IPCC 2018, 2019). These dynamics could compromise irreplaceable forest functions such as oxygen production, CO₂ absorption, and biodiversity conservation, and in the future could cause not only environmental but also social and economic repercussions, considering that the forest covers about 30% of the Earth's surface and contains about 45% of the Earth's carbon (Schimel 1995, WBGU 1998, Marchetti 2023). Critical changes in climatic conditions in the past have been preceded by a characteristic slowdown in climate fluctuations that begins well before the actual change (Dakos et al. 2012). In our case, anthropogenically induced alterations are very rapid, and our ability to accurately model these systems is still too limited to predict if and when future climate change might bring us to a critical threshold (Dakos et al. 2008). Therefore, the contribution of research in understanding forest dynamics in response to climate change is crucial.

1.1 The climate is changing

In recent decades, climate change and extreme events have become increasingly frequent. The release of greenhouse gases into the atmosphere by anthropogenic activities has caused a global temperature increase of 1°C compared to pre-industrial levels, with an estimated increase of 0.2 C° per decade (IPCC 2018).

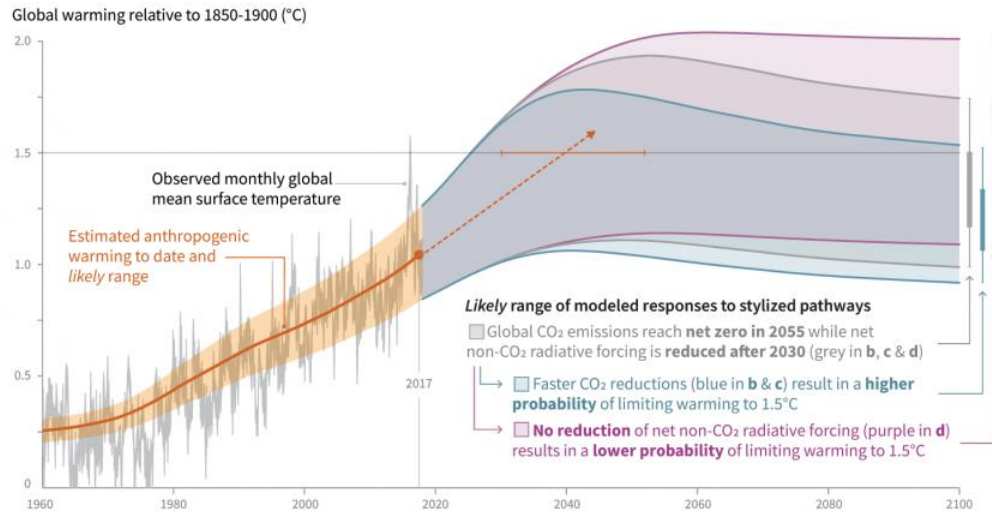


Figure 1. Global temperature increase reported by the IPCC 2018 report and future values obtained from models based on anthropogenic emission trends

Climate alterations result not only in heat waves, but also in a high variability of precipitation with prolonged periods of drought (IPCC 2019, IPCC 2022). In the Mediterranean basin these phenomena are much more intense, in fact the increase in average temperatures is 0.4°C higher than the global average (Cramer et al. 2018) with a significant reduction in precipitation. Frequent dry spells and heat waves can cause large-scale alterations of entire forest ecosystems, causing physiological stress phenomena that makes vegetation susceptible to other processes such as insect attacks, diseases and pathogens. (Thomas et al. 2002, McDowell et al. 2008).

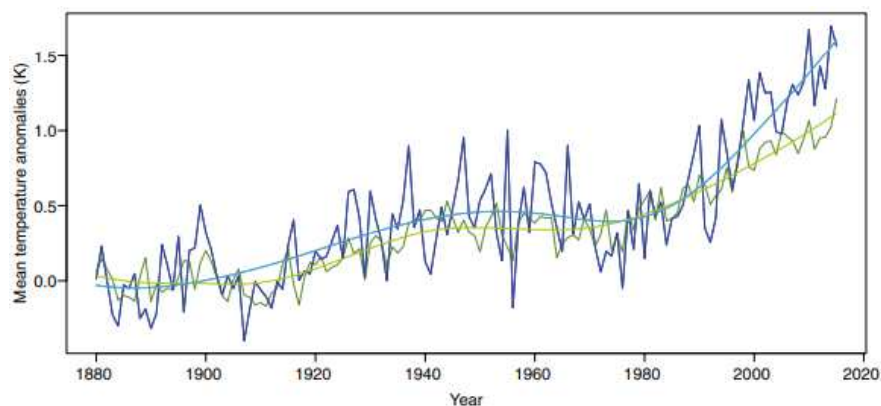


Figure 2. Chronology of rising temperatures globally (in green) and in the Mediterranean basin (in blue), (by Cramer et al, 2018).

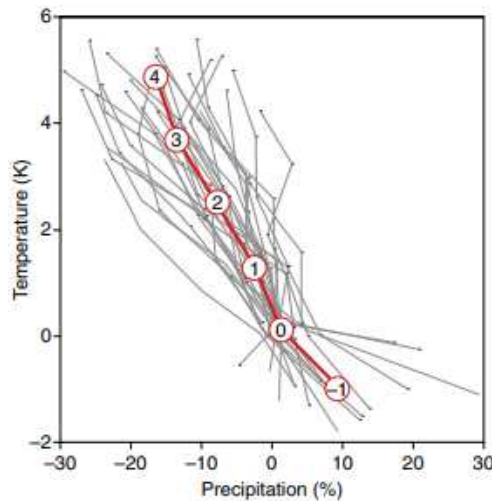


Figure 3. Evolution of the Mediterranean climate towards a trend towards warmer and lower precipitation (by Cramer et al, 2018).

Extreme climate events make forests vulnerable, exposing them to dieback and mortality. Vulnerability can be defined as the degree of susceptibility of the system, i.e. the inability to cope with the negative effects of climate change (IPCC 2007). In this context, forest vulnerability can be defined as the reduction/absence of response to such events in terms of resistance, recovery and resilience resulting in the dieback and death of entire forests.

1.2 Drivers of forest dieback and mortality

The dynamics responsible for forest mortality induced by extreme weather events are complex and multifaceted; several studies have identified hydraulic failure and carbon starvation, followed by attacks by biotic agents, as the main mechanisms of mortality (Thomas et al. 2002, McDowell et al. 2008, 2011, Adams et al., 2017). Failure of the hydraulic system results from an imbalance between plant transpiration and water uptake, which in hot and dry conditions, causes increasingly negative xylem pressure with the formation of gas bubbles in the xylem ducts that interrupt the flow of water in the xylem system, and consequent stress to the tree (Borghetti et al. 2020). Studies based on this concept have observed that there is a global convergence in the vulnerability of forests to drought; highlighting that different forest biomes are equally vulnerable to hydraulic system failure, i.e.

drought-induced forest dieback is occurring not only in arid regions, but also in wet forests not considered drought-prone (Choat et al. 2012). Extensive assessments have been carried out to understand the drought-induced hydrological vulnerability of forests, trying to define what the hydraulic safety margin is before hydraulic system collapse occurs (Klein et al. 2013, Hammond et al. 2019). Nevertheless, the existence of additional factors makes this relationship very complex, in fact each species may have different drought response strategies, so hydraulic safety margins will be different and must be evaluated for each forest system (Hammond et al. 2019). However, in general, greater resistance to embolism has been observed in gymnosperms than in angiosperms (Choat et al. 2012). Conversely, angiosperms may have a greater ability to reverse the embolism by dissolving gases and filling xylem ducts. This process can occur in several ways, by dissolution of the bubbles once the xylem pressure approaches atmospheric pressure, by positive root/stem pressure, or by repairing the damage through the production of new xylem (Klein et al. 2018). However, the reversal of embolism is still a poorly understood process, but it would appear that sugars and ions released in the ducts cause osmotic gradients by channelling the flow of water through the parenchyma, phloem and xylem (Klein et al. 2018). Repeated drought events could cause chronic stress and thus result in the inability to refill the embolised vessels (Klein et al. 2018). Carbon starvation mortality is a phenomenon that occurs because the plant, in order to limit water loss through transpiration, closes its stomatal openings during water stress, resulting in a poor supply of CO₂ (McDowell et al. 2008). The main consequence of carbon starvation is the reduction of carbohydrate synthesis; the plant begins to utilise carbohydrates stored in the root structures that cannot be restored if water stress conditions persist. Glucose and other non-structural carbon compounds (NSC) play many roles in plant functioning, not only as sources of energy, but can interact in water balance, root growth or repair of xylem emboli. In addition, drought negatively affects phloem transport with a reduction in cell turgor, preventing the translocation of useful carbon to the plant (Sevanto et al. 2014). The minimum NSC thresholds required for survival are currently unknown and precise methodologies for determining absolute carbohydrate concentrations have not yet emerged (Hartmann 2015). The two mechanisms are therefore connected: xylem

embolism reduces hydraulic conductivity and limits photosynthesis, further causing NSC dependence and further reducing the availability of carbohydrates for metabolism to the of carbon starvation (McDowell 2011). A reduction in tree health results not only in reduced photosynthetic activity, but also in a subsequent reduction in tree radial growth, characterised by the formation of smaller vessels in the earlywood and narrower growth rings (Levanič et al. 2011, Colangelo et al. 2017b).

Dieback phenomena are characterised by obvious symptoms represented by, crown thinning caused by abnormal abscission of twigs along the stem and significant desiccation of shoots and branches in the upper crown region. Other symptoms include clumped leaves, canopy yellowing, microphyllia, epicormal shoot development, necrosis of cambium tissues and reduced diametrical growth (Thomas et al. 2002, Gentilesca et al. 2017). These symptoms do not occur simultaneously and may affect part of the crown or the entire tree. Should environmental conditions improve, the vegetation, if not severely compromised, may recover the vigour of the canopy with a restoration of health; on the contrary, the succession of adverse environmental conditions, or further stress factors, may lead to a progressive reduction of the canopy until complete desiccation.

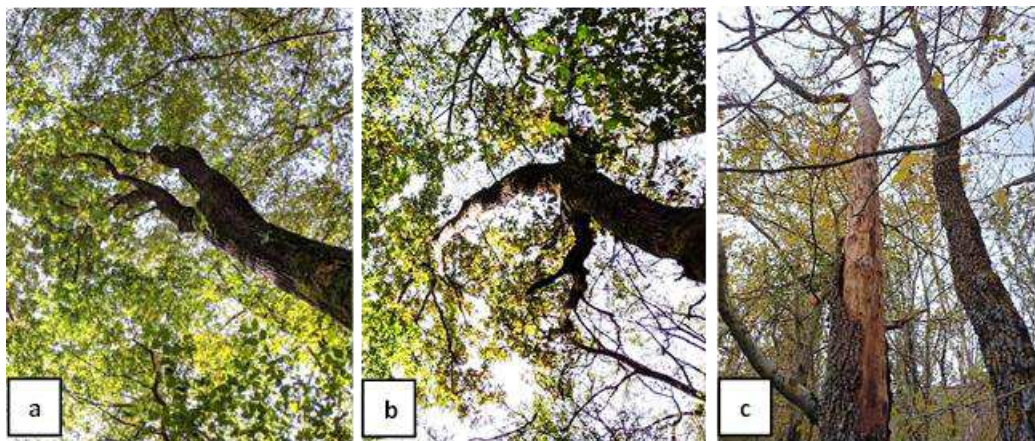


Figure.4. a) leaf yellowing and abscission of twigs along the stem, b) desiccation of branches and shoots in the upper part of the crown with considerable thinning of the crown, c) tissue necrosis and complete desiccation of the tree.

Forest dynamics in relation to climate change and the resulting dieback phenomena can occur in a site-specific manner and with wide variability. Vegetation responses to extreme climatic events may depend on multiple factors, e.g. characteristics of each site such as, latitude, altitude, slope (Rita et al. 2019), species abundance, in fact generally the greater the species mix the better the stand response to disturbance (Lloret et al. 2007), type and availability of nutrients (González de Andrés et al. 2022), variability between conifers and broadleaf trees (Choat et al. 2012, Gazol et al. 2018, DeSoto et al. 2020).

In mixed forests, in fact, the mixing of species allows the adoption of different water consumption strategies (anisohydric and isohydric) that can be implemented in a complementary way; or, in other cases, deep-rooted species could facilitate hydraulic water uplift favouring species with superficial roots (Pretzsch 2013). Tree size and stand structure can also influence the forest's response to climatic stresses. For example, according to recent studies (Xu et al. 2018), medium-height trees are less susceptible to cavitation than very tall trees, and have a more developed root system than shorter trees. These differences may have favoured a medium-height forest structure showing greater drought resistance (Xu et al. 2018). Competition also influences the response of forests (Castagneri et al. 2021), e.g. the reduction of competitors, could have positive effects for surviving individuals due to increased resource availability (Lloret et al. 2012). While an excessive density results in a tree canopy that is able to intercept rainfall considerably with subsequent evaporation of water before it reaches the soil and reduced soil water storage. A very high LAI also leads to increased transpiration, negatively affecting soil water availability (Castagneri et al. 2021). Genetic factors also affect the response of forests to climate change, e.g. investigations (Depardieu et al. 2020), conducted on silver fir in a common garden, with trees from different sites with different climatic conditions, made it possible to analyse the response of the vegetation according to their geographic areas. Trees from drier geographic areas under water stress conditions showed greater resilience than trees from wetter geographic areas. This highlights adaptive genetic variation in response to climatic conditions, reflecting local adaptation and consequently different resilience and recovery after periods of drought. Thus, forests respond, adapting to the surrounding environmental

conditions, but this happens very slowly over time, while extreme weather events have become increasingly frequent in recent decades. Therefore, the response of forests to climate change is influenced by several factors and is extremely complex, which is why the study of these phenomena is increasingly important.

1.3 Forest dieback around the world and the Mediterranean basin

Climate change and in particular drought, is causing dieback phenomena with a clear increase in mortality of forest systems globally (Allen et al. 2010), affecting several forest species on all continents. In addition to having a direct impact on forest health, environmental stress can amplify other agents of mortality, such as insects, diseases and cause changes in fire regimes. In the southwestern United States since the late 1990s, multiple tree species have been substantially affected by the drought that has killed millions of hectares of forest (Allen 2007). Radial tree growth, in recent decades, has shown unstable climatic responses and growth trends, including in China Siberian larch (*Larix sibirica*) and Schrenk spruce (*Picea schrenkiana*) forests, exhibiting clear evidence of radial growth decline, tree mortality and stand dieback induced by climate warming (Jiao et al. 2019). The 2018 drought and subsequent dry years also impacted Central Europe, affecting *Fagus sylvatica* forests in Switzerland (Neycken et al. 2022), while in Germany the 2015 drought affected *Pinus silvestris*, showing widespread mortality (Buras et al. 2018).

The area most affected by these phenomena is the Mediterranean basin, which will face warmer and drier conditions in the future due to the expected increase in temperature and decrease in precipitation (Lindner et al. 2010). In Greece, it has been estimated (Fyllas et al. 2017) for forests dominated by *Abies borisii - regis*, *Abies cephalonica*, *Fagus sylvatica*, *Pinus nigra* and *Quercus frainetto* in response to climate change a retreat of less drought-resistant species and an upward spread of more drought-resistant species (*Pinus nigra* and *Quercus frainetto*). Drought-resistant species also showed changes in xylem wood traits with an increase in their average growth and a decrease in average wood density (Fyllas et al. 2017). Another Mediterranean area affected by dieback and mortality phenomena is Tunisia where

the decline of *Quercus suber* has been observed since 1988 following extreme drought conditions (Touhami et al. 2020). Cedar forests in north-eastern Algeria are also disappearing due to drought, with massive tree mortality (areas with more than 95 % dead trees) (Kherchouche et al. 2012). Further studies have also identified dieback phenomena in Spain, showing a marked reduction in growth caused by different periods of water stress in several forest species *Abies alba*, *Fagus sylvatica*, *Pinus sylvestris*, *Pinus nigra* (Camarero et al. 2018). In particular, silver fir in the Spanish Pyrenees shows ongoing defoliation processes since 1980 and recent studies have shown higher levels of defoliation especially in low-elevation sites with lower growth rates limited by evaporative demand in late summer (Valeriano et al. 2023). In south-eastern France, phenomena of *Pinus sylvestris* dieback were reported with greater intensity in areas with drier topographic and climatic conditions that also favoured the spread of biotic agents, mistletoe and pine processionary (Lemaire et al. 2022). Dieback processes have also been reported in the forests of north-eastern Italy, within the Ticino Regional Park, with regard to the pedunculate oak (*Quercus robur*) (Colangelo et al. 2018). While other phenomena of this type have been observed in central Italy, after periods of drought several species (*Fagus sylvatica*, *Quercus pubescens*, *Quercus cerris*, *Quercus ilex* and *Phillyrea latifolia*) suffered severe crown defoliation, leaf desiccation and mortality (Pollastrini et al. 2019). Studies conducted in southern Italian forests, particularly in Mediterranean oak groves, have shown a reduction in the growth rate of dieback plants compared to healthy ones, starting in 2000 following very dry years characterised by less than 400 mm of annual precipitation (Gentilesca et al. 2014). Further studies on forests in southern Italy confirmed a decline in the viability of *Quercus frainetto*, with growth declining between 44% and 49% in response to very hot and dry spring conditions between 2002 and 2009 (Colangelo et al. 2017a). Further studies confirmed the impact of the 2017 drought in several mixed forests in southern Italy consisting of numerous species (*Quercus pubescens*, *Fraxinus ornus*, *Pinus pinaster*, *Acer monspessulanum*, *Abies alba*, *Carpinus orientalis*) characterised overall by crown browning and widespread defoliation (Coluzzi et al. 2020). Therefore, forests around the world, and in particular

Mediterranean forests, are severely tested and are increasingly vulnerable to the influence of climate change.

1.4 Monitoring forest health

The analysis and monitoring of mortality phenomena have been addressed by various authors using different methodologies, such as field surveys, dendrochronology, qualitative analysis of vegetation conditions and remote sensing techniques. For example, Mannerucci et al. (2006), in order to study and understand the severity of the vulnerability of Mediterranean forests, carried out a qualitative analysis using an empirical scale to assign a viability class on the basis of visible symptoms of dieback (0 = healthy tree; 1 = crown dieback up to 20%; 2 = crown dieback of 21 to 50%; 3 = crown dieback of 51 to 99%; 4 = 100% crown dieback and epicormic shoots from the stem; 5 = dead crown and stem; living stump with production of new shoots; 6 = dead plant). This study highlighted post-drought dieback phenomena in the areas studied, in southern Italy, with a canopy dieback of over 20%, but the method applied is qualitative and visual and therefore not fully suitable for assessing the health conditions of the trees. More detailed information and thus more accurate analyses, such as physiological, dendroecological and structural surveys, are required to quantitatively assess forest dieback phenomena. For example, dendroecological investigations allows to associate plant growth and anatomy with environmental conditions. Dendrochronological and dendroanatomical analyses permit to measure radial growth increments, ring area, vessel lumen, vessel density, hydraulic diameter and hydraulic conduction, etc., all important parameters for analysing vegetation health. Some authors (Colangelo et al. 2017a) applying this type of analysis observed lower ring growth and lower BAI (Basal Area Increment) values at very low SPEI values, i.e. during periods of drought. In agreement with other studies, trees under drought conditions show a reduction in vessel lumen and a consequent reduction in hydraulic diameter and hydraulic conductivity (Levanič et al. 2011). Furthermore, when comparing dendrochronological data, i.e. radial growth trends and growth responses to climate and drought, a significant growth divergence between dieback and non-dieback trees can be observed. Trees in dieback show lower radial growth rates than their

non-dieback counterparts and tend to show less growth variability (Camarero et al. 2021). These are unequivocal signs of the tree's state of physiological stress and irreversible growth decline can occur long before death, even 10 years earlier (Colangelo et al. 2017b). Low growth before mortality is consistent with carbon deficiency leading to mortality phenomena over time (Levanič et al. 2011).

Studies such as those mentioned (qualitative analysis, dendrochronology and wood anatomy) are applicable on single sites or small areas, while dieback phenomena occur on a large scale. To obtain information on a large scale, remote sensing can be very useful; in fact, with the development of remotely sensed vegetation indices, this discipline is contributing to the study of forest vulnerability. For example, Lloret et al. (2007) studied the health of forests in north-eastern Spain at different altitudes after a drought event by estimating the NDVI (Normalized Different Vegetation Index), an index sensitive to photosynthetic activity. The water deficit was identified by low values of the NDVI index estimated through VEGETATION SPOT satellite images with a spatial resolution of 1km x 1km. The results showed lower NDVI values after the summer of 2003, mainly in drier locations with less species abundance. Lloret et al. (2007) showed that the response of vegetation to water stress varies not only due to the physiological stress to which the forest species is subjected, but also according to the exposure of the site and the abundance of plant species present. Other studies have used remotely sensed indices, e.g. on Mediterranean holm oak (*Quercus Ilex*) forests (Ogaya et al., 2015), MODIS data with 250mX250m spatial resolution were used to obtain two vegetation indices NDVI and EVI (Enhanced Vegetation Index), an enhanced index to overcome saturation problems and with correction factors for atmospheric aerosol. The study conducted on the Mediterranean holm oak forests showed that mortality and increases in forest biomass are well correlated with climatic conditions and well represented by the vegetation indices used, confirming that NDVI and EVI are good indicators of forest dieback. In recent years, several studies have been investigating the use of high-resolution satellite data to carry out remote monitoring even on a small scale. An example is that of Coluzzi et al. (2020) who monitored the effects of extreme weather events on Mediterranean forests. Using Sentinel-2 images with a resolution of 10m X 10m and field-collected data on tree health conditions

(qualitative analysis), they observed a heterogeneous response of different sites, details that could not be captured with low-resolution images.

Therefore, dendrochronological analysis and remote sensing appear useful methods for monitoring and analysing the complex response of forests to climate change, but, as reported in the following chapters, they require further refinement to ensure appropriate information on complex forest dynamics.

1.5 Resistance, recovery and resilience of forests

The studies conducted so far point to the evolution towards an increasingly hotter and drier climate as the main hypothesis, suggesting an increase in forest stress and dieback phenomena; but how would forests really react to such climatic events? Some authors (e.g. Lloret et al. 2011) analysed, through the study of radial growth, the resilience components of forests located in the northern Rocky Mountains (USA). By measuring growth increments before, during and after disturbance, Resistance, Recovery, and Forest Resilience after Drought were estimated. Applying this investigation to trees of different ages, the authors observed greater resistance of younger trees compared to greater resilience of older trees (Lloret et al. 2011). This work proposed very interesting parameters for evaluating vegetation response, which have been widely used for further studies. For example, Andivia et al. (2018), analysed the growth, resilience and resistance of under-canopy saplings and saplings in open areas after extreme drought events in pine forests of the central Iberian Peninsula. The responses in terms of growth, resilience and resistance showed a better response to drought in adult under-canopy saplings, which were larger than those in open areas. Thus, using resilience indices Andivia et al. (2018) analysed the dynamics driving regeneration after extreme drought events. In Germany Pretzsch et al. (2013) applied resilience parameters for pure and mixed stands. In some cases, they showed a higher risk of morphological changes, cavitation and leaf loss, and slower recovery after drought stress for single-species stands, compared to higher resistance and resilience in mixed stands. Overall, this observation reflects the importance of forest biodiversity in the response to

disturbances (Bochenek et al. 2017, Lloret et al. 2007). Heterogeneous systems tend to have a better resilience as they gradually adapt to change (Scheffer et al. 2012).

The resilience response of forests has also been analysed using remote sensing indices to examine the stability of different terrestrial biomes. Huang et al. (2019), using the Enhanced vegetation index (EVI) derived from the MODIS satellite, estimated the resistance of forest biomes as the ability to keep EVI levels unchanged during drought, and resilience as the ability to restore pre-drought EVI levels. Overall, Huang et al. (2019) identified an increasing trend in the severity and duration of annual drought events over the period 2000-2014. In the areas analysed, the resistance and resilience, of biomes, to drought were largely influenced by temperature and solar radiation. Other studies (Khoury et al. 2020), carried out for large forest areas in Spain, used a time series of the NDVI (MODIS data) to assess resilience as the ability of the canopy to return to a pre-drought state. In these cases, resistance and resilience appear as constancy or recovery of green foliage analysed through vegetation indices. Khoury et al. (2020) observed good resilience of Spanish forests to drought over the last 18 years. In order to better understand these phenomena, Khoury et al. (2020) recommend combining remote sensing with field analyses to better assess mortality processes in Mediterranean forests. Using remotely sensed data, recent studies (Senf et al. 2021) estimated several satellite indices (NDVI, EVI, mSAVI, NBR and NDMI) to examine the recovery and resilience of European forest canopies. Forest resilience was quantified as the ratio of canopy disturbance intervals to recovery intervals, with critical resilience defined for those forest areas where canopy disturbances occurred faster than canopy recovery. Most European forests showed canopy recovery before disturbance within 30 years, thus showing good resilience, except for 14% of them, which are affected by disturbance more frequently than the time it takes the canopy to recover. Senf et al. (2021) estimated a risk of system collapse with an average disturbance interval of 25 years. Thus, resilience depends not only on the system's ability to recover, but also on the frequency of disturbances. The limitations of the remote sensing approach have been attributed to the low spatial resolution of the data (often coarse) which may underestimate disturbances on a smaller scale and thus lead to an approximate view of recovery dynamics on a continental scale. These critical

issues could be ameliorated with in situ studies to obtain regional-scale information and proximal remote sensing applications. The time scale of remote sensing data is also very short and verification of information with long-term data such as dendrochronological data would be an added value.

Long-term monitoring is very important to assess resilience, because drought effects can last for decades and these effects influence not only growth, but also leaf and shoot production, water and carbon use (Camarero et al. 2018). European forests appear to be resilient to past disturbance regimes, however, changes in current climate, regimes and disturbance frequencies could erode their resilience (Senf et al. 2021).

1.6 Future scenarios and possible actions

The impact and exposure to climate change are different depending on bioclimatic zones and forest types; in Europe, we can identify three main bioclimatic zones, boreal, temperate and Mediterranean, each with a different scenario of changes (Lindner et al. 2010). The most critical area is the Mediterranean; for this area, a further temperature increase of 3-4 C° is expected in the 21st century, with peaks during the summer period, and a reduction in average precipitation of up to 20 % and summer precipitation of up to 50 % (Lindner et al. 2010). The new climate scenarios could favour large fires in Mediterranean areas with consequent soil erosion, and the new conditions could limit the renewal of the most demanding species by favouring the spread of more competitive species (Lindner et al. 2010). Trees that survive or resist extreme climatic events turn out to be very interesting individuals from a genetic point of view. Indeed, some authors (Vinceti et al. 2020) have evaluated the management of forest genetic resources as a strategy for adapting forests to future scenarios. This strategy consists of using forest material, both of the same species from other areas (hot and dry areas) and new species, to help the forest adapt to future environmental conditions and perpetuate the ecosystem and environmental services. However, assisted migration actions could entail risks of genetic pollution, maladaptation and the risk of exposing forests to new pathogens.

Forests, throughout their long evolutionary history, have demonstrated the ability to adapt and respond to climate change. However, natural processes alone are too slow to cope with the rapid changes that have occurred in recent years. Forests must be considered as complex and adaptive ecosystems, organised in a plurality of interacting parts that often generate non-linear dynamics (Borghetti 2012). Therefore, for future management, it is necessary to consider adaptive silviculture, i.e. a flexible method of action that takes into account ongoing changes. Therefore, after having identified the stands affected by climate change-induced dieback and mortality phenomena, it is necessary to identify appropriate adaptive forest management strategies with the aim of perpetuating forest growth, carbon sequestration, health and vitality of the forest system, reducing competition, structural homogeneity and promoting high biodiversity, thus giving the ecosystem greater resistance to environmental changes (Fabbio et al. 2014). From the silvicultural point of view, therefore, action must be taken to favour the adaptation of forest systems to future scenarios. Useful, in the early stages of dieback (in less affected sites), would be interventions to reduce grasses, shrubs and undergrowth vegetation to increase the soil's hydrological balance (Gentilesca et al. 2017), including through the use of controlled grazing (Sharro & Fletcher 1994). The aim is to retain water in the soil, promote organic matter degradation and nutrient availability. In fact, nutrient and mineral uptake in the soil is reduced during dry periods (González de Andrés et al. 2022). Moreover, in dense stands affected by dieback phenomena, reduced competition can promote survival (Lloret et al. 2012, Tonelli et al. 2023) and forest stand resistance to drought events (Castagneri et al. 2021). Therefore, selective thinnings could be performed, both in coppices and in high forest stands, reducing intra and interspecific competition (Gentilesca et al. 2017), always favouring a mixed forest composition that can increase the resilience of the system (Scheffer et al. 2012). Furthermore, in highly degraded sites, reproduction from seed should be encouraged and the production of non-viable seeds that occurs with senescence should be prevented (Gentilesca et al. 2017). Therefore, regeneration cuts could be anticipated in order to accelerate forest evolution and genetic mixing (Vinceti et al. 2020), maintaining a high level of

biodiversity and promoting forest adaptation to climatic conditions (Lindner et al. 2010).

1.7 Purposes and aims

The analysis of forest vulnerability is very complex, many factors can influence the response of stands to climate change, and management methods that could promote stand adaptation are still poorly experimented. The integrated approach of field and remotely sensed data to analyse forest health appears to be promising, but these studies still require further investigation to fully clarify how and according to which dynamics different forests, species and forest systems respond to ongoing changes. With this work, we wanted to assess critically the potential of the combined use of growth rings and remote sensing. We applied these methods to analyse some Mediterranean sites, characterised by mixed stands with symptoms of dieback, with the aim of improving our understanding of the vulnerability of Mediterranean forests to climate change and to provide useful information on this very critical issue at planetary scale.

1.8 References

1. Adams H.D., Zeppel M.J., Anderegg W.R., Hartmann H., Landhäusser S.M., Tissue D.T., McDowell N.G., 2017. *A multi-species synthesis of physiological mechanisms in drought-induced tree mortality*. Nat. Ecol. Evol., 1, 1285–1291. <https://doi.org/10.1038/s41559-017-0248-x>
2. Allen C. D., Breshears D. D. Breshears and McDowell N. G., 2015. *On underestimation of global vulnerability to tree mortality and forest die-off from hotter drought in the Anthropocene*. Ecosphere 6(8):129 <http://dx.doi.org/10.1890/ES15-00203.1>
3. Allen C. D., Macalady A. K., Chenchouni H., Bachelet D., McDowell N., Vennetier M., Kitzberger T., Rigling A., Breshears D. D., Hogg E. H., Gonzalez P., Fensham R., Zhang Z., Castro J., Demidova N., Lim J. H., Allard G., Running S. W., Semerci A., Cobb N., 2010. *A global overview of drought and heat-induced*

- tree mortality reveals emerging climate change risks for forests*. Forest Ecology and Management 259, 660-684. DOI:10.1016/j.foreco.2009.09.001
4. Allen C. D., 2007 *Interactions across spatial scales among forest dieback, fire, and erosion in northern New Mexico landscapes*. *Ecosystems*, 10.5: 797-808. <https://doi.org/10.1007/s10021-007-9057-4>
 5. Andivia E., Madrigal-Gonzalez J., Villar-Salvador P., and Zavala M.A., 2018. *Do adult trees increase conspecific juvenile resilience to recurrent droughts? Implications for forest regeneration*. *Ecosphere*, 9 (6):e02282.10.1002/ecs2.2282, <https://doi.org/10.1002/ecs2.2282>
 6. Bochenek Z., Ziolkowski D., Bartold M., Orłowska K. & Ochtyra A., 2017. *Monitoring forest biodiversity and the impact of climate on forest environment using high resolution satellite images*. *European Journal Of Remote Sensing* 51:1,166-181. DOI:10.1080/22797254.2017.1414573
 7. Borghetti M., 2012. *Principi fondanti, mosaico delle conoscenze e selvicoltura adattativa*. *Forest@* 9, 166-169. DOI: 10.3832/efor0699-009
 8. Borghetti M., Gentilesca T., Colangelo M., Ripullone F., Rita A., 2020. *Xylem Functional Traits as Indicators of Health in Mediterranean Forests*. *Curr Forestry Rep* 6, 220–236. <https://doi.org/10.1007/s40725-020-00124-5>
 9. Buras, A., Schunk, C., Zeiträg, C., Herrmann, C., Kaiser, L., Lemme, H., ... & Menzel, A., 2018. *Are Scots pine forest edges particularly prone to drought-induced mortality?*. *Environmental Research Letters*, 13(2), 025001. DOI 10.1088/1748-9326/aaa0b4
 10. Camarero J. J., Gazol A, Sangüesa-Barreda G., Cantero A., Sánchez-Salguero R., Sánchez-Miranda A., Granda E., Serra-Maluquer X. and Ibáñez R., 2018. *Forest Growth Responses to Drought at Short- and Long-Term Scales in Spain: Squeezing the Stress Memory from Tree Rings*. *Front. Ecol. Evol.* 6:9. DOI: 10.3389/fevo.2018.00009
 11. Camarero J.J., Colangelo M., Gazol A., Azorín-Molina C., 2021. *Drought and cold spells trigger dieback of temperate oak and beech forests in northern Spain*. *Dendrochronologia* 66, 125812 <https://doi.org/10.1016/j.dendro.2021.125812>

12. Castagneri D., Vacchiano G., Hacket-Pain A., DeRose R.J., Klein T. and Bottero A., 2021. *Meta-analysis Reveals Different Competition Effects on Tree Growth Resistance and Resilience to Drought*. *Ecosystems* <https://doi.org/10.1007/s10021-021-00638-4>
13. Choat B., Jansen S., Brodribb T.J., Cochard H., Delzon S., Bhaskar R., Bucci S.J., Field T.S., Gleason S.M., Hacke U.G., Jacobsen A.L., Lens F., Maherali H., Martinez-Vilalta J., Mayr S., Mencuccini M., Mitchell P.J., Nardini A., Pittermann J., Pratt R.B., Sperry J.S., Westoby, Zanne I.J.W., 2012. *Global convergence in the vulnerability of forests to drought*. *Nature* 491, 752-755. DOI:10.1038/nature11688
14. (a) Colangelo M., Camarero J.J., Battipaglia G., Borghetti M., De Micco V., Gentilesca T. and Ripullone F., 2017. *A multi-proxy assessment of dieback causes in a Mediterranean oak species*. *Tree Physiology* 37, 617–631. DOI:10.1093/treephys/tpx002
15. (b) Colangelo M., Camarero J.J., Borghetti M., Gazol A., Gentilesca T. and Ripullone F., 2017. *Size Matters a Lot: Drought-Affected Italian Oaks Are Smaller and Show Lower Growth Prior to Tree Death*. *Front. Plant Sci.* 8,135. DOI: 10.3389/fpls.2017.00135
16. Colangelo M., Camarero J.J., Ripullone F., Gazol A., Sánchez-Salguero R., Oliva J. and Redondo M. A., 2018. *Drought Decreases Growth and Increases Mortality of Coexisting Native and Introduced Tree Species in a Temperate Floodplain Forest*. *Forests*, 9, 205. DOI:10.3390/f9040205
17. Coluzzi R., Fascetti S., Imbrenda V., Italiano S. S. P., Ripullone F. and Lanfredi M., 2020. *Exploring the Use of Sentinel-2 Data to Monitor Heterogeneous Effects of Contextual Drought and Heatwaves on Mediterranean Forests*. *Land*, 9, 325. DOI:10.3390/land9090325
18. Cramer W., Guiot J., Fader M., Garrabou J., Gattuso J. P., Iglesias A., Lange M. A., Lionello P., Llasat M. C., Paz S., Peñuelas J., Snoussi M., Toreti A., Tsimplis M. N. and Xoplaki E., 2018. *Climate change and interconnected risks to sustainable development in the Mediterranean*. *Nature Climate Change*, 8 (11), pp.972 - 980. <https://doi.org/10.1038/s41558-018-0299-2>

19. Dakos V., Carpenter S.R., Brock W.A., Ellison A.M., Guttal V., Ives A.R., Ke'fi S., Livina V., Seekell D.A., van Nes E.H., Scheffer M., 2012. *Methods for Detecting Early Warnings of Critical Transitions in Time Series Illustrated Using Simulated Ecological Data*. PLoS ONE 7(7):e41010. DOI:10.1371/journal.pone.0041010
20. Dakos V., Scheffer M., van Nes E.H., Brovkin V., Petoukhov V. and Held H., 2008. *Slowing down as an early warning signal for abrupt climate change*. PNAS vol. 105: 14308–14312. www.pnas.org/cgi/doi/10.1073/pnas.0802430105
21. Depardieu C., Girardin M. P., Nadeau S., Lenz P., Bousquet J. and Isabel N., 2020. *Adaptive genetic variation to drought in a widely distributed conifer suggests a potential for increasing forest resilience in a drying climate*. New Phytologist, 227: 427–439. DOI: 10.1111/nph.16551
22. DeSoto L., Cailleret M., Sterck F., Jansen S., Kramer K., Robert E.M.R., Aakala T., Amoroso M.M., Bigler C., Camarero J.J., Cufar K., Gea-Izquierdo G., Gillner S., Haavik L.J., Heres A., Kane J.M., Kharuk V.I., Kitzberger T., Klein T., Levanič T., Linares J.C., Mäkinen H., Oberhuber W., Papadopoulos A., Rohner B., Sangüesa-Barreda G., Stojanovic D.B., Suárez M. L., Villalba R. & Martínez-Vilalta J., 2020. *Low growth resilience to drought is related to future mortality risk in trees*. Nature Communications, 11:545. <https://doi.org/10.1038/s41467-020-14300-5>
23. Fabbio, G., Cantiani, P., Ferretti, F., Chiavetta, U., Bertini, G., Becagli, C., ... & De Cinti, B., 2014. Adaptive silviculture to face up to the new challenges: the ManForCBD experience. In *Proceedings 2nd International Congress of Silviculture. Florence* (Vol. 1, pp. 531-538). <http://dx.doi.org/10.4129/2cis-gf-ada>
24. Fyllas, N. M., Christopoulou, A., Galanidis, A., Michelaki, C. Z., Giannakopoulos, C., Dimitrakopoulos, P. G., ... & Gloor, M., 2017. *Predicting species dominance shifts across elevation gradients in mountain forests in Greece under a warmer and drier climate*. *Regional Environmental Change*, 17, 1165-1177. <https://doi.org/10.1007/s10113-016-1093-1>
25. Gazol A., Camarero J.J., Vicente-Serrano S.M., Sánchez-Salguero R., Gutiérrez E., de Luis M., Sangüesa-Barreda G., Novak K., Rozas V., Tiscar P.A., Linares J.C., Martín-Hernández N., Martínez del Castillo E., Ribas M., García-

- González I., Silla F., Camisón A., Génova M., Olano J.M., Longares L.A., Hevia A., Tomàs-Buguera M., Galván J.D., 2018. *Forest resilience to drought varies across biomes*. *Glob Change Biol.*, 24:2143–2158. DOI: 10.1111/gcb.14082
26. Gentilesca T., Camarero J. J., Colangelo M., Nolè A., Ripullone F., 2017. *Drought induced oak decline in the western Mediterranean region: an overview on current evidences, mechanisms and management options to improve forest resilience*. *IForest*, 10: 796-806. DOI: 10.3832/ifor2317-010
27. Gentilesca, T., Camele, I. N., Colangelo, M., Lauteri, M., Lapolla, A., & Ripullone, F., 2015. Oak forest decline in Southern Italy: the study case of Gorgoglione forest. In *ATTI del Secondo Congresso Internazionale di Selvicoltura* (Vol. 2, pp. 123-129). Accademia Italiana Di Scienze Forestali. <http://dx.doi.org/10.4129/2cis-tg-dec>
28. González de Andrés E., Gazol A., Querejeta J.I., Igual J.M., Colangelo M., Sánchez-Salguero R., Linares J.C., Camarero J.J., 2022. *The role of nutritional impairment in carbon-water balance of silver fir drought-induced dieback*. *Glob Change Biol.* 2022;00:1–20, DOI: 10.1111/gcb.16170.
29. Hammond W.M., Yu K., Wilson L.A., Will R.E., Anderegg W.R.L. and Adams H.D., 2019. *Dead or dying? Quantifying the point of no return from hydraulic failure in drought-induced tree mortality*. *New Phytologist*, 223: 1834–1843.
DOI: 10.1111/nph.15922
30. Hartmann H., 2015. *Carbon starvation during drought-induced tree mortality – are we chasing a myth?*. *Journal of Plant Hydraulics*, 2: e-005. <https://doi.org/10.20870/jph.2015.e005>
31. Huang K., Xia J., 2019. *High ecosystem stability of evergreen broadleaf forests under severe droughts*. *Glob Change Biol.*, 25:3494–3503. DOI: 10.1111/gcb.14748
32. IPCC, 2018: *Summary for Policymakers*. In: *Global warming of 1.5°C. An IPCC Special Report on the impacts of global warming of 1.5°C above pre-industrial levels and related global greenhouse gas emission pathways, in the context of strengthening the global response to the threat of climate change, sustainable development, and efforts to eradicate poverty*; Masson-Delmotte V.,

- Zhai P., Pörtner H.O., Roberts D., Skea J., Shukla P.R., Pirani A., Moufouma-Okia W., Péan C., Pidcock R., Connors S., Matthews J.B.R., Chen Y., Zhou X., Gomis M.I., Lonnoy E., Maycock T., Tignor M., Waterfield T. (eds.). World Meteorological Organization, Geneva, Switzerland, 32 pp.
33. IPCC. Summary for Policymakers. In *Climate Change 2007: The Physical Science Basis. Contribution of Working Group I to the Fourth Assessment Report of the Intergovernmental Panel on Climate Change*; Solomon S., Qin D., Manning M., Chen Z., Marquis M., Averyt K.B., Tignor M., Miller H.L., Eds.; Cambridge University Press: Cambridge, UK; New York, NY, USA, 2007.
34. IPCC. Summary for Policymakers. In *Climate Change 2022: Mitigation of Climate Change. Contribution of Working Group III to the Sixth Assessment Report of the Intergovernmental Panel on Climate Change*; Shukla P.R., Skea J., Slade R., Al Khourdajie A., van Diemen R., McCollum D., Pathak M., Some S., Vyas, P., Fradera R., Eds.; Cambridge University Press: Cambridge, UK; New York, NY, USA, 2022
35. IPCC. 2019: Summary for Policymakers. In *Climate Change and Land: An IPCC Special Report on Climate Change, Desertification, Land Degradation, Sustainable Land Management, Food Security, and Greenhouse Gas Fluxes in Terrestrial Ecosystems*; Shukla P.R., Skea J., Calvo Buendia E., Masson-Delmotte V., Pörtner H.O., Roberts D.C., Zhai P., Slade R., Connors S., Van Diemen R., et al., Eds.; Intergovernmental Panel on Climate Change: Geneva, Switzerland, 2019; ISBN 978-92-9169-154-8.
36. Jiao L., Jiang Y., Zhang W., Wang M., Wang S., & Liu X., 2019. *Assessing the stability of radial growth responses to climate change by two dominant conifer trees species in the Tianshan Mountains, northwest China. Forest Ecology and Management*, 433, 667-677. DOI:10.1016/j.foreco.2018.11.046
37. Kherchouche D., Kalla M., Gutiérrez E. M., Attalah S. & Bouzghaia M., 2012. *Impact of droughts on Cedrus atlantica forests dieback in the Aurès (Algeria). Journal of Life Sciences*, 6(11), 1262.

38. Khoury S., Coomes D. A., 2020. *Resilience of Spanish forests to recent droughts and climate change*. *Glob Change Biol.* 2020;26:7079–7098. DOI: 10.1111/gcb.15268
39. Klein T, Zeppel M.J.B., Anderegg W.R.L., Bloemen J., De Kauwe M.G., Hudson P., Ruehr N.K., Powell T.L., von Arx G., Nardini A., 2018. *Xylem embolism refilling and resilience against drought-induced mortality in woody plants: processes and trade-offs*. *Ecological Research*, 33(5). DOI: 10.1007/s11284-018-1588-y
40. Klein T., Yakir D., Buchmann N and Grünzweig J.M., 2013. *Towards an advanced assessment of the hydrological vulnerability of forests to climate change-induced drought*. *New Phytologist*, 201: 712-716.
41. Lemaire J., Vennetier M., Prévosto B. & Cailleret M., 2022. *Interactive effects of abiotic factors and biotic agents on Scots pine dieback: A multivariate modeling approach in southeast France*. *Forest Ecology and Management*, 526, 120543. <https://doi.org/10.1016/j.foreco.2022.120543>
42. Levanič T., Čater M. and McDowell N. G., 2011. *Associations between growth, wood anatomy, carbon isotope discrimination and mortality in a Quercus robur forest*. *Tree Physiology*, 31, 298–308. DOI:10.1093/treephys/tpq111
43. Lindner M., Maroschek M., Netherer S., Kremer A., Barbati A., Garcia-Gonzalo J., Seidl R., Delzon S., Corona P., Kolström M., Lexer M.J., Marchetti M., 2010. *Climate change impacts, adaptive capacity, and vulnerability of European forest ecosystems*. *Forest Ecology and Management*, 259, 698–709. DOI:10.1016/j.foreco.2009.09.023
44. Lloret F., Escudero A., Iriondo O. M., Martínez-Vilalta J. and Valladares F., 2012. *Extreme climatic events and vegetation: the role of stabilizing processes*. *Global Change Biology*, 18, 797–805. DOI: 10.1111/j.1365-2486.2011.02624.x
45. Lloret F., Keeling E. G. and Sala A., 2011. *Components of tree resilience: effects of successive low-growth episodes in old ponderosa pine forests*. *Oikos*, 120: 1909–1920. DOI: 10.1111/j.1600-0706.2011.19372.x.
46. Lloret F., Lobo A., Estevan H., Maisongrande P., Vayreda J. and Terradas J., 2007. *Woody plant richness and NDVI response to drought events in*

- Catalonian (Northeastern Spain) forests*. *Ecology*, 88(9), 2007, pp. 2270–2279. DOI: 10.1890/06-1195.1
47. Mannerucci F., Sicoli G. and Luisi N., 2006. *Oak decline in Apulia, southern Italy: an ecological indicator of landscape evolution?*. *Landscape ecology*, 4th Meeting of IUFRO 8.01.03.
48. Marchetti M., 2023. *I conflitti per la terra, minaccia primaria per la biodiversità*. *L'Italia forestale e montana*, 78(2), 77-94. DOI: 10.36253/ifm-1101
49. McDowell N., Pockman W.T., Allen C.D., Breshears D.D., Cobb N., Kolb T., Plaut J., Sperry J., West A., Williams D.G. and Yezzer E.A., 2008. *Mechanisms of plant survival and mortality during drought: why do some plants survive while others succumb to drought?*. *New Phytologist*, DOI: 10.1111/j.1469-8137.2008.02436.x.
50. McDowell N.G., 2011. *Mechanisms Linking Drought, Hydraulics, Carbon Metabolism, and Vegetation Mortality*. *Plant Physiology*, Vol. 155, pp. 1051–1059. www.plantphysiol.org/cgi/doi/10.1104/pp.110.170704
51. Neycken, A., Scheggia, M., Bigler, C., & Lévesque, M., 2022. *Long-term growth decline precedes sudden crown dieback of European beech*. *Agricultural and Forest Meteorology*, 324, 109103. <https://doi.org/10.1016/j.agrformet.2022.109103>
52. Ogaya R., Barbeta A., Basnou C., Peñuelas J., 2015. *Satellite data as indicators of tree biomass growth and forest dieback in a Mediterranean holm oak forest*. *Annals of Forest Science*, Springer Verlag/EDP Sciences, 72 (1), pp.135-144. DOI:10.1007/s13595-014-0408-y
53. Pollastrini M., Puletti N., Selvi F., Iacopetti G. & Bussotti, F., 2019. *Widespread crown defoliation after a drought and heat wave in the forests of Tuscany (central Italy) and their recovery—A case study from summer 2017*. *Frontiers in Forests and Global Change*, 2, 74. DOI:10.3389/ffgc.2019.00074
54. Pretzsch H., Schütze G. & Uhl E., 2013. *Resistance of European tree species to drought stress in mixed versus pure forests: evidence of stress release by interspecific facilitation*. *Plant Biology*, 15, 483–495. DOI:10.1111/j.1438-8677.2012.00670.x

55. Rita A., Camarero J.J., Nolè A., Borghetti M., Brunetti M., Pergola N., Serio C., Vicente-Serrano S. M., Tramutoli V., Ripullone F., 2019. *The impact of drought spells on forests depends on site conditions: The case of 2017 summer heat wave in southern Europe*. *Global Change Biology*; 00:1–13. DOI: 10.1111/gcb.14825
56. Scheffer M., Carpenter S.R., Lenton T.M., Bascompte J., Brock W., Dakos V., van de Koppel J., van de Leemput I. A., Levin S.A., van Nes E.H., Pascual M., Vandermeer J., 2012. *Anticipating Critical Transitions*. *SCIENCE* - Vol 338, pp. 344-348, DOI: 10.1126/science.1225244
57. Schimel D.S., 1995. *Terrestrial Ecosystems and the Carbon Cycle*. *Global Change Biology*, 1: 77-91. <https://doi.org/10.1111/j.1365-2486.1995.tb00008.x>
58. Senf C., Seidl R., 2021. *Post-disturbance canopy recovery and the resilience of Europe's forests*. *Global Ecol Biogeogr*. 00:1–12, DOI: 10.1111/geb.13406.
59. Sevanto S, McDowell NG, Dickman LT, Pangle R, Pockman WT., 2014. *How do trees die? A test of the hydraulic failure and carbon starvation hypotheses*. *Plant, Cell & Environment* 37: 153-161). <https://doi.org/10.1111/pce.12141>
60. Sharrow S.H.S., Fletcher R.A., 1994. *Trees and pastures: 40 years of agro-silvopastoral experience in Western Oregon*. In: *Proceedings of the Symposium "Agroforestry and Sustainable Systems"*. Fort Collins (CO, USA) 7-10 Aug 1994. NAC, Lincoln, NE, USA, pp. 47-53.
61. Tonelli E., Vitali A., Brega F., Gazol A., Colangelo M., Urbinati C., & Camarero J. J., 2023. *Thinning improves growth and resilience after severe droughts in Quercus subpyrenaica coppice forests in the Spanish Pre-Pyrenees*. *Dendrochronologia*, 77, 126042. <https://doi.org/10.1016/j.dendro.2022.126042>
62. Thomas F.M., Blank R. and Hartman G., 2002. *Abiotic and biotic factors and their interactions as causes of oak decline in Central Europe*. *For. Path.* 32, 277–307.
63. Touhami I., Chirino E., Aouinti H., El Khorchani A., Elaieb M. T., Khaldi A. & Nasr Z., 2020. *Decline and dieback of cork oak (Quercus suber L.) forests in the Mediterranean basin: A case study of Kroumirie, Northwest Tunisia*. *Journal of Forestry Research*, 31, 1461-1477. <https://doi.org/10.1007/s11676-019-00974->

1

64. Valeriano C., Tumajer J., Gazol A., de Andrés E. G., Sánchez-Salguero R., Colangelo M., ... & Camarero J. J., 2023. *Delineating vulnerability to drought using a process-based growth model in Pyrenean silver fir forests*. *Forest Ecology and Management*, 541, 121069. DOI:10.1016/j.foreco.2023.121069
65. Vinceti B., Manica M., Lauridsen N., Verkerk P.J., Lindner M., Fady B., 2020. *Managing forest genetic resources as a strategy to adapt forests to climate change: perceptions of European forest owners and managers*. *European Journal of Forest Research*, 139:1107–1119. <https://doi.org/10.1007/s10342-020-01311-6>
66. WBGU (Wissenschaftlicher Beirat der Bundesregierung Globale Umweltveränderungen), Beese F., Fraedrich K., Klemmer P., Kokott J., Kruse-Graumann L., et al., 1998. *The Accounting of Biological Sinks and Sources under the Kyoto Protocol: A Step Forward or Backwards for Global Environmental Protection?*, Special report, Bremerhaven, Alfred Wegener Institut.
67. Xu P., Zhou T., Yi C., Fang W., Hendrey G. and Zhao X., 2018. *Forest drought resistance distinguished by canopy height*. *Environ. Res. Lett.*, 13, 075003. <https://doi.org/10.1088/1748-9326/aacadd>

2. ASSESSING FOREST VULNERABILITY TO CLIMATE CHANGE COMBINING REMOTE SENSING AND TREE-RING DATA: ISSUES, NEEDS AND AVENUES

2.1 Abstract

Forests around the world are facing climate change. Increased drought stress and severe heat waves in recent decades have negatively impacted on forest health, making them more vulnerable and prone to dieback and mortality phenomena. Although the term vulnerability is used to indicate an increased susceptibility of forests to climate change with a worsening of their vigour status that can compromise their ability to respond to further climate extreme events, there are still uncertainties on how to evaluate it. Indeed, evaluation of forest vulnerability is complex both because of some critical issues in the estimation methods used and because of the multiple factors influencing the response of forests to ongoing climate change. A way to assess the vulnerability to environmental stresses is by combining remote sensing and dendroecological data. However, these two approaches entail multiple uncertainties, including growth/photosynthetic relationships, carbon allocation dynamics, biases of tree-ring data and noisy remote sensing data, which require further clarification for proper monitoring of pre- and post-drought forest trajectories. Our review aims to create an overview of the current literature and knowledge to understand the critical issues, needs and possible solutions that forest vulnerability research is addressing. We focus on Mediterranean forests located in a climate warming hotspot and showing a high vulnerability to increased aridification.

Keywords: climate change; drought; dieback; forest vulnerability

2.2 Introduction

Average temperatures in Mediterranean regions have risen +1.4 °C since the late 19th century, an increase of +0.4 °C above the global average. Overall, these conditions are leading to a significant reduction in summer precipitation availability and more frequent heat waves and droughts (Cramer et al. 2018, IPCC 2019). Such climatic alterations can affect forest ecosystems by causing dieback and consequent changes in forest composition, structure and distribution, making some stands more susceptible to pests, pathogens (Thomas et al. 2002) and fires (Jones et al. 2022). Thus, overall, ongoing climate change makes our forests more vulnerable by compromising their ecosystem services such as CO₂ uptake, climate change mitigation, biodiversity conservation, soil protection, water regulation, etc.

Tree mortality phenomena, due to the physiological stress to which forests are subjected, have been attributed to interconnected abiotic and biotic stress factors. Hydraulic failure and carbon starvation, followed by attacks by biotic agents, have been identified as the main mechanisms of mortality (McDowell et al. 2008).

Hydraulic failure, which occurs in hot and dry conditions, results from an imbalance between plant transpiration and water uptake, which causes an increasingly negative xylem pressure, leading to widespread xylem embolism, interruption of water flow and canopy desiccation (McDowell et al. 2008). Carbon starvation, on the other hand, occurs because the plant, under water stress conditions, closes its stomata to limit water loss through transpiration, resulting in reduced CO₂ supply and carbohydrate synthesis (McDowell et al. 2008). Plants initially utilise stored carbohydrates to cope with stress (Martínez-Vilalta et al. 2016); these reserves cannot be restored if water stress conditions persist, and therefore the plant goes into starvation. Furthermore, drought negatively affects phloem transport with a reduction in cell turgor, preventing carbon translocation in the plant (Hartmann 2015). Therefore, the uptake of nutrients and minerals in the soil is reduced during dry periods, causing generalised stress (González de Andrés et al. 2022). Hydraulic failure and carbon starvation are mechanisms that can occur simultaneously (McDowell 2011, Adams et al. 2017) and can therefore trigger a reduction in photosynthetic activity (defoliation, canopy desiccation)

and growth rate (very narrow growth rings) (Levanič et al. 2011, Colangelo et al. 2017b).

Climate can also influence insect, pathogen and disease cycles (Patterson et al. 1999). The combination of various factors, such as drought and excess nitrogen due to anthropogenic emissions (NH₃, N₂O, NO_x), causes a reduction in the concentration of allelochemicals in plant leaves (Thomas et al. 2002), secondary metabolites produced by plants, which can have a defensive function against pests; the reduction of these substances can therefore make trees more susceptible to pathogens.

Thus, abiotic and biotic factors are interconnected and it is clear how climate change can trigger dieback phenomena and influence the vulnerability and growth of forests. Vulnerability can be defined as the degree of susceptibility of a system and its inability to cope with the adverse effects of climate change (IPCC 2007), or, more precisely, as the reduction/absence of response to such adverse climatic events (e.g., drought). In the case of forests, a loss of resilience or recovery capacity can result in forest dieback and higher mortality rates of trees, stands or entire forests (DeSoto et al. 2020).

Thus, heat waves and drought periods are causing the death of several forest tree species in most continents: North America, Europe, Australia, continental Asia and Russia, showing a sharp increase in mortality events from 1998 to 2000 (Allen et al. 2010, Allen et al. 2015). In the Mediterranean basin, forest dieback phenomena have been reported in temperate oaks (*Quercus robur* L., *Quercus petraea* Matt. Liebl) in northeastern Italy (Colangelo et al. 2018, Pericolo et al. 2023) and northern Spain (Camarero et al. 2021), while in southern Italy, dieback has affected oak species such as *Quercus cerris* L., *Quercus pubescens* Willd. (Gentilesca et al. 2017) and *Quercus frainetto* Ten. (Colangelo et al. 2017a). Other dieback phenomena have been reported in several conifers, such as *Pinus pinaster* Aiton. in southeastern Spain (Navarro-Cerrillo et al. 2018), *Pinus pinea* L. in northeastern Spain (Moreno-Fernández et al. 2022) and *Pinus sylvestris* L., *Pinus halepensis* Mill. and *Abies alba* Mill. in eastern Spain (Camarero et al. 2015). In the case of *A. alba*, the species showed a marked reduction in growth in some Pyrenean populations compared to cooler and wetter sites in eastern and central Europe

(Camarero et al. 2011, Gazol et al. 2015). Furthermore, several Greek stands of *P. sylvestris* L. and *Abies cephalonica* Loudon have shown dieback triggered by climate change and assisted by pathogen outbreaks (Chrysopolitou et al. 2013). In Greece, the increase in temperature caused mortality phenomena in *Pinus brutia* Ten., highlighting vulnerability to global warming (Christopoulou et al. 2022), while *Abies borisii-regis* Mattf. manifested greater adaptability to increasing temperatures but susceptibility to drought periods (Kastridis et al. 2022). In addition, climate change causes changes in the composition and distribution of species, leading to alterations in ecosystems. Recent studies (Batllori et al. 2020) have shown, through analysis of different biomes around the world (131 sites), that tree mortality caused by drought phenomena led to a short-term (on average 5 years) conversion of vegetation type. Species self-replacement involved changes in community composition, e.g., from mesic forests to more xeric communities, with the spread of shrubs or non-woody vegetation. Thus, extreme drought could act as an environmental filter for species particularly sensitive to water deficit, highlighting a potential reorganisation of the ecosystem (Batllori et al. 2020).

The phenomena of forest dieback are mainly manifested through symptoms such as crown defoliation and wilting, branch desiccation, crown decay, epicormic shoot production, longitudinal bark cracking, biomass reduction, necrosis of absorbing roots, growth decline, etc. (Manion 1992, Gentilesca et al. 2017). Clearly, the assessment of forest vulnerability as linked to dieback is not straightforward; this complexity is due to some critical issues in the estimation methods used and to the many factors that influence the response of forests to climate, including site characteristics (exposure, altitude, slope) (Rita et al. 2020), nutrient availability and soil type (González de Andrés et al. 2022), species abundance (Lloret et al. 2007), isohydric (water-sparing) vs. anisohydric (water-spending) strategies (Pretzsch et al. 2013), the availability of reserves such as non-structural carbohydrates (Hartmann 2015, Trugman et al. 2018), stand structure (Xu et al. 2018, Ripullone et al. 2020), tree age (Lloret et al. 2011, Colangelo et al. 2021) and mitigation or compensation processes (Lloret et al. 2012), as well as management and human activities (Bussotti et al. 2015).

Therefore, the response of forests to climate change is influenced by several factors

and variables, but since the repercussions of climate anomalies on forests are mainly translated into a reduction in radial increment and photosynthetic activity, the study of forest vulnerability can be conducted through dendroecological surveys, to analyse the increment of growth rings, and remote sensing vegetation indices, which provide information on the state of canopies (Table 1).

Field surveys and dendroecological/anatomical studies of wood in relation to climatic data (Camarero et al. 2016) are fundamental; in fact, by analysing tree rings and anatomical variables of wood, it has been possible to understand that drought is the triggering factor of dieback in Mediterranean forests (Camarero et al. 2015, Gentilesca et al. 2017), while remote sensing surveys represent a widely used method to study forest dynamics over large areas (Lloret et al. 2007, Ogaya et al. 2015) and to observe the response of forests to disturbances (drought, heat waves, fires) in spectral terms (Coluzzi et al. 2020).

However, the methods used to estimate vulnerability may present some criticalities; for example, in some cases, the radial increment estimated with dendrochronology does not correspond to climatic dynamics, which may be due to the translocation of reserve carbohydrates used by woody plants to grow during periods of stress (Michelot et al. 2012). Or, in other cases, satellite information does not correspond to field observations. Indeed, coarse spatial resolution (Brehaut et al. 2018), cover mix (tree canopy, undergrowth, soil, etc.) (Chen et al. 2018) and density (Wang et al. 2022) or plant diversity (Vicente-Serrano et al. 2020), could lead to overestimated or underestimated spectral index values. Therefore, studying the vulnerability of forests to climate change is still an evolving challenge for researchers and survey methods need further implementation to understand how forests are able to respond to climate change and how resilient they are to such events. In this article, we provide an overview of the state of the art to reason about the studies and the main critical issues that have emerged regarding the combined use of tree rings and remote sensing to examine the vulnerability of forests.

Table 1. Recent articles with a combination of dendroecological and remote sensing approaches: MXD (maximum latewood density), TRW (tree-ring width), TRWi (tree-ring width index), BAI (Basal area increment), RWI (ring width index), GPP (gross primary production); VI (vegetation index): NDVI (Normalized Difference Vegetation Index), EVI (Enhanced Vegetation Index), NDWI (Normalized Difference Water Index).

Reference	Species	Variables	Correlation
Moreno-Fernández et al. 2022	<i>Pinus pinea</i> L., 1753	BAI, NDVI, NDWI	different responses to drought between indices and low BAI – VI correlation
Ogaya et al. 2015	<i>Quercus ilex</i> L., 1753	Defoliation, BAI, NDVI, EVI	positive correlation between defoliation and vegetation indices
Coluzzi et al. 2020	Mixed forest of oaks and ash trees	Defoliation, NDVI	positive correlation
Brehaut et al. 2018	<i>Picea glauca</i> (Moench) Voss, 1907 <i>Picea mariana</i> (Mill.) Britton, Sterns & Poggenb., 1888 <i>Salix glauca</i> L., 1753 <i>Alnus crispa</i> (Aiton) Pursh, 1814 <i>Populus tremuloides</i> Michx., 1803, at different sites	TRW, NDVI	low correlation
Vicente-Serrano et al. 2020	15 species In different biomes	TRW, GPP, NDVI	site-dependent relationships
Wang et al. 2021	<i>Pinus densiflora</i> Siebold & Zucc., 1842	RWI, NDVI	positive correlation
Castellaneta et al. 2022	<i>Pinus sylvestris</i> L., 1753 <i>Quercus pubescens</i> Willd., 1805 <i>Quercus frainetto</i> Ten., 1813 <i>Juniperus phoenicea</i> L., 1753	BAI, NDVI	positive correlations

Table 1 (cont.)

Gazol et al. 2018	11 tree species between gymnosperms and angiosperms	TRWi, NDVI	positive correlation
D'Andrea et al. 2022	<i>Picea abies</i> (L.) H.Karst., 1881	RWI, NDVI	inconsistent trend
Lapenis et al. 2013	<i>Picea abies</i> (L.) H.Karst., 1881	TRW, NDVI	inconsistent trend
Vicente-Serrano et al. 2016	100 tree species in different biomes	TRW, NDVI	different relationships between growth and vegetation indices; stronger correlation in dry sites
Beck et al. 2013	Treeline vegetation mix in different forests	TRW, MXD, NDVI	positive NDVI-MXD correlation
D'Arrigo et al. 2000	<i>Picea glauca</i> (Moench) Voss, 1907 <i>Larix gmelinii</i> (Rupr.) Kuzen, 1854	MXD, NDVI	good correlation

2.3 Resilience Indexes to Assess the Vulnerability of Forests

As described above, the vulnerability of forests results in a loss of resilience, i.e., a reduced ability to return to pre-disturbance conditions, that over time can cause mortality phenomena (DeSoto et al. 2020). Therefore, to assess forest resilience, resilience indices (Lloret et al. 2011) can be applied based on dendroecological information, i.e., the performance of radial growth (e.g., BAI basal area increment) before (PreDr), during (Dr) and after (PostDr) drought episodes. These indicators are obtained through simple formulae and are represented by: resistance ($R_t = Dr/PreDr$), recovery ($R_c = PostDr/Dr$) and resilience itself ($R_s = PostDr/PreDr$). By applying these indices, it is possible to understand the dynamics of a forest stand in response to stress episodes. Lloret et al. (2011), analysing tree rings in *Pinus ponderosa* Douglas trees in remote Rocky Mountain forests, observed low radial growth correlated with drought periods, and estimating the components of R_t , R_c and R_s showed that impacts from a previous event and cumulative effects from the past, resulting in lower growth, caused a decrease in resilience (Lloret et al. 2011).

Further studies conducted in Germany (Pretzsch et al. 2013) applied resilience parameters (Lloret et al. 2011) to quantify the growth response of trees to periods of water stress. Resistance, recovery and resilience (R_t , R_c and R_s) were estimated for three different species, *Fagus sylvatica* L., *Picea abies* L. and *Quercus petraea* Matt. Liebl, for both pure and mixed stands. In all cases, the species effect on R_t , R_c and R_s was significant; i.e., Norway spruce is easily affected by dry spells but recovers quickly and oak is more resistant but recovers more slowly, while beech's reaction is in the middle, showing greater resistance and resilience when mixed with oak than when monospecific (Pretzsch et al. 2013). Other studies (DeSoto et al. 2020) applied these indices (R_t , R_c , R_s) using a pan-continental tree ring width (TRW) database for entire biomes (118 sites and 3500 individuals) with different angiosperm and gymnosperm species. Overall, the TRW time series study showed reduced growth associated with higher mortality risk, and resilience indices showed that drought-dead trees were less resilient to drought events prior to their death than surviving trees for both gymnosperms and angiosperms.

Therefore, these indicators provide information on the resilience of forest stands, based on dendrochronological measurements, so even these indices could suffer from some criticalities linked to possible cases of inconsistencies between growth rings and climate (Schweingruber 1988, Michelot et al. 2012, Schwarz et al. 2020), which we will discuss in the following sections.

2.4 Methods for Monitoring and Studying Forest Vulnerability

2.4.1 Tree Crown Evaluations

The analysis and monitoring of dieback and mortality phenomena have been addressed through various methodologies, such as visual analysis of vegetation conditions, field surveys, remote sensing techniques and many others. Some studies in the past have used a visual and qualitative assessment of trees (vitality classes) to evaluate the severity of dieback (Mannerucci et al. 2006). This approach consists of assigning each observed plant a vitality class, i.e., a numerical value in the range from 1 to 6 (healthy to dead plant) (Mannerucci et al. 2006, Coluzzi et al. 2020). However, this method, being a visual and qualitative assessment of the state of the canopy, is not very objective, so it depends on the operator's ability to distinguish

between the different vitality classes. Other studies (Dobbertin 2005, Camarero et al. 2016), for example, have differentiated between declining and non-declining trees based on the current percentage of crown transparency or defoliation. This is a widely used practical approach to characterise tree vigour; nevertheless, this approach has been subject to some criticism. Indeed, establishing a fixed threshold of defoliation to distinguish trees in decline from those that are not can be questioned because crown transparency can change from year to year. Thus, a defoliated tree may recover, while some non-defoliated trees may start to die back. However, there are defoliation thresholds that, once exceeded, are not reversible. Other studies have used remote sensing to assess forest cover. Indeed, it has been shown that airborne Lidar (Laser Imaging Detection and Ranging), through the acquisition of point clouds, can detect defoliation in terms of LAI (Solberg et al. 2006) and thus provide feedback on canopy and forest vigour (Meng et al. 2022). Given the complexity of forest systems and their response to disturbances, visual or remote canopy assessment methods must always be accompanied and validated by quantitative field surveys and measurements to ensure representativeness and correlation between the data obtained.

2.4.2 Dendroecology

Qualitative observations of canopies alone, therefore, are not sufficient to best discriminate the state of forests and, consequently, their vulnerability. Quantitative investigations to examine forest dieback phenomena can be obtained using dendroecological data; an example of this type of investigation is that employed by several studies (Camarero et al. 2016, Colangelo et al. 2017a), in which, in addition to an initial visual assessment of canopy transparency, time series of tree rings were also obtained. Trees under drought conditions show a reduction in the radial increment and area of the vasa lumen and a consequent reduction in hydraulic conductivity (Colangelo et al. 2017a). Following frequent extreme weather events that trigger dieback phenomena, a decline in the growth of trees is observed long before their death, which can vary in intensity and duration. This phenomenon results in divergent growth trends between trees that experience dieback and those that do not (Colangelo et al. 2017b, Camarero et al. 2021). Thus, the reduction in

growth immediately before death could be due to a generalised water failure and/or secondary stress factors (diseases and pathogens) favoured by a loss of tree vigour, while a slow growth slowdown could be associated with a gradual decline in hydraulic performance and depletion of carbon reserves (Cailleret et al. 2017).

Therefore, tree rings and their anatomical variations are considered important proxies for studying the response of forests to environmental changes by retrospectively analysing, with high temporal resolution, the climatic dynamics permanently recorded in the wood structure (Fonti et al. 2010).

However, even the growth ring does not always show reductions in growth during a particularly hot and droughty year, e.g., the formation of early wood in porous ring species depends on the remobilisation of stored carbon, thus not exclusively reflecting the climatic conditions during that actual growth period (Schweingruber 1988, Michelot et al. 2012). In other words, growth is maintained during drought through the use of stored carbohydrates, but this can cause depletion of non-structural carbohydrate (NSC) reserves and reduce the trees' resistance to further drought events, making them prone to death (DeSoto et al. 2020). In addition, drought responses may vary depending on vegetative earliness, i.e., two species in the same area may show different growth responses depending on the time of sprouting, and thus the growth ring may or may not highlight the drought event (Schwarz et al. 2020).

In spite of these difficulties, to date dendrochronological surveys have been the most suitable for providing information and quantifying forest dieback phenomena, but these types of studies can only be applied to single sites on a small scale and require considerable resources, so even these alone do not allow for the study of large areas such as those affected by dieback.

2.4.3 Remote Sensing

To obtain information on forest vulnerability on a large scale and save the time and resources needed for field surveys, remote sensing can assist. Indeed, satellite-based vegetation indices have made it possible to switch from individual- to forest-scale studies. Therefore, the combination of the dendrochronological approach and remote sensing is promising for assessing forest decline (Vicente-Serrano et al.

2013, Wang et al., 2021). A widely used remote sensing index on which many other indices are based is the Normalized Difference Vegetation Index (NDVI) (Rouse et al. 1973). This index is widely used as a proxy for forest photosynthetic activity (Coluzzi et al. 2020, Wang et al. 2021, Castellaneta et al. 2022) and productivity in drought-prone Mediterranean biomes (Vicente-Serrano et al. 2020). Thus, after drought events or heat waves, which lead to a reduction in photosynthetic activity, the NDVI tends to assume lower values, while higher values of the index indicate favourable conditions for plant health. Therefore, this index has been used to study mortality phenomena or increases in biomass related to climatic conditions (Ogaya et al. 2015). For example, some studies (Gazol et al. 2018) have shown the existence of a positive correlation between resilience indices (Lloret et al. 2011), obtained using growth in terms of tree ring width indices (TRWi) and forest productivity in terms of NDVI. However, it must be remembered that the response of forests, as expressed by the remote indices, can differ depending on the type of forest site, tree species and the degree of stand mixing (Bochenek et al. 2017).

2.5 Decoupling of NDVI–Growth Relationship

NDVI is an index that measures photosynthetically active biomass (canopy of trees and greenness), but its relationship to growth is complex (Glenn et al. 2008, Brehaut et al. 2018). Indeed, changes in carbon allocation may favour foliage over woody biomass, leading to a weakening of the relationship between tree-ring growth and the remote sensing signal. This can cause inconsistency phenomena between trends (D’Andrea et al. 2022), i.e., the presence of positive NDVI trends when negative tree-ring trends are observed (Lapenis et al. 2013). To study these relationships, Vicente-Serrano et al. (2016) compared tree ring data with NDVI time series on a global scale, finding a high spatial and temporal divergence in forest growth responses. In fact, growth rates and vegetative recovery between coexisting species may differ and, respectively, carbon sequestration may vary and influence the growth of rings with respect to NDVI. Therefore, the different phenology of wood and leaf formation could explain the decoupling between NDVI and growth (Vicente-Serrano et al. 2016).

Other cases where NDVI may not provide an accurate account of radial growth are

surveys in ecotone areas (Beck et al. 2013), i.e., at forest edges where there is a transition from tree to shrub vegetation, greening trends with increasing shrub biomass could alter vegetation indices. Furthermore, it has been shown that not only vegetation composition, but also slope (Wang et al. 2021), exposure and altitude, influence the climatic response, which means that in an area, different vegetation types or trends may confound the NDVI–ring width relationship. Consequently, low image resolution, changes in resource allocation in trees and site characteristics may interact to limit the correlation between NDVI and annual radial growth (Brehaut et al. 2018). These limitations increase with the complexity of the landscape, such as for highly heterogeneous Mediterranean ecosystems that manifest articulated responses to extreme events, so response patterns and tree-ring growth on NDVI time scales may not be fully representative (Vicente-Serrano et al. 2020). On the other hand, if species composition is homogeneous or if the proportion of dominant species responds similarly to climatic variations, then there should be a positive correlation between NDVI and trends in ring width (D’Arrigo et al. 2000).

In order to use these two indicators (NDVI and tree rings) congruently, one could consider the observed positive correlations between MXD (maximum latewood density), NDVI and temperature during the growing season (Beck et al. 2013) and perform satellite analyses at a higher spatial and temporal resolution that could allow for a better investigation. Certainly, an examination of the relationship between NDVI and processes at the tree/species level, date of sprouting or root growth may lead to a better understanding of these dynamics (Brehaut et al. 2018). Thus, appropriate research is needed to understand the physiological and phenological processes that explain the dependence between wood formation and photosynthetic processes underlying NDVI and the relative time intervals in which these processes occur (Vicente-Serrano et al. 2016).

In addition, the use of high-resolution satellite data could improve remote sensing information; in fact, Sentinel-2 10 m X 10 m space resolutions have given good results in small-scale monitoring (Coluzzi et al. 2020) of the effects of extreme weather events on mixed Mediterranean forests in southern Italy, showing a good correspondence between NDVI and qualitative data collected in the field. To obtain

highly detailed resolutions, an alternative could be remote sensing with drones, which allows lower material and operational costs and greater flexibility in spatio-temporal resolution than satellites (Tang et al. 2015). Recent studies (Vivar-Vivar et al. 2022) have used unmanned aerial vehicles (UAVs) to monitor mixed coniferous and deciduous forests in northern Mexico with excellent results. Using specific sensors, they calculated tree height, canopy area and number of trees, and with a multispectral camera (PM4), with a resolution of up to 10 cm per pixel, they accurately estimated a number of multi-spectral indices related to vegetation activity. However, even then, seasonal monitoring is recommended to obtain an accurate estimate of photosynthetic activity and determine the seasonality of plant response. Furthermore, higher-quality mapping requires new research paradigms and the need to adapt algorithms according to forest stand characteristics (Vivar-Vivar et al. 2022).

2.6 Low Spatial Resolution and Remote Sensing Signal Anomalies

Remote sensing therefore has great potential in forest monitoring, but most satellites have a low to moderate spatial resolution, which means that a pixel contains a mixture of tree vegetation, undergrowth, soil, shade, etc. (Chen et al. 2018, Wang et al. 2022). This could lead to anomalous index values, particularly in sparse forests and those affected by climate-change-induced mortality (Wang et al. 2022).

Therefore, it is necessary to estimate the fractional coverage of photosynthetic vegetation, non-photosynthetic vegetation and bare soil. Guerschman et al. (2009) developed a very interesting approach, i.e., they used the NDVI and the Cellulose Absorption Index (CAI) to distinguish the different cover types. Analysing large areas of Australia characterised by different cover types (Closed Forest > 80% cover, Non Forest < 20% cover, Open Forest 50%–80% cover and Woodland 21%–50% cover) and using data from the EO-1 Hyperion satellite, with a hyperspectral sensor (30 m spatial resolution), they showed that green vegetation is represented by high NDVI values and an intermediate CAI; dry vegetation and litter by low NDVI values and a high CAI; and bare soil by low NDVI values and a low CAI. In other words, CAI increases linearly with increasing non-photosynthetic vegetation

(Nagler et al. 2003). Furthermore, the work of Guerschman et al. (2009) showed that the ratio between the SWIR3 and SWIR 2 bands of MODIS (bands 7 and 6 at 500 m resolution) is linearly correlated with NDVI and CAI derived from Hyperion. Therefore, fractional vegetation cover can be analysed with satellite data (Hyperion and MODIS satellites), but it is still a moderate resolution.

Over time, in order to solve the surface discrimination problem, attempts have been made to reduce the soil signal in the presence of low vegetation cover by adding soil correction factors, resulting in indices such as the Soil-Adjusted Vegetation Index (SAVI) (Huete 1988), Modified Soil Adjusted Vegetation Index (MSAVI) (Qi et al. 1994), Optimisation of Soil-Adjusted Vegetation Index (OSAVI) (Rondeaux et al. 1996) and Generalized Soil-Adjusted Vegetation Index (GSAVI) (Gilabert et al. 2002); alternatively, weighting coefficients were added to improve vegetation signals, as in the case of the indices Enhanced Vegetation Index (EVI) (Huete et al. 2002), Wide Dynamic Range Vegetation Index (WDRVI) (Gitelson et al. 2004) and Near-Infrared Reflectance of terrestrial vegetation (NIRv) (Badgley et al. 2017). However, these satellite-derived indices are not yet able to accurately capture surface phenological changes due to their limited spatial resolution (Wang et al. 2022). In addition, shading causes alterations in indices values, as with NDVI, reducing the accuracy of land cover classification (Liu et al. 2012).

An approach that could improve this problem could come from comparing NDVI values obtained from satellites, results obtained from radiometers attached to field towers and field data obtained from drones. Wang et al. (2022) conducted such an approach in Israel, analysing a *Pinus halepensis* Mill. forest located between the Mediterranean Sea and the Dead Sea, using drones with multispectral cameras with high spatial resolution (around 5 cm at a flight height of 50 m), have improved the accuracy of pine canopy segmentation, vegetation indices and shaded area classification. It was also determined that the satellite data (Landsat 8) were dominated by soil signals (70%), while the tower data were dominated by canopy signals (95%). With these results, discrepancies in NDVI values were recovered and corrected.

Therefore, once again, the use of drones, with the possibility of obtaining high-resolution images, can solve some of the problems encountered by remote sensing

with satellites. Of course, in order to use these devices, one must perform a series of systemic time flights over the affected area to obtain an adequate time series. In this way, proximal remote sensing could become increasingly important for forest monitoring, both for the acquisition of remote data and for the calibration/correction of coarser data.

2.7 Conclusions

Studies undertaken so far converge in a single direction characterised by warmer and drier conditions leading to forest dieback and mortality phenomena. The combination of dendrochronology with remote sensing data allow analysing these phenomena from individual trees to global scales. However, this approach presents challenges such as: the decoupling of the NDVI–growth relationship or alterations in remote-sensing indices due to mixed pixels and site features. Moreover, considering that the impacts and exposure to climate change are different according to bioclimatic zones and forest types (Lindner et al. 2010, IPCC 2022), the assessment of forest response and vulnerability will also have to be site-specific and interdisciplinary, with greater caution especially in more heterogeneous regions, such as the Mediterranean basin.

Therefore, to refine the NDVI–growth relationship, it would be useful to analyse the relationships between NDVI and physiological processes at the tree/species level during the growing season in addition to using high-resolution images, such as those obtained from drones, improving the accuracy of the remote sensing indices.

Thus, a multi-proxy analysis could be applied to refine this study, following a cascade flow of qualitative and quantitative information at different scales (in the field and remotely) (Figure 1). Reliable and rapid metrics could be combined to examine large forest areas while preserving local-scale information (proximal remote sensing), along with accurate in situ, dendroecological, physiological (regarding the control of carbon stock, to understand the minimum NSC thresholds required for survival) (Hartmann 2015, Hagedorn et al. 2016) and phenological (concerning the relationships between seasonal tree-ring growth trends and NDVI signal) (Vicente-Serrano et al. 2016) analyses. In this way, it would be possible to

overcome the criticalities of each of the methods used to date and obtain a detailed, large-scale view of forest dieback phenomena. As a result, by improving the understanding of the response of different forest types to climate change, it will be possible to analyse their vulnerability more accurately.

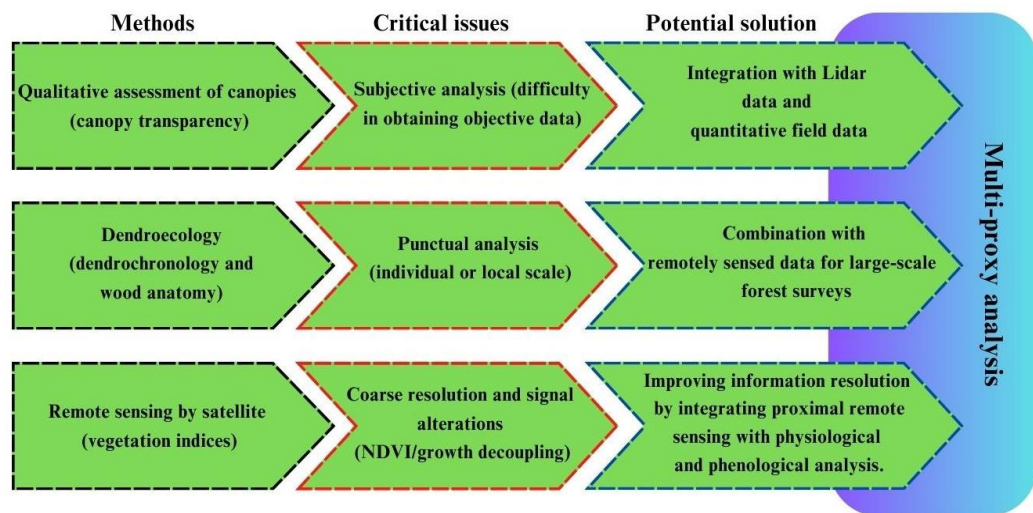


Figure 1. Overview summary.

2.8 References

1. Adams H.D., Zeppel M.J., Anderegg W.R., Hartmann H., Landhäusser S.M., Tissue D.T., McDowell N.G., 2017. *A multi-species synthesis of physiological mechanisms in drought-induced tree mortality*. Nat. Ecol. Evol., 1, 1285–1291. DOI: 10.1038/s41559-017-0248-x
2. Allen C.D., Breshears D.D., McDowell N.G., 2015. *On underestimation of global vulnerability to tree mortality and forest die-off from hotter drought in the Anthropocene*. Ecosphere, 6, 1–55. <https://doi.org/10.1890/ES15-00203.1>
3. Allen C.D., Macalady A.K., Chenchouni H., Bachelet D., McDowell N., Vennetier M., Cobb N., 2010. *A global overview of drought and heat-induced tree mortality reveals emerging climate change risks for forests*. For. Ecol. Manag., 259, 660–684. DOI:10.1016/j.foreco.2009.09.001
4. Badgley G., Field C.B., Berry J.A., 2017. *Canopy near-infrared*

- reflectance and terrestrial photosynthesis*. *Sci. Adv.*, 3, e1602244. DOI: 10.1126/sciadv.1602244
5. Batllori E., Lloret F., Aakala T., Anderegg W.R., Aynekulu E., Bendixsen D.P., Zeeman B., 2020. *Forest and woodland replacement patterns following drought-related mortality*. *Proc. Natl. Acad. Sci. USA*, 117, 29720–29729. <https://doi.org/10.1073/pnas.2002314117>
 6. Beck P.S.A., Andreu-Hayles L., D'Arrigo R., Anchukaitis K.J., Tucker C.J., Pinzón J.E., Goetz S.J., 2013. *A large-scale coherent signal of canopy status in maximum latewood density of tree rings at arctic treeline in North America*. *Glob. Planet. Change.*, 100, 109–118. <http://dx.doi.org/10.1016/j.gloplacha.2012.10.005>
 7. Bochenek Z., Ziolkowski D., Bartold M., Orłowska K., Ochtyra A., 2017. *Monitoring forest biodiversity and the impact of climate on forest environment using high resolution satellite images*. *Eur. J. Remote Sens.*, 51, 166–181. DOI:10.1080/22797254.2017.1414573
 8. Brehaut L., Danbya R.K., 2018. *Inconsistent relationships between annual tree ring-widths and satellite measured NDVI in a mountainous subarctic environment*. *Ecol. Indic.*, 91, 698–711. <https://doi.org/10.1016/j.ecolind.2018.04.052>
 9. Bussotti F., Pollastrini M., Holland V., Brüggemann W., 2015. *Functional traits and adaptive capacity of European forests to climate change*. *Environ. Exp. Bot.*, 111, 91–113. DOI:10.1016/j.envexpbot.2014.11.006
 10. Cailleret M., Jansen S., Robert E.M., Desoto L., Aakala T., Antos J.A., Beikircher B., Bigler C., Bugmann H., Caccianiga M., et al., 2017. *A synthesis of radial growth patterns preceding tree mortality*. *Glob. Change. Biol.*, 23, 1675–1690. DOI: 10.1111/gcb.13535
 11. Camarero J.J., Bigler C., Linares J.C., Linares J.C., Gil-Pelegrín E., 2011. *Synergistic effects of past historical logging and drought on the decline of Pyrenean silver fir forests*. *For. Ecol. Manag.*, 262, 759–769. DOI:10.1016/j.foreco.2011.05.009
 12. Camarero J.J., Colangelo M., Gazol A., Azorín-Molina C., 2021. *Drought and cold spells trigger dieback of temperate oak and beech forests in northern*

- Spain*. *Dendrochronologia*, 66, 125812. DOI:10.1016/j.dendro.2021.125812
13. Camarero J.J., Gazol A., Sangüesa-Barreda G., Oliva J., Vicente-Serrano S.M., 2015. *To die or not to die: Early warnings of tree dieback in response to a severe drought*. *J. Ecol.*, 103, 44–57. DOI:10.1111/1365-2745.12295
 14. Camarero J.J., Sangüesa-Barreda G., Vergarechea M., 2016. *Prior height, growth, and wood anatomy differently predispose to drought-induced dieback in two Mediterranean oak species*. *Ann. For. Sci.*, 73, 341–351. DOI:10.1007/s13595-015-0523-4
 15. Castellaneta M., Rita A., Camarero J.J., Colangelo M., Ripullone F., 2022. *Declines in canopy greenness and tree growth are caused by combined climate extremes during drought-induced dieback*. *Sci. Total Environ.*, 813, 152666. <http://dx.doi.org/10.1016/j.scitotenv.2021.152666>
 16. Chen X., Wang D., Chen J., Wang C., Shen M., 2018. *The mixed pixel effect in land surface phenology: A simulation study*. *Remote Sens. Environ.*, 211, 338–344. <https://doi.org/10.1016/j.rse.2018.04.030>
 17. Christopoulou A., Sazeides C.I., Fyllas N.M., 2022. *Size-mediated effects of climate on tree growth and mortality in Mediterranean Brutia pine forests*. *Sci. Total Environ.*, 812, 151463. <https://doi.org/10.1016/j.scitotenv.2021.151463>
 18. Chrysopolitou V., Apostolakis A., Avtzis D., Avtzis N., Diamandis S., Kemitzoglou D., Dafis S., 2013. *Studies on forest health and vegetation changes in Greece under the effects of climate changes*. *Biodivers. Conserv.*, 22, 1133–1150. DOI:10.1007/s10531-013-0451-2
 19. (a) Colangelo M., Camarero J.J., Battipaglia G., Borghetti M., De Micco V., Gentilesca T., Ripullone F., 2017. *A multi-proxy assessment of dieback causes in a Mediterranean oak species*. *Tree Physiol.*, 37, 617–631. DOI:10.1093/treephys/tpx002
 20. (b) Colangelo M., Camarero J.J., Borghetti M., Gazol A., Gentilesca T., Ripullone F., 2017. *Size Matters a Lot: Drought-Affected Italian Oaks Are Smaller and Show Lower Growth Prior to Tree Death*. *Front. Plant Sci.*, 8, 135. DOI:10.3389/fpls.2017.00135
 21. Colangelo M., Camarero J.J., Gazol A., Piovesan G., Borghetti M., Baliva

- M., Gentilesca T., Rita A., Schettino A., Ripullone F., 2021. *Mediterranean old-growth forests exhibit resistance to climate warming*. *Sci. Total Environ.*, 801, 149684. DOI:10.1016/j.scitotenv.2021.149684
22. Colangelo M., Camarero J.J., Ripullone F., Gazol A., Sánchez-Salguero R., Oliva J., Redondo M.A., 2018. *Drought Decreases Growth and Increases Mortality of Coexisting Native and Introduced Tree Species in a Temperate Floodplain Forest*. *Forests*, 9, 205. DOI:10.3390/f9040205
23. Coluzzi R., Fascetti S., Imbrenda V., Italiano S.S.P., Ripullone F., Lanfredi M., 2020. *Exploring the Use of Sentinel-2 Data to Monitor Heterogeneous Effects of Contextual Drought and Heatwaves on Mediterranean Forests*. *Land*, 9, 325. DOI:10.3390/land9090325
24. Cramer W., Guiot J., Fader M., Garrabou J., Gattuso J.P., Iglesias A., Lange M.A., Lionello P., Llasat M.C., Paz S., 2018. *Climate change and interconnected risks to sustainable development in the Mediterranean*. *Nat. Clim. Change.*, 8, 972–980. DOI: 10.1038/s41558-018-0299-2
25. D’Andrea G., Šimu^o nek V., Castellaneta M., Vacek Z., Vacek S., Pericolo O., Ripullone F., 2022. *Mismatch between annual tree-ring width growth and NDVI index in Norway spruce stands of Central Europe*. *Forests*, 13, 1417. <https://doi.org/10.3390/f13091417>
26. D’Arrigo R.D., Malmstrom C.M., Jacoby G.C., Los S.O., Bunker D.E., 2000. *Correlation between maximum latewood density of annual tree rings and NDVI based estimates of forest productivity*. *Int. J. Remote Sens.*, 21, 2329–2336. DOI:10.1080/01431160050029611
27. DeSoto L., Cailleret M., Sterck F., Jansen S., Kramer K., Robert E.M.R., Aakala T., Amoroso M.M., Bigler C., Camarero J.J., et al., 2020. *Low growth resilience to drought is related to future mortality risk in trees*. *Nat. Commun.*, 11, 545. DOI:10.1038/s41467-020-14300-5
28. Dobbertin M., 2005. *Tree growth as indicator of tree vitality and of tree reaction to environmental stress: A review*. *Eur. J. Forest Res.*, 124, 319–333. <https://doi.org/10.1007/s10342-005-0085-3>
29. Fonti P., Arx G., García-González I., Eilmann B., Sass-Klaassen U., Gärtner H., Eckstein D., 2010. *Studying global change through investigation of*

- the plastic responses of xylem anatomy in tree rings*. *New Phytol.*, 185, 42–53. DOI: 10.1111/j.1469-8137.2009.03030.x
30. Gazol A., Camarero J.J., Gutiérrez E., Popa I., Andreu-Hayles L., Motta R., Nola P., Ribas M., Sangüesa-Barreda G., Urbinati C., et al., 2015. *Distinct effects of climate warming on populations of silver fir (Abies alba) across Europe*. *J. Biogeogr.*, 42, 1150–1162. DOI:10.1111/jbi.12512
31. Gazol A., Camarero J.J., Vicente-Serrano S.M., Sánchez-Salguero R., Gutiérrez E., de Luis M., Galván J.D., 2018. *Forest resilience to drought varies across biomes*. *Glob. Change. Biol.*, 24, 2143–2158. DOI: 10.1111/gcb.14082
32. Gentilesca T., Camarero J.J., Colangelo M., Nolè A., Ripullone F., 2017. *Drought induced oak decline in the western Mediterranean region: An overview on current evidences, mechanisms and management options to improve forest resilience*. *iForest*, 10, 796–806. DOI: 10.3832/ifor2317-010
33. Gilabert M.A., González-Piqueras J., García-Haro F.J., Meliá J., 2002. *A generalized soil-adjusted vegetation index*. *Remote Sens. Environ.*, 82, 303–310. [https://doi.org/10.1016/S0034-4257\(02\)00048-2](https://doi.org/10.1016/S0034-4257(02)00048-2)
34. Gitelson A.A., 2004. *Wide dynamic range vegetation index for remote quantification of biophysical characteristics of vegetation*. *J. Plant Physiol.*, 161, 165–173. <https://doi.org/10.1078/0176-1617-01176>
35. Glenn E.P., Huete A.R., Nagler P.L., Nelson S.G., 2008. *Relationship Between Remotely-sensed Vegetation Indices, Canopy Attributes and Plant Physiological Processes: What Vegetation Indices Can and Cannot Tell Us About the Landscape*. *Sensors*, 8, 2136–2160. DOI: 10.3390/s8042136
36. González de Andrés E., Gazol A., Querejeta J.I., Igual J.M., Colangelo M., Sánchez-Salguero R., Linares J.C., Camarero J.J., 2022. *The role of nutritional impairment in carbon-water balance of silver fir drought-induced dieback*. *Glob. Change. Biol.*, 28, 4439–4458. DOI:10.1111/gcb.16170
37. Guerschman J.P., Hill M.J., Renzullo L.J., Barrett D.J., Marks A.S., Botha E.J., 2009. *Estimating fractional cover of photosynthetic vegetation, non-photosynthetic vegetation and bare soil in the Australian tropical savanna region upscaling the EO-1 Hyperion and MODIS sensors*. *Remote Sens. Environ.*, 113, 928–945. DOI:10.1016/j.rse.2009.01.006

38. Hagedorn F., Joseph J., Peter M., Luster J., Pritsch K., Geppert U., Arend M., 2016. *Recovery of trees from drought depends on belowground sink control*. *Nat. Plants*, 2, 16111. DOI: 10.1038/NPLANTS.2016.111
39. Hartmann H., 2015. *Carbon starvation during drought-induced tree mortality—are we chasing a myth?* *J. Plant Hydraul.*, 2, e005. DOI:10.20870/jph.2015.e005
40. Huete A., Didan K., Miura T., Rodriguez E.P., Gao X., Ferreira L.G., 2002. *Overview of the radiometric and biophysical performance of the MODIS vegetation indices*. *Remote Sens. Environ.*, 83, 195–213. [https://doi.org/10.1016/S0034-4257\(02\)00096-2](https://doi.org/10.1016/S0034-4257(02)00096-2)
41. Huete A.R., 1988. *A soil-adjusted vegetation index (SAVI)*. *Remote Sens. Environ.*, 25, 295–309. [https://doi.org/10.1016/0034-4257\(88\)90106-X](https://doi.org/10.1016/0034-4257(88)90106-X)
42. IPCC. *Summary for Policymakers. In Climate Change 2007: The Physical Science Basis. Contribution of Working Group I to the Fourth Assessment Report of the Intergovernmental Panel on Climate Change*; Solomon S., Qin D., Manning M., Chen Z., Marquis M., Averyt K.B., Tignor M., Miller H.L., Eds.; Cambridge University Press: Cambridge, UK; New York, NY, USA, 2007.
43. IPCC. *Summary for Policymakers. In Climate Change 2022: Mitigation of Climate Change. Contribution of Working Group III to the Sixth Assessment Report of the Intergovernmental Panel on Climate Change*; Shukla P.R., Skea J., Slade R., Al Khourdajie A., van Diemen R., McCollum D., Pathak M., Some S., Vyas P., Fradera R. Eds.; Cambridge University Press: Cambridge, UK; New York, NY, USA, 2022.
44. IPCC. *Summary for Policymakers. In Climate Change and Land: An IPCC Special Report on Climate Change, Desertification, Land Degradation, Sustainable Land Management, Food Security, and Greenhouse Gas Fluxes in Terrestrial Ecosystems*; Shukla P.R., Skea J., Calvo Buendia E., Masson-Delmotte V., Pörtner H.O., Roberts D.C., Zhai P., Slade R., Connors S., Van Diemen R., et al., Eds.; Intergovernmental Panel on Climate Change: Geneva, Switzerland, 2019; ISBN 978-92-9169-154-8.
45. Jones M.W., Abatzoglou J.T., Veraverbeke S., Andela N., Lasslop G., Forkel M., Smith A.J.P., Burton C., Betts R.A., van der Werf G.R., et al., 2022.

- Global and regional trends and drivers of fire under climate change*. Rev. Geophys., 60, e2020RG000726. <https://doi.org/10.1029/2020RG000726>
46. Kastridis A., Kamperidou V., Stathis D., 2022. *Dendroclimatological Analysis of Fir (A. borisii-regis) in Greece in the frame of Climate Change Investigation*. Forests, 13, 879. <https://doi.org/10.3390/f13060879>
47. Lapenis A.G., Lawrence G.B., Heim A., Zheng C., Shortle W., 2013. *Climate warming shifts carbon allocation from stemwood to roots in calcium-depleted spruce forests*. Glob. Biogeochem. Cycles, 27, 101–107. DOI:10.1029/2011GB004268
48. Levanič T., Čater M., McDowell N.G., 2011. *Associations between growth, wood anatomy, carbon isotope discrimination and mortality in a Quercus robur forest*. Tree Physiol., 31, 298–308. DOI:10.1093/treephys/tpq111
49. Lindner M., Maroschek M., Netherer S., Kremer A., Barbati A., Garcia-Gonzalo J., Seidl R., Delzon S., Corona P., Kolström M. et al., 2010. *Climate change impacts, adaptive capacity, and vulnerability of European forest ecosystems*. For. Ecol. Manag., 259, 698–709. DOI:10.1016/j.foreco.2009.09.023
50. Liu W., Yamazaki F., 2012. *Object-Based Shadow Extraction and Correction of High-Resolution Optical Satellite Images*. IEEE J. Sel. Top. Appl. Earth Obs. Remote Sens., 5, 1296–1302. DOI: 10.1109/JSTARS.2012.2189558
51. Lloret F., Escudero, A., Iriondo O.M., Martínez-Vilalta J., Valladares F., 2012. *Extreme climatic events and vegetation: The role of stabilizing processes*. Glob. Change. Biol., 18, 797–805. DOI: 10.1111/j.1365-2486.2011.02624.x
52. Lloret F., Keeling E.G., Sala A., 2011. *Components of tree resilience: Effects of successive low-growth episodes in old ponderosa pine forests*. Oikos, 120, 1909–1920. DOI: 10.1111/j.1600-0706.2011.19372.x
53. Lloret F., Lobo A., Estevan H., Maisongrande P., Vayreda J., Terradas J., 2007. *Woody plant richness and NDVI response to drought events in Catalanian (Northeastern Spain) forests*. Ecology, 88, 2270–2279. doi:10.1890/06-1195.1
54. Manion P.D., 1992. *Forest Decline Concepts*; American Phytopathological Society: Saint Paul, MN, USA, ISBN 10 0890541434.
55. Mannerucci F., Sicoli G., Luisi N., 2006. *Oak decline in Apulia, southern*

Italy: An ecological indicator of landscape evolution? In Patterns and Processes in Forest Landscapes. Consequences of Human Management; Laforteza, R., Sanesi, G., Eds.; Locorotondo: Bari, Italy.

56. Martínez-Vilalta J., Sala A., Asensio D., Galiano L., Hoch G., Palacio S., Lloret F., 2016. *Dynamics of non-structural carbohydrates in terrestrial plants: A global synthesis.* Ecol. Monogr., 86, 495–516. <https://doi.org/10.1002/ecm.1231>

57. McDowell N., Pockman W.T., Allen C.D., Breshears D.D., Cobb N., Kolb T., Yezpe E.A., 2008. *Mechanisms of plant survival and mortality during drought: Why do some plants survive while others succumb to drought?* New Phytol., 178, 719–739. DOI: 10.1111/j.1469-8137.2008.02436.x

58. McDowell N.G., 2011. *Mechanisms linking drought, hydraulics, carbon metabolism, and vegetation mortality.* Plant Physiol., 155, 1051–1059. <https://doi.org/10.1104/pp.110.170704>

59. Meng P., Wang H., Qin S., Li X., Song Z., Wang Y., Yang Y., Gao J., 2022. *Health assessment of plantations based on LiDAR canopy spatial structure parameters.* Int. J. Digit. Earth, 15, 712–729. DOI:10.1080/17538947.2022.2059114

60. Michelot A., Simard S., Rathgeber C., Dufrêne E., Damesin C., 2012. *Comparing the intra-annual wood formation of three European species (Fagus sylvatica, Quercus petraea and Pinus sylvestris) as related to leaf phenology and non-structural carbohydrate dynamics.* Tree Physiol., 32, 1033–1043. doi:10.1093/treephys/tps052

61. Moreno-Fernández D., Camarero J.J., García M., Lines E.R., Sánchez-Dávila J., Tijerín J., Ruiz-Benito P., 2022. *The Interplay of the Tree and Stand-Level Processes Mediate Drought-Induced Forest Dieback: Evidence from Complementary Remote Sensing and Tree-Ring Approaches.* Ecosystems, 25, 1738–1753. <https://doi.org/10.1007/s10021-022-00793-2>

62. Nagler P.L., Inoueb Y., Glenn E.P., Russc A.L., Daughtry C.S.T., 2003. *Cellulose absorption index (CAI) to quantify mixed soil–plant litter scenes.* Remote Sens. Environ., 87, 310–325. DOI:10.1016/j.rse.2003.06.001

63. Navarro-Cerrillo R.M., Rodríguez-Vallejo C., Silveiro E., Hortal A.,

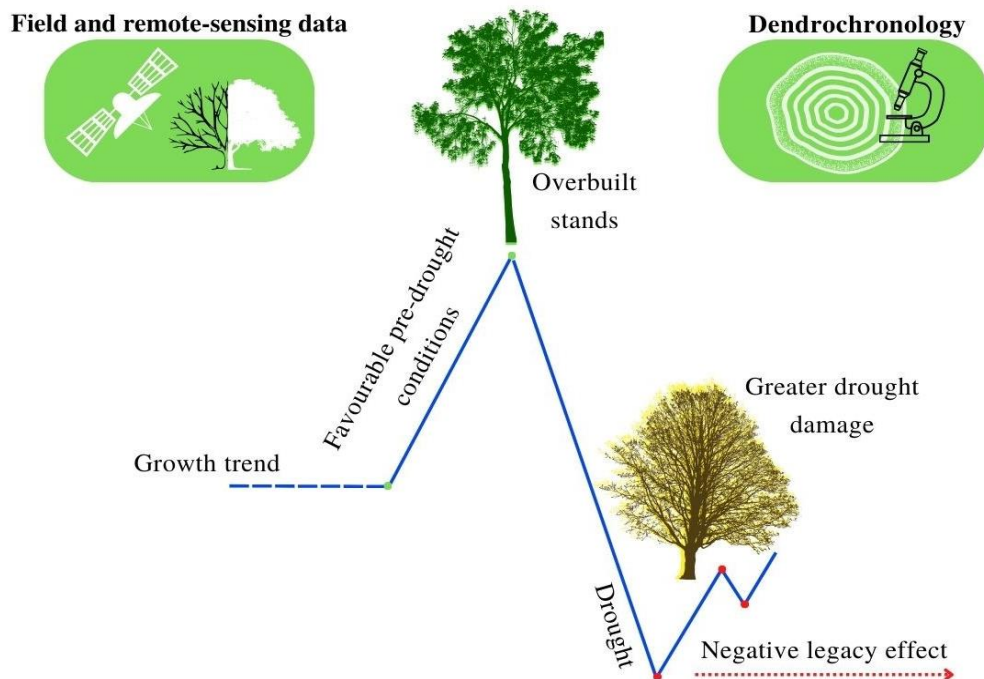
- Palacios-Rodríguez G., Duque-Lazo J., Camarero J.J., 2018. *Cumulative Drought Stress Leads to a Loss of Growth Resilience and Explains Higher Mortality in Planted than in Naturally Regenerated Pinus pinaster Stands*. *Forests*, 9, 358. DOI:10.3390/f9060358
64. Ogaya R., Barbeta A., Basnou C., Peñuelas J., 2015. *Satellite data as indicators of tree biomass growth and forest dieback in a Mediterranean holm oak forest*. *Ann. For. Sci.*, 72, 135–144. DOI:10.1007/s13595-014-0408-y
65. Patterson D.T., Westbrook J.K., Joyce R.J.V., Lingren P.D., Rogasik J., 1999. *Weeds, insects, and diseases*. *Clim. Change.*, 43,711–727. <https://doi.org/10.1023/A:1005549400875>
66. Pericolo O., Camarero J.J., Colangelo M., Valeriano C., Sánchez-Salguero R., Borghetti M., Castellaneta M., Nola P., Ripullone F., 2023. *Species specific vulnerability to increased drought in temperate and Mediterranean floodplain forests*. *Agric. For. Meteorol.*, 328, 109238. <https://doi.org/10.1016/j.agrformet.2022.109238>
67. Pretzsch H., Schütze G., Uhl E., 2013. *Resistance of European tree species to drought stress in mixed versus pure forests: Evidence of stress release by inter-specific facilitation*. *Plant Biol.*, 15, 483–495. DOI:10.1111/j.1438-8677.2012.00670.x
68. Qi J., Chehbouni A., Huete A.R., Kerr Y.H., Sorooshian S., 1994. *A modified soil adjusted vegetation index*. *Remote Sens. Environ.*, 48, 119–126. [https://doi.org/10.1016/0034-4257\(94\)90134-1](https://doi.org/10.1016/0034-4257(94)90134-1)
69. Ripullone F., Camarero J.J., Colangelo M., Voltas J., 2020. *Variation in the access to deep soil water pools explains tree-to-tree differences in drought-triggered dieback of Mediterranean oaks*. *Tree Physiol.*, 40, 591–604. DOI:10.1093/treephys/tpaa026
70. Rita A., Camarero J.J., Nolè A., Borghetti M., Brunetti M., Pergola N., Serio C., Vicente-Serrano S.M., Tramutoli V., Ripullone F., 2020. *The impact of drought spells on forests depends on site conditions: The case of 2017 summer heat wave in southern Europe*. *Glob. Change. Biol.*, 26, 851–863. DOI: 10.1111/gcb.14825
71. Rondeaux G., Steven M., Baret F., 1996. *Optimization of soil-adjusted*

- vegetation indices. *Remote Sens. Environ.*, 55, 95–107.
[https://doi.org/10.1016/0034-4257\(95\)00186-7](https://doi.org/10.1016/0034-4257(95)00186-7)
72. Rouse J., Haas R., Schell J., Deering D., 1973. *Monitoring Vegetation Systems in the Great Plains with ERTS. Third ERTS Symp.* NASA, 1, 309–317.
73. Schwarz J., Skiadaresis G., Kohler M., Kunz J., Schnabel F., Vitali V., Bauhus J., 2020. *Quantifying Growth Responses of Trees to Drought—a Critique of Commonly Used Resilience Indices and Recommendations for Future Studies.* *Curr. For. Rep.*, 6, 185–200. DOI:10.1007/s40725-020-00119-2
74. Schweingruber F.H., 1988. *Tree Rings: Basics and Applications of Dendrochronology*; Kluwer Academic Publishers: Dordrecht, The Netherlands. DOI: 10.1007/978-94-009-1273-1
75. Solberg S., Næsset E., Hanssen K.H., Christiansen E., 2006. *Mapping defoliation during a severe insect attack on Scots pine using airborne laser scanning.* *Remote Sens. Environ.*, 102, 364–376. DOI:10.1016/j.rse.2006.03.001
76. Tang L., Shao G., 2015. *Drone remote sensing for forestry research and practices.* *J. For. Res.*, 26, 791–797. DOI: 10.1007/s11676-015-0088-y
77. Thomas F.M., Blank R., Hartman G., 2002. *Abiotic and biotic factors and their interactions as causes of oak decline in Central Europe.* *For. Pathol.*, 32, 277–307. DOI:10.1046/j.1439-0329.2002.00291.x
78. Trugman A.T., Detto M., Bartlett M.K., Medvigy D., Anderegg W.R.L., Schwalm C., Schaffer B., Pacala S.W., 2018. *Tree carbon allocation explains forest drought-kill and recovery patterns.* *Ecol. Lett.*, 21, 1552–1560. DOI: 10.1111/ele.13136
79. Vicente-Serrano S.M., Camarero J.J., Olanob J.M., Martín-Hernández N., Peña-Gallardo M., Tomás-Burguera M., Gazol A., Azorin-Molina C., Bhuyan U., El Kenawy A., 2016. *Diverse relationships between forest growth and the Normalized Difference Vegetation Index at a global scale.* *Remote Sens. Environ.*, 187, 14–29. <https://doi.org/10.1016/j.rse.2016.10.001>
80. Vicente-Serrano S.M., Gouveiab C., Camarero J.J., Begueríae S., Trigo R., López-Morenoa J.I., Azorín-Molina C., Pashoa E., Lorenzo-Lacruza J., Revueltoa J. et al., 2013. *Response of vegetation to drought time-scales across*

- global land biomes*. Proc. Natl. Acad. Sci. USA, 110, 52–57.
<https://doi.org/10.1073/pnas.1207068110>
81. Vicente-Serrano S.M., Martin-Hernandez N., Camarero J.J., Gazol A., Sanchez-Salguero R., Pena-Gallardo M., El Kenawy A., Domínguez-Castro F., Tomas-Burguera M., Gutiérrez E., et al., 2020. *Linking tree-ring growth and satellite-derived gross primary growth in multiple forest biomes. Temporal-scale matters*. Ecol. Indic., 108, 105753.
<https://doi.org/10.1016/j.ecolind.2019.105753>
82. Vivar-Vivar E.D., Pompa-García M., Martínez-Rivas J.A., Mora-Tembre L.A., 2022. *UAV-Based Characterization of Tree-Attributes and Multispectral Indices in an Uneven-Aged Mixed Conifer-Broadleaf Forest*. Remote Sens., 14, 2775. <https://doi.org/10.3390/rs14122775>
83. Wang H., Muller J.D., Tatarinov F., Yakir D., Rotenberg E., 2022. *Disentangling Soil, Shade, and Tree Canopy Contributions to Mixed Satellite Vegetation Indices in a Sparse Dry Forest*. Remote Sens., 14, 3681.
<https://doi.org/10.3390/rs14153681>
84. Wang Z., Lyu L., Liu L., Liang H., Huang J., Zhang Q.B., 2021. *Topographic patterns of forest decline as detected from tree rings and NDVI*. Catena, 198, 105011. <https://doi.org/10.1016/j.catena.2020.105011>
85. Xu P., Zhou T., Yi C., Fang W., Hendrey G., Zhao X., 2018. *Forest drought resistance distinguished by canopy height*. Environ. Res. Lett., 13, 075003. DOI:10.1088/1748-9326/aacadd

Submitted: 13 October 2023

3. DROUGHT LEGACIES IN MIXED MEDITERRANEAN FORESTS: EFFECTS OF OVERSHOOT DROUGHTS, SPECIES CHARACTERISTICS AND SITE CONDITIONS



Graphical Abstract

3.1 Abstract

Previous favourable climate conditions may stimulate growth making forests more vulnerable to hotter droughts. The so-called structural overshoot contributes to forest dieback and growth decline, but evidences are still scarcely understood because of the limited integrated, retrospective field data. Here, we used tree-ring width data to assess the recovery, resilience and legacy effects of the 2017 summer drought which affected several Mediterranean tree species in southern Italy (*Fraxinus ornus*, *Quercus pubescens*, *Acer monspessulanum*, *Pinus pinaster*).

Legacy effects were assessed by calculating differences between observed and predicted basal area increment (BAI). We also used remote sensing data (NDVI) to characterize the drought impacts on canopy cover. Overall the growth response of forest stands to the 2017 drought was contingent on site conditions and species characteristics. Most sites presented a BAI reduction during the drought, but the growth responses to drought were contingent on site conditions and species characteristics. Growth decline was followed by a quick recovery and positive legacy effects, particularly in the case of *F. ornus*. However, we found negative drought legacies lasting in some species (e.g., *Q. pubescens*, *A. monspessulanum*) and sites. In those sites showing negative legacies, high growth rates prior to drought in response to previous wet winter-spring conditions may have predisposed trees to drought damage and subsequent negative legacies. Vice versa, the positive drought legacy found on *F. ornus* in some study site was probably due to post-drought release in competition due to widespread oak decline and mortality. Therefore, we found evidences of structural overshoot in some study sites. These findings highlight that historical effects (i.e. pre-drought conditions) should be explicitly considered when studying drought impacts on forests and mismatches between available and required soil water in overbuilt stands.

Keywords: *Acer monspessulanum*, dendroecology, drought overshoot, *Fraxinus ornus*, legacy effects, resilience.

3.2 Introduction

Warmer conditions are increasing evaporative demand and reducing soil moisture availability, causing hotter droughts which trigger forest dieback episodes worldwide (Allen et al. 2015, Choat et al. 2018). Therefore, it is critical to determine how vulnerable trees are to such droughts and how they will recover because a low resiliency capacity could threaten many tree populations if the frequency and severity of such dry spells increase (Schwalm et al. 2017). Post-drought recovery informs on stress impacts and growth resilience (Lloret et al. 2011, Guada et al. 2016, Ingrisich and Bahn 2018). For instance, partial recovery can lead to drought legacy or carryover effects often characterized by incomplete retrieval of prior

growth rates (Anderegg et al. 2015, Kannenberg et al. 2020). Previous growth conditions can also influence drought legacies (Peltier and Ogle 2019) and thus growth recovery after drought (Fritts 1976, Ogle et al. 2015, Camarero et al. 2018, Pretzsch 2021). For example, recurrent mild drought stress may improve drought resistance through physiological adjustments or metabolic changes (Backhaus et al. 2014). Thus, environmental events (dry and wet years) over time drive growth responses to drought (Serra-Maluquer et al. 2021). In sum, both pre- and post-drought climatic conditions can modify forest recovery after water shortage and warm conditions (Sergent et al. 2014).

Wet, post-drought conditions can compensate growth losses due to prior dry conditions (Jiang et al. 2019), while favorable conditions that stimulate growth before a drought event could also predispose to dieback. In this regard, structural overshoot, i.e. the development of high shoot-to-root ratios of woody vegetation in response to favorable weather conditions, could predispose to drought damage and amplify dieback risk (Jump et al. 2017). Such temporal mismatches between water availability and requirement could make some stands overbuilt and predispose them to subsequent stressful, dry conditions. However, there is still a lack of information on the dynamics of recovery in different tree species, considering pre- and post-drought conditions.

Considering also that species mixing and thus biodiversity can moderate the impact of disturbances (Lloret et al. 2007, Pretzsch et al. 2013, Bochenek et al. 2018), mixed forests, as in this study case, with combinations of oak, pine, ash and maple trees, may respond differently to drought than pure stands (Camarero et al. 2021) by adopting different strategies. For example, *Quercus pubescens* Willd. is a species that adopts a water-wasting (anisohydric) strategy (Damesin and Rambal 1995, Poyatos et al. 2008); thus, severe droughts may expose this species more to hydraulic collapse. However, *Fraxinus ornus* L. seems to have a relatively isohydric strategy with rapid post-drought recovery making it more tolerant to severe droughts (Tomasella et al. 2019). Other studies have showed that oaks present a more rapid post-drought recovery and shorter legacies as compared with pines (Anderegg et al. 2015); as is well known, Mediterranean pines (such as *Pinus pinaster*) have a strong regulation of leaf water potential regardless of

environmental conditions and close their stomata during drought (Valeriano et al. 2021). This rapid recovery is probably due to the ability of oaks to compensate for the loss of hydraulic conductivity by forming new rings with wide vessels (Cavender-Bares and Holbrook 2001). The other species we studied here, *Acer monspessulanum* L. is considered drought-tolerant and resistant to xylem cavitation (Tissier et al. 2004), with growth performances similar to oaks in seasonally dry sites (Portoghesi et al. 2008).

Regrettably, there is still very little knowledge on the responses to drought of rare hardwood Mediterranean species, such as *F. ornus* and *A. monspessulanum*, despite their ecological and economic relevance. For example, in some rural areas *F. ornus* is used as source of firewood and it is still cultivated for the production of “manna”, the crystallised sap used for pharmaceutical and food industry, well appreciated by grazing animals (Caudullo and Rigo 2016). Further the ability to resprout after cutting makes this ash species also well adapted to grow in areas disturbed by animal browsing, wildfires, landslides and logging. The maple *A. monspessulanum* forms hard and compact wood which is used for tools construction (Pignatti 1982). Further, this species shows a high resistance to drought and it is often considered a suitable species for future climatic change scenarios (Kowarik 2023). In fact, according to some studies, its role as a species capable of reconstituting degraded stands in seasonally dry regions should be considered (Portoghesi et al. 2008).

There is also little information on how site conditions can influence recovery in relation to factors such as soil depth and water retention capacity, slope, stand structure, etc. (Bréda et al. 2006, Ruehr et al. 2019). Indeed, different recovery paces among coexisting tree species or in sites with different quality are components of ecological memory which can affect post-disturbance forest resilience (Johnstone et al. 2016). Disturbances generate biological legacies that interact with soil properties such as water and nutrient availability (Gonzalez de Andres et al. 2022). Recently, others illustrated how site-specific conditions mediate species responses to drought in southern Europe (Rita et al. 2020).

In this study we analyzed the recovery trajectories after the severe 2017 summer drought which strongly affected Mediterranean forests in southern Italy (Italiano et al. 2023). We investigated six sites characterized by different tree species (the

hardwood *F. ornus*, *Q. pubescens* and *A. monspessulanum*, the softwood *Pinus pinaster*) and differences in slope, aspect, elevation, soil/substrate, but all impacted by the 2017 drought (Coluzzi et al. 2020). The general aim of this study design was to identify differences in drought response in species coexisting in mixed Mediterranean forests. Achieving this aim is relevant to forecast which species will better tolerate forecasted aridification and have better chance of establish or replace species with a low drought tolerance (Batllori et al. 2020). Our specific aims were: (i) to reconstruct radial growth rates (i.e. to obtain the dendrochronological series of each species studied and estimate their growth increments), (ii) to assess radial growth responses to climate variables (temperature, precipitation) and drought severity, (iii) to quantify post-drought growth recovery and legacies. We hypothesize that trees showed high growth rates prior to that drought, in response to previous favorable winter-spring wet conditions, may have experienced a structural overshoot. In other words, such conditions may have predisposed stands to drought damage and the resulting negative legacies.

3.3 Materials and methods

3.3.1 Study sites

We selected six sites located in the Basilicata region (southern Italy, longitude 15.46–16.15° E, latitude 40.52–40.62° N) which presented damage after the 2017 severe summer drought (Fig. 1, Table 1). These sites were identified because they showed visual symptoms of decay following this drought phenomenon and thus were considered suitable for studying the response of forest stands to climatic disturbances. Damage symptoms included premature leaf browning and shedding, canopy and shoot dieback and elevated tree mortality (see Italiano et al. 2023). Sites showed different elevations (530–790 m a.s.l.), slopes (15–50%), aspects (mainly N-NW but also S-SE in site Castellmezzano) and substrate or soil types (mainly sandstone but also limestone in Vietri di Potenza site and clay in Orto Siderio site). Climate conditions in each study site were characterized using short-term records (period 2006–2020) from nearby meteorological stations (see Table S1 and Table 1). In the study area, warmest and driest conditions occur in July and August and

coldest conditions in January and February, whilst March and November are the wettest months.

The Palazzo site (hereafter AP), located in the Accettura municipality, is characterized by an average annual rainfall of 734 mm and mean annual temperature is 16 °C. The forest consists of *Q. pubescens* mixed with *F. ornus* managed as coppice. The Grotta dell'Angelo site (hereafter GA), located in the Savoia di Lucania municipality, vegetation consists of thermophilic broad-leaved trees (*F. ornus*, *Carpinus orientalis* Mill, *Quercus ilex* L.) and conifer plantations (*Pinus pinaster* Ait.). The average annual rainfall is 889 mm and the mean annual temperature is 13.0 °C. The Orto Siderio site (hereafter OS) also located in the Savoia di Lucania municipality, is dominated by *Q. pubescens*, *F. ornus*, *Carpinus orientalis*, *Quercus cerris* L. and *Ostrya carpinifolia* Scop. and the climatic conditions are similar to those in site GA site. Moreover, at the site (OS), oak dieback was very evident in several patches. The Vietri di Potenza site (hereafter VP) located in the Vietri di Potenza municipality is dominated by *Q. pubescens* and other broadleaves (*A. monspessulanum*, *C. orientalis*, *Crataegus monogyna* Jacq.). The average annual rainfall is 943 mm and the average annual temperature is 14.5 °C. The Pietrapertosa site (hereafter PI) located in the Pietrapertosa municipality is dominated by oak, ash, *O. carpinifolia*, *C. orientalis* and *Pistacia terebinthus* L. The average annual rainfall is 671 mm and the average annual temperature is 12.7 °C. Lastly, the Castelmezzano site (hereafter CA) located in the Castelmezzano municipality consists of *Q. pubescens*, *F. ornus*, *A. monspessulanum*, *Cornus mas* L. and *P. terebinthus*. Climate conditions are as in site PI.

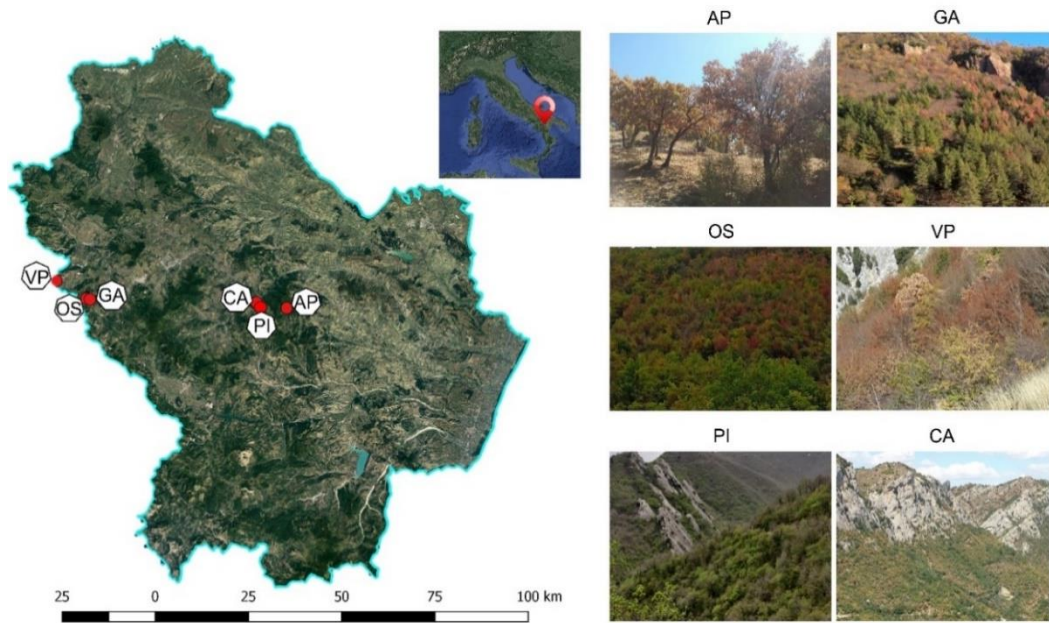


Figure 1. Map showing the location of the six study sites in the Basilicata region (southern Italy) and images showing impacts of the 2017 summer drought (brown crowns, leaf shedding) in the six study sites (see sites' codes in Table 1).

3.3.2 Climate data, soil moisture and drought index

Long-term monthly or seasonal climate data (mean temperature, total precipitation) were obtained for the period 1950–2021 (Figs. S1 and S2). They corresponded to the 0.1°-gridded E-OBS ver. 22.0 climate dataset, which has been subjected to quality and homogeneity tests (Cornes et al. 2018). We selected this dataset because it provides long-term regional climate records, allowing us to perform climate-growth correlations analysis with respect to the time span (50-60 years), whereas local climate stations records are short and each station has heterogeneous time series (10 to 20 years).

Changes in drought severity were evaluated by using the Standardized Precipitation Evapotranspiration Index (SPEI) which was downloaded from the Global Drought Monitor webpage at 0.5° resolution (<http://spei.csic.es/index.html>). The SPEI is a multiscalar drought index that considers effects of temperature and evapotranspiration on water availability with negative and positive values corresponding to dry and wet conditions, respectively (Vicente-Serrano et al. 2010).

We obtained 3-, 6- and 12-month long SPEI values to assess drought severity at different temporal resolutions (Fig. S3).

In order to get an idea of the phenomena that affected the study area before 2017, we also took into account two previous droughts which affected the forests of the study region (Basilicata, southern Italy) in 2003 and 2012 (Gentilesca et al. 2017, Colangelo et al. 2017, 2018). Looking at the SPEI variability, it is possible to appreciate the three drought periods considered (2003, 2012 and 2017) and the greater severity of the last drought event is evident (Fig. S3).

Gridded (0.1° resolution), monthly soil moisture data at 0-10 cm depth were also obtained for the period 1992–2018 based on land surface model simulations with observations-based forcing (precipitation data) (Rodell et al. 2004). To better characterize the drought under study (2017), we also obtained daily data (period 2012–2020) of relative humidity from meteorological stations located near the study sites (Table S1, Fig. S4).

3.3.3 Tree-ring width data and field sampling

At each site, an area of 5000 m² (circular in shape) was identified, representative of the entire stand in which we randomly sampled at least 15 dominant trees for each of the two most abundant species, thus 30 trees per site, for a total of 180 trees were analyzed. For each plant, the diameter of the breast height (dbh) was measured at 1.3 m, and the percentage of living or dead trees and the percentage of defoliation (crown transparency > 50% or < 50%) was also assessed for each site (Dobbertin 2005, Camarero et al. 2016) (Table 2).

Sampling was carried out by randomly selecting the dominant trees to avoid the effects of competition on the growth rings, as they are less affected by competition for light, nutrients and water than submissive trees. The selected stands were all heavily affected by the 2017 summer drought. We took the wood cores from each tree from the bark to the pith at 1.3 m using a Pressler increment borer. Cores were air-dried, and their surfaces were cut using a sledge core microtome to clearly distinguish ring boundaries (Gärtner and Nievergelt 2010). All cores were successfully cross-dated. Tree rings were visually cross-dated under the binocular microscope by assigning characteristic rings (i.e. rings whose growth was strongly

influenced by environmental events over time) (Fritts 1976). The tree-ring widths (TRW) were measured to the nearest 0.01 mm using the LINTAB package (Rinntech, Heidelberg, Germany). The COFECHA program (Holmes 1983) was used to evaluate the visual cross-dating of the tree-ring series by calculating moving correlations between individual series and the mean series of each species in each site (see Table 3).

To assess the growth trend over time of the analyzed forest stands, we calculated the basal area increment (BAI) assuming a circular shape of stems. This index is used for forestry growth modelling studies, as it provides an accurate quantification of the wood production determined by the diametric increment of a growing tree. The individual TRW series were transformed BAI series because it is a two-dimensional measure of stem increment in area, which is known to reduce the geometric effect associated with increasing tree dbh and better reflects the growth of the entire tree than the one-dimensional width of the ring:

$$\text{BAI} = \pi (R^2_t - R^2_{t-1}) \quad (1)$$

where R^2_t and R^2_{t-1} are the radii corresponding to the current (t) and prior (t-1) years, respectively.

To remove the BAI trends, the individual BAI series were detrended by fitting cubic smooth splines with a length of 67% of the series using the ARSTAN software ver. 49 (Cook et al. 2017). Afterwards, an autoregressive model was applied to each detrended series to remove the first-order autocorrelation. This allowed obtaining residual or pre-whitened series of BAI. Mean BAI series were obtained by using bi-weight robust averages of detrended individual BAI series within each site and species (obtaining, $n = 12$ mean series). These mean series were used in further analyses considering the common, best-replicated 1980–2020 period. We used detrended BAI data for climate-growth relationships. Further, by detrending analysis we removed the growth pattern to highlight drought in the analysis. Legacy effects have been assessed by subtracting observed BAI from the predicted BAI (Fig. 5), as they are carryover impacts of the drought, calculated by removing the effects of post-drought climate conditions (Anderegg et al. 2015). In addition, the

diameter annual increment was retrospectively calculated for each tree from ring-width measurements assuming non-eccentricity of tree stem.

3.3.4 Characterizing impacts of the drought using remote sensing data

Here we used the Normalized Different Vegetation Index (NDVI) only to further characterize each site and further highlight the impact of the 2017 drought on canopy cover (Tucker and Sellers 1986), as this index allows us to detect the loss of canopy and green cover (Coluzzi et al. 2020).

The NDVI index was obtained using Sentinel-2 products (MSI: MultiSpectral Instrument, Level-1C), already effectively used to monitor the effects of drought on the studied stands at a resolution of 10 m x 10 m (Coluzzi et al. 2020).

The NDVI values were obtained from Google Earth Engine (https://developers.google.com/earth-engine/datasets/catalog/COPERNICUS_S2). The NDVI data were checked to exclude outliers (due to cloudiness). For each of the 6 analyzed stands, a polygon of 5000 m² was located in the middle of each stand to obtain mean monthly NDVI values during the growing season (April-September) and from 2016 to 2018. Finally, we calculated the ratios between the NDVI values measured in 2017 and 2016 ($NDVI_{2017} / NDVI_{2016}$) and between those measured in 2018 and 2017 ($NDVI_{2018} / NDVI_{2017}$) (see Table 1).

3.3.5 Correlations between growth, climate variables, soil moisture and drought

To evaluate growth responses to climate variability and drought severity we calculated Pearson correlation coefficients between detrended mean BAI series, monthly climate data (mean temperature and precipitation) and the SPEI (using 3-, 6- and 12-month temporal scales). Correlations were calculated from previous October to current September to account for lagged effects of prior climate conditions on tree growth. In the case of soil moisture, correlations were calculated for the same temporal window but considering the period 1992–2018. We considered the 0.05 and 0.01 significance levels in these analyses. Certainly, the climate and humidity data (0.1° degrees approx. 10 km) and SPEI (0.5° approx. 55.5 km) have coarse resolutions. However, for the selected sites there are no other

long-term climate data available that can provide information on a small scale, and the data from nearby weather stations do not have useful time series.

3.3.6 Resilience indices

To analyze post-drought growth recovery after selected extreme drought years (2003, 2012 and 2017), characterised by SPEI values < -2 (see Fig. S3), we used the resilience indices proposed by Lloret et al. (2011): resistance (hereafter R_t), recovery (hereafter R_c), resilience (hereafter R_s), relative resilience (hereafter R_r) and impact (hereafter I). By considering tree radial growth performance (BAI) before, during and after a disturbance, indices have been defined that allow quantifying the components of resilience and understanding how the forest system can or cannot cope with extreme events such as droughts. Resilience indices (R_t , resistance; R_c , recovery; R_s , resilience; R_r , relative resilience and I , impact) were calculated as follows:

$$R_t = D_r / \text{PreDr} \quad (2)$$

$$R_c = \text{PostDr} / D_r \quad (3)$$

$$R_s = \text{PostDr} / \text{PreDr} \quad (4)$$

$$R_r = (\text{PostDr} - D_r) / \text{PreDr} \quad (5)$$

$$I = (\text{PreDr} - D_r) / \text{PreDr} \quad (6)$$

where PreDr , D_r and PostDr indicate mean BAI values before, during and after the drought, respectively.

- ❖ Resistance (R_t) is the ability to resist growth reduction during the disturbance episode, $R_t = 1$ is complete resistance; the lower the value $R_t < 1$, the lower the resistance.
- ❖ Recovery (R_c) is the increase in growth compared to the minimum growth during the stress episode, $R_c = 1$ indicates the persistence of a low level of growth even after the dry period; $R_c < 1$ indicates a further decline, and $R_c > 1$ indicates recovery from the level reached during the dry period.

- ❖ Resilience (R_s) is the ability to reach pre-episode growth levels; $R_s \geq 1$ indicates full recovery of pre-episode performance or even increased growth after episodic stress, while $R_s < 1$ indicates a decline in growth and low resilience.
- ❖ Relative resilience (R_r) which is the resilience weighted by the damage suffered during the episode, i.e. the ability to recover pre-disturbance levels depends on the impact of the episode itself. The closer this value is to 1, the greater the relative resilience, while the closer it is to 0, the lower the resilience. Relative resilience can have negative values if post-disturbance performance is lower than during the disturbance event.
- ❖ Impact (I), the closer the value is to 1 the greater the impact suffered, while the closer the value is to 0 the less impact suffered. Negative values, on the other hand, logically occur when during the disturbance there has been an increase in growth contrary to what is expected.

We chose 3-year intervals to calculate these indices since legacy effects have been shown to be strong 1-3 years after drought (Anderegg et al. 2015). We note that some of these indices are statistically related since $R_s = R_c * R_t$ (Schwarz et al. 2020).

3.3.7 Statistical analyses

We used Mann-Kendall trend tests to assess if there were significant ($p < 0.05$) trends in climate data at seasonal resolution. Pearson and Spearman correlations were used to quantify relationships in the case of variables following or not following the normal distribution, respectively. Mann-Whitney tests were used to compare resilience indices among sites, species and droughts.

To observe how and whether growth increments and stand responses to drought can be influenced by the other variables, we used linear mixed models (LMMs; Pinheiro and Bates 2000) to model (log-transformed) BAI and resilience indices (R_t , R_c , R_s , R_r). BAI was modeled as a function of site, species, tree dbh, calendar year, BAI of the previous year, drought severity (6-month SPEI); and tree was considered the random factor. The 2017 resilience indices were modeled as a function of: tree age

and dbh, 2003 and 2012 resilience indices; in this case, species and site were regarded as random factors.

We considered random effects in the models and quantified intra-class correlation coefficient (ICC) accounted by each factor, which is meaningful to understand how much of the overall variation in the response variable is explained by grouping random effects, with higher values corresponding to greater between-group variability. Variances were estimated using restricted maximum likelihood (REML) methods. We also calculated the proportion of variance explained by fixed and by fixed plus random terms, which corresponded to the marginal (R^2_m) and conditional R^2 (R^2_c) values, respectively (Nakagawa et al. 2017). These were obtained using `r.squared GLMM` function in the `MuMIn` package (Barton 2022). Finally, a residual diagnosis was performed to check model assumptions, namely normality and homoscedasticity of residuals. LMMs' parameters were estimated using the `lme4` R library (Bates et al. 2015). All statistical analyses were carried out with R (R Core Team. 2022).

3.4 Results

3.4.1 Climate trends and drought severity

The seasonal maximum and minimum temperatures increased in the study area from 1950 to 2020 (about 2-3 °C, see Fig. S1). Also precipitation significantly increased in spring (about 3 mm day⁻¹, see Fig. S2). The SPEI values showed three major recent droughts occurring in 2003, 2012 and 2017, although drought severity peaked in 2017 (Fig. S3). The low relative air humidity values confirmed the elevated evaporative demand experienced by vegetation during 2012 and 2017 summers (Fig. S4). The 2017 drought was preceded by high winter-to-spring precipitation in the late 2000s and early 2010s.

3.4.2 Growth patterns

The tree-ring widths and BAI ranged 0.8–3.1 mm and 1.2–23.7 cm² yr⁻¹, respectively (Table 3). Minimum and maximum growth rates corresponded to *F. ornus* (site OS) and *P. pinaster* (site GA), respectively. The oak (*Q. pubescens*) showed the highest first-order autocorrelation (site CA) and mean sensitivity (site PI) values, whilst *A.*

monspessulanum presented the lowest autocorrelation (site VP). The mean correlation between the individual series and their corresponding mean site series ranged between 0.5 (site OS, *F. ornus*) and 0.7 (site VP, *Q. pubescens*) indicating a reliable cross-dating (Table 3).

Most sites presented a BAI reduction during the 2017 drought, but there were exceptions to this pattern such as *F. ornus* and *Q. pubescens* in site AP (Fig. 2). Here, both species showed a growth reduction in 2018. In the case of *F. ornus* in site GA, the 2017 growth drop was preceded by low BAI values in 2015 and 2016. Growth recovery after 2017 was evident in several sites such as, GA, OS, VP, PI and CA, particularly in the case of *F. ornus*. A growth release was evident for *F. ornus* in site OS since BAI in the period 2018-2020 increased three times as compared with BAI in 2017. However, in the case of *Q. pubescens* from site CA growth declined after 2017. In general, growth reductions were also observed during the 2003 and 2012 droughts. In contrast, growth increases during the early 2010s occurred in some species and sites (*F. ornus* in site GA, *Q. pubescens* in OS, *A. monspessulanum* in VP).

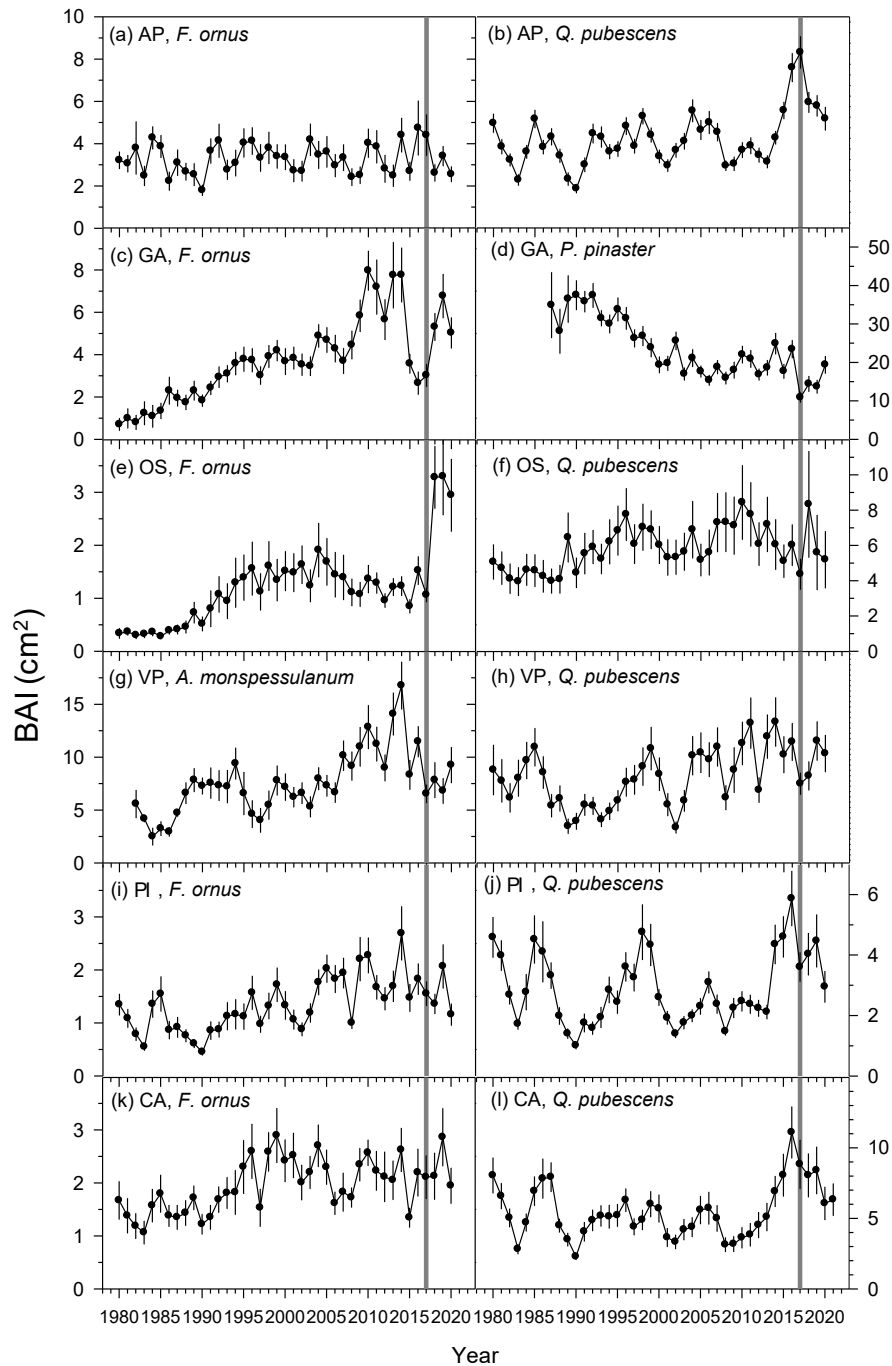


Figure 2. Basal area increment (BAI) measured in the study sites and species (values are means \pm SE). The vertical grey lines indicate the 2017 drought.

3.4.3 Growth responses to climate

Warm and dry spring conditions were associated with lower growth rates of *F. ornus* (Fig. S10). However, there were local exceptions with sites where growth responded more to cool spring (site AP) or wet prior winter conditions (site PI). In the case of *A. monspessulanum* growth increased with higher precipitation from

prior winter to summer and also in response to lower summer temperatures. In *Q. pubescens*, wet winter and spring conditions again increased growth. Usually, a prior warm winter and a cool spring enhanced growth in this species and in *P. pinaster*, but in site OS low temperatures in the prior fall were also a main positive driver of growth. Lastly, for *P. pinaster* growth increased with late summer precipitation.

3.4.4 Growth responses to drought and soil moisture

Growth significantly increased as drought severity decreased in most sites and species, excepting *F. ornus* and *Q. pubescens* in site AP (Fig. 3). The highest correlations were found from May to July considering 3-month SPEI values in the case of *A. monspessulanum*, *P. pinaster*, *F. ornus* in site OS, and *F. ornus* and *Q. pubescens* in site CA. However, more consistent growth-drought associations were found in the other sites showing responses to drought considering either 6- (*Q. pubescens* in OS site, *F. ornus* and *Q. pubescens* in PI site) or 12-month (*Q. pubescens* in VP site) SPEI values.

The highest correlations between growth and soil moisture were found in May and June (Fig.S11), and peaked in the case of *Q. pubescens* in sites VP and PI and *F. ornus* in site PI. The geographic influence of the relationships between growth and soil moisture in responsive species and sites (*Q. pubescens* in site VP) was broad, as showed the significant spatial correlations found across southern Italy (Fig. S5).

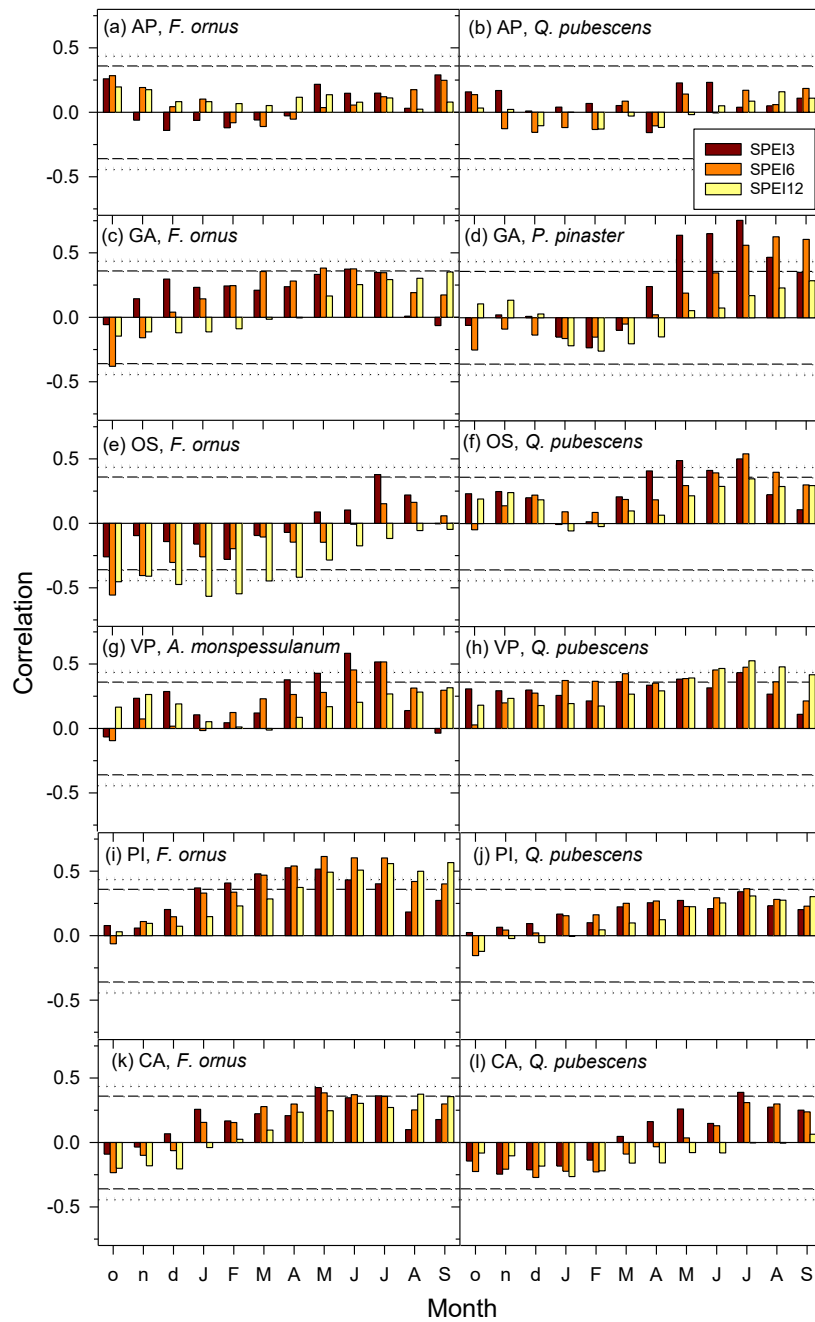


Figure 3. Drought-growth Pearson correlations calculated for the study sites and species considering 3- (SPEI3), 6- (SPEI6) and 12-month (SPEI12) long SPEI values. The window of analyses was from prior October to current September. Months of the previous year are abbreviated by lowercase letters. Dashed and dotted horizontal lines show the 0.05 and 0.01 significance levels, respectively.

3.4.5 Growth resilience indices

The calculated resilience indices based on BAI data and 3-year periods (Fig. 4) were similar to those obtained based on 1-year long periods (Fig. S6). Therefore, we comment the results based on 3-year periods. In sites GA and OS, and *F. ornus* presented very high recovery indices after the 2017 drought, followed by *P. pinaster* in site GA (Fig. 4, Table S2). Resistance after 2017 was lower than in the other two droughts. The post-2017 resilience was high in *F. ornus* from site OS illustrating the effect of the post-drought growth release (Figs. 2 and 4). However, the resilience and relative resilience after 2017 tended to be lower than after the 2003 and 2012 droughts, whereas the impact tended to increase.

Considering the comparisons of resilience indices among coexisting species, *Q. pubescens* showed higher resilience after 2017 than *F. ornus* in sites AP and VP, but lower recovery in sites OS and CA (Table S3). Relative resilience and impact were usually higher in *F. ornus*. Considering the NDVI responses to the 2017 drought, the lowest resistance values ($\text{NDVI}_{2017} / \text{NDVI}_{2016}$) were observed in sites CA, PI and VP, whilst the highest recovery values ($\text{NDVI}_{2018} / \text{NDVI}_{2017}$) were found in sites GA, VP and CA (Table 1).

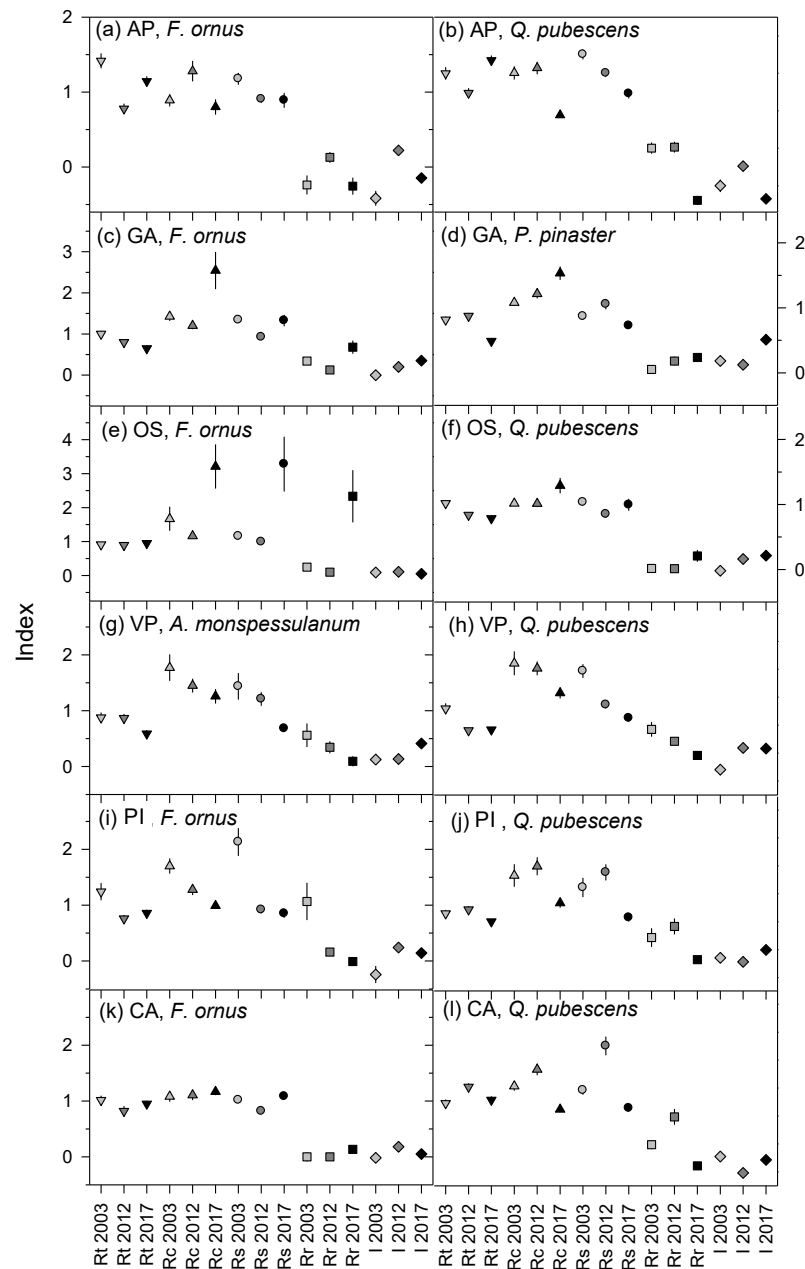


Figure 4. Basal area increment resilience indices based on 3-year long periods and considering three droughts (2003, 2012 and 2017). Values are means \pm SE. Abbreviations of resilience indices are: Rt, resistance; Rc, recovery; Rs, resilience; Rr, relative resilience; I, impact. See comparisons in Tables S2 and S3.

3.4.6 Modeling post-drought recovery and legacies

Regarding the 2017 resilience indices, models were able to explain a low amount of variance as function of fixed factors, ranging between 2% (recovery, relative resilience) and 8% (resistance) (Table S4). Tree age was positively associated to

resistance after 2017, but dbh was negatively related (Fig. S7). Tree age was also negatively associated to the impact after 2003 and 2017 droughts (Fig. S8). The resilience in 2017 was negatively related to 2012 resilience (Fig. S7).

The BAI models resulted in robust fits (Fig. S9, Tables 4 and S5). BAI depended on prior growth, tree species and tree dbh. The fixed factors accounted for 12% (site VP) to 42 % (site GA) of the total BAI variance, showing that random effects accounted for most growth variability.

Legacy effects were calculated by subtracting observed versus predicted BAI values (Fig. 5). Negative legacy effects lasting two years were found in sites VP (*Q. pubescens* and *A. monspessulanum*) and GA (only in *P. pinaster*). Positive and high residuals during 2017, suggesting no negative impact of the 2017 drought on growth, were found for *F. ornus* in site AP and *Q. pubescens* in site CA. Lastly, slight positive legacy effects were observed in the case of *F. ornus* in sites OS and AP, and *Q. pubescens* in sites PI and CA.

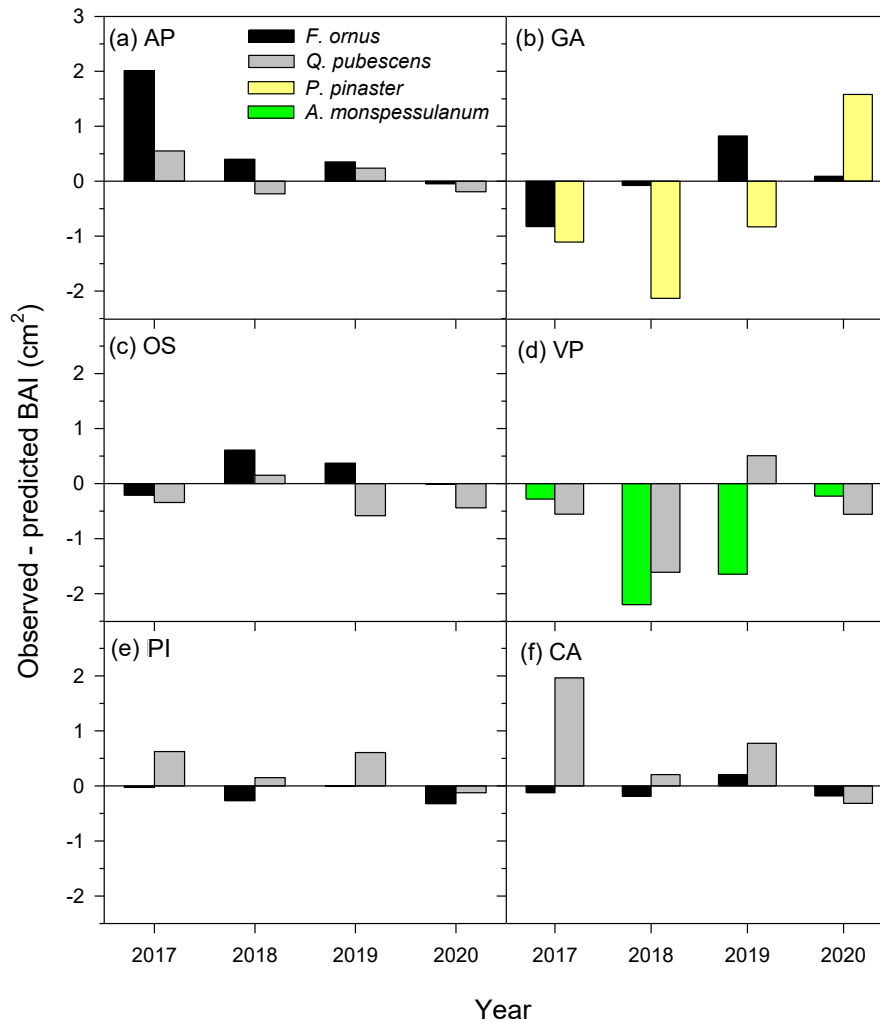


Figure 5. Legacy effects of the 2017 drought calculated as differences between observed and predicted basal area increment (BAI).

3.5 Discussion

In general, consistent growth-drought associations were found showing responses to drought considering either mid to long-term droughts (6- to 12-month SPEI values) for most sites and species. Growth significantly decreased as drought severity increased. The highest correlations between growth and soil moisture were found in late spring and early summer, peaking in the case of *Q. pubescens* and *F. ornus* in site PI.

In most study sites and species, the 2017 drought was followed by a fast recovery and positive legacy effects. This finding confirms the general tendency of Mediterranean hardwood species to show a fast growth recovery after extreme

drought events as highlighted also in previous studies (Gazol et al. 2018). Even so, these authors indicated that the recovery potential of Mediterranean tree species could be constrained if extreme drought events become more frequent. In this study, we also contribute to explain forest vulnerability to drought by considering structural overshoot, which may be a key characteristic of Mediterranean and other seasonally dry forests (e.g., monsoon-affected forests in SW North America) subjected to a high year-to-year precipitation variability.

Negative drought legacies were found in sites GA and VP (see Fig. 5), which lasted longer (2 years). They were stronger at the VP site, particularly in the case of *A. monspessulanum*, which also exhibited greater crown defoliation (41%) than the coexisting oak (23%) in 2017. Consequently, low NDVI values were observed at this site. While for the GA site the negative legacies mainly involved *P. pinaster*, even in this case the pine also manifested greater crown defoliation (by 24%) than the co-occurring *F. ornus* (0%). Analogously, forests with different composition and age structures showed contrasting post-drought legacies in terms of productivity (Yu et al. 2022).

We found support for our hypothesis of strong legacy effects in the extreme drought event of 2017 that mainly affected two sites (GA and VP) and in particular the species *P. pinaster* and *A. monspessulanum*. The reason for the lack of common legacy effects in the extreme drought of 2017 could be explained by drought tolerance and the different strategies shown by coexisting tree species. Certainly in the case of the GA site, pine, being a planted and non-native species, could be more affected by climate extremes than native species such as ash (Camarero et al. 2021). Furthermore, *P. pinaster* performs a significant decrease in root carbohydrates under drought conditions, i.e. a shift in the root carbon balance during defoliation. This decrease in carbohydrate supply during defoliation may not counterbalance the use of carbon for mineral and water uptake (Jacquet et al. 2014) especially in harsh sites.

While *F. ornus* has shown remarkable recovery not only in comparison to pine, but also in other sites compared to oak. The ash is also the species that showed the lowest crown defoliation (ranging 0 to 10%), further confirming its resistance to drought.

It is a species that shows good control of reserves for rapid post-drought recovery (Tomasella et al. 2019), and it tends to allocate relatively more to leaf biomass and conductive phloem under water shortage conditions (Kiorapostolou et al. 2019).

In the second site where more negative drought legacies were observed (site VP), the two coexisting species (*A. monspessulanum*, *Q. pubescens*) are drought-tolerant, so in terms of resilience indices they behaved similarly. However, the maple was more affected by the drought event, bringing with it negative legacies in the 2 years following the drought (see Fig. 5), compared to oak with an extremely anisohydric character (Damesin and Rambal 1995, Poyatos et al. 2008), which probably gave it a small extra advantage with negative legacies evident only in the year following 2017.

The fact that drought legacies were observed in planted (*P. pinaster*) and natural (*A. monspessulanum*) stands suggests that their different structure did not explain their responses to drought, but this should be validated by considering more sites and different stand structures of each species. The GA and VP sites illustrate how the structural overshoot predisposed trees to show increased drought damage in 2017 and subsequent negative legacies, as trees showed high pre-drought growth rates in response to previous wet winter-spring conditions. Thus, the damage was conditioned by previous moisture conditions that led to overbuilt stands. Our findings are very important if considered at a large scale given how widespread forest dieback phenomena are (Allen et al. 2015). For instance, a recent global study estimated that structural overshoot contributed to exacerbate negative impacts in about 11% of drought events in the period 1981-2015 (Zhang et al. 2021), causing faster decline and greater impacts on forest stands affected by droughts and heat waves.

However, we cannot exclude that impacts observed in response to the 2017 droughts were caused by other concomitant variables or factors not/or partially recognized in our analyses (i.e., stand basal area and density, aboveground biomass, etc.). In fact, drought effects can be linked to whole stand water usage and not only to individual tree overshoot. Furthermore, mixed stands such as Mediterranean forests have greater resistance and resilience to drought events than single-species stands, but the beneficial effect of the species mix cannot be generalized because it

is strongly modulated by the type of mixing and the identity of the tree species (Pardos et al. 2021) as well as the characteristics of the site.

Overall, our results indicate that the negative growth responses to the 2017 drought were contingent on site conditions (slope, soil, exposure) and species characteristics. For instance, the *F. ornus* growth release observed in the OS site may be explained by the elevated oak dieback observed there, which could have reduced competition for soil water and nutrients in favour of *F. ornus*. A long-term legacy with a slow recovery in oak comparing to ash could be also due to differences in structural damage after drought that affects the regrowth of lost and damaged tissues (Gessler et al. 2020). In fact, drought mitigation, and thus the repair and regrowth of post-drought, damaged organs can even exacerbate the depletion of non-structural carbon (Ouyang et al. 2021).

In some study stands, a replacement of *Q. pubescens* by *F. ornus* could occur if more severe droughts occur. In fact, increasing aridity has accelerated shifts of forest composition towards communities dominated by drought resistant species at a global scale (Batllori et al. 2020). The growth increase observed in *Q. pubescens* in some sites such as AP may be explained because *Q. pubescens* could have formed most of their ring before the summer drought started or because they relied on stored non-structural carbohydrates to form the 2017 ring (Colangelo et al. 2017). Indeed, *Q. pubescens* showed a greater resistance than *F. ornus* during the 2017 drought. Moreover, AP is the warmest site where trees may be already adapted to cope with heat waves. For example, recent studies have observed that drought resilience is increased, especially in mixed stands that vegetate in the driest and hottest sites (Pardos et al. 2021).

In addition, the mismatch or the temporal overlap between growth phenology and drought timing influences the legacy of tree growth recovery and may determine growth decline (Camarero et al. 2015, Huang et al. 2018). Recent greenhouse experiments show how differences in growth phenology determine the post-drought growth recovery (van Kampen et al. 2022).

One might think that competition between trees might influence forest resistance, but recent studies (Castagneri et al. 2022) have concluded that there is no universal model of resilience to growth after drought in relation to competition.

In general, the impact of summer drought greatly depended on site conditions since elevation, exposure and vegetation type influenced this response (Rita et al. 2020). In addition, differences between coexisting species were observed and could be due to their different soil water uptake strategies which affect gas-water exchange dynamics (Lemoine et al. 2001).

3.6 Conclusions

We found that growth resilience and drought legacies depended on site conditions and species characteristics. Most of the investigated forest sites showed a growth reduction during the 2017 drought. This growth reduction was followed by a quick recovery and positive legacy effect, which may be a feature characteristic of some Mediterranean hardwood forests. Negative drought legacies, lasting up to two years after drought, were mainly found in sites with more unfavorable growing conditions. In these sites, trees showed high growth rates prior to drought in response to previous favorable winter-spring wet conditions which predisposed to drought damages and subsequent negative legacies.

We also emphasize that we are reporting dendrochronological data of understudied but relevant Mediterranean tree species, such as the ash *F. ornus* and the maple *A. monspessulanum*, and also provide information on mixed Mediterranean forests that are often little studied due to their complexity. In general *Q. pubescens* showed a greater resistance than *F. ornus* during the 2017 drought, while *F. ornus* presented high recovery indices. The maple *A. monspessulanum* showed similar responses to drought as *Q. pubescens*, and also a good resistance to drought. All broadleaf trees studied showed a better response to disturbance than the planted pine (*P. pinaster*). Overall, *F. ornus* seems to be the species that responded best to drought showing excellent recovery. These resilient hardwood species could be compared with more widely distributed but less drought-tolerant tree species as alternatives for warmer and drier climate scenarios.

This study could represent an important step in documenting the ecological consequences of drought overshoot in Mediterranean forest dynamics. Our results may give indications of possible changes in composition towards communities dominated by more drought-tolerant tree species. Certainly, to have more specific

information on post-drought stand dynamics it would be necessary to carry out specific monitoring and measure variables responsive to drought stress such as wood anatomy, non-structural carbohydrate concentrations and soil water and nutrient availability and uptake.

3.7 Tables

Table 1. Characteristics of the six study sites. The temperature and precipitation values come from the records of the local meteorological stations (Tab. S1). MAT and TAP are the annual average and total annuals of temperature and precipitation, respectively, for each site.

Site	Longitude E (°)	Latitude N (°)	Elevation (m a.s.l.)	Slope (%)	Aspect	Substrate	MAT (°C)	TAP (mm)	Rainfall in 2017 compared to the average (%)
Accettura Palazzo (AP)	16.148	40.516	790	15	W	Sandstone	16	734	-25
Grotta dell'Angelo (GA)	15.558	40.570	760	30	N-NW	Clay	13	889	-29
Orto Siderio (OS)	15.546	40.573	600	35	N-NW	Clay	13	889	-29
Vietri di Potenza (VP)	15.460	40.617	530	30	NW	Limestone	14,5	943	-35
Pietrapertosa (PI)	16.058	40.533	625	35	N-NW	Sandstone	12,7	671	-18
Castellmezzano (CA)	16.054	40.534	665	50	S-SE	Sandstone	12,7	671	-18

Table 2. Characteristics of the six stands analyzed. Stem diameter values (dbh) are means \pm SD. The remote sensing indices are the ratio of the NDVI value pre and during the disturbance to the ratio post and during the disturbance.

Site	Sampled species	Code	Age (years)	Dbh (cm)	Dead trees (%)	Crown defoliation 51–100% (%)	NDVI ₂₀₁₇ / NDVI ₂₀₁₆	NDVI ₂₀₁₈ / NDVI ₂₀₁₇
AP	<i>Fraxinus ornus</i>	APFO	56	16 \pm 3.8	0	0	1.178	0.887
	<i>Quercus pubescens</i>	APQP	66	19 \pm 6.6	0	45		
GA	<i>Fraxinus ornus</i>	GAFO	35	13 \pm 3.2	0	0	1.064	0.940
	<i>Pinus pinaster</i>	GAPP	33	33 \pm 5.5	18	24		
OS	<i>Fraxinus ornus</i>	OSFO	42	9 \pm 3.2	0	7	1.049	0.900
	<i>Quercus pubescens</i>	OSQP	65	18 \pm 6.8	61	89		
VP	<i>Acer monspessulanum</i>	VPAM	30	19 \pm 5.8	0	41	0.939	1.116
	<i>Quercus pubescens</i>	VPQP	45	22 \pm 6.7	0	23		
PI	<i>Fraxinus ornus</i>	PIFO	58	7 \pm 0.7	0	0	0.963	0.821
	<i>Quercus pubescens</i>	PIQP	47	14 \pm 5.1	11	45		
CA	<i>Fraxinus ornus</i>	CAFO	43	8 \pm 2.4	3	10	0.897	0.943
	<i>Quercus pubescens</i>	CAQP	50	16 \pm 6.5	19	84		

Table 3. Growth data of the study sites and species. Basal area increment (BAI) was calculated for the common period 1980–2020 (BAI values are means \pm SE). Abbreviations: SD, standard deviation; AR1, first-order autocorrelation; MS, mean sensitivity. See sites' codes in Table 1.

Site	Interval	Tree-ring width (mm)	SD (mm)	AR1	MS	Correlation between growth series	BAI (cm ²)
APFO	1938-2021	1.03	0.50	0.62	0.31	0.55	3.28 \pm 0.11
APQP	1931-2021	1.14	0.63	0.72	0.26	0.66	4.22 \pm 0.20
GAFO	1977-2021	1.65	0.66	0.61	0.29	0.57	3.71 \pm 0.30
GAPP	1983-2021	3.11	1.80	0.83	0.23	0.68	23.68 \pm 1.31
OSFO	1958-2021	0.76	0.40	0.61	0.31	0.48	1.20 \pm 0.11
OSQP	1940-2021	1.20	0.57	0.71	0.22	0.53	5.84 \pm 0.19
VPAM	1976-2021	2.19	0.83	0.46	0.33	0.54	7.60 \pm 0.48
VPQP	1966-2021	1.90	1.00	0.66	0.32	0.71	8.18 \pm 0.42
PIFO	1953-2021	0.82	0.48	0.66	0.33	0.58	1.35 \pm 0.08
PIQP	1951-2021	1.07	0.80	0.73	0.36	0.65	2.90 \pm 0.18
CAFO	1969-2021	0.93	0.45	0.61	0.30	0.55	1.95 \pm 0.08
CAQP	1968-2021	1.50	1.13	0.86	0.27	0.63	5.47 \pm 0.30

Table 4. Summary statistics (factor; SE, standard error) of linear mixed models of basal area increment (BAI) in the six study sites as a function of tree species (Spp), calendar year, BAI of the previous year (BAI_{t-1}), diameter at breast height (dbh), and 6-month SPEI (spei6). Species' abbreviations: QP, *Quercus pubescens*; FO, *Fraxinus ornus*; PP, *Pinus pinaster*; AM, *Acer monspessulanum*. Tree ID is the random term. The last line shows the proportion of variance explained by fixed (R²m) and by fixed plus random terms (R²c). Significance levels: * p < 0.05, ** p < 0.01, *** p < 0.001.

Predictors	AP		GA		OS		VP		PI		CM	
	factor	SE	factor	SE	factor	SE	factor	SE	factor	SE	factor	SE
Intercept	0.34	0.28	1.00 ***	0.22	2.83 ***	0.51	0.28	0.19	0.70	0.37	1.08 **	0.34
Spp [QP]	-0.78	0.42			-3.14 ***	0.73	0.39 ***	0.03	-1.11 *	0.54	-1.97 ***	0.51
year	-0.23 ***	0.05	-0.34 ***	0.05	-0.32 ***	0.05	-0.16 **	0.05	0.40 ***	0.03	-0.44 ***	0.06
BAI _{t-1}	0.36 ***	0.03	0.39 ***	0.03	0.33 ***	0.03	-0.32	0.27	-0.21 ***	0.05	0.38 ***	0.03
Spp [FO] * dbh	0.77 ***	0.22	1.63 ***	0.25	3.46 ***	0.63			1.05 **	0.38	1.53 ***	0.40
Spp [QP] * dbh	1.15 ***	0.22			1.51 *	0.60	0.69 **	0.26	1.43 ***	0.37	2.05 ***	0.40
Spp [FO] * spei6	0.02	0.02	0.05 **	0.02	0.02	0.01			0.05 *	0.03	0.03	0.02
Spp [QP] * spei6	0.03	0.02			0.04 **	0.01	0.06 **	0.02	0.09 ***	0.02	0.07 ***	0.02
Spp [PP]			-0.77 *	0.33								
Spp [PP] * dbh			0.56 **	0.20								
Spp [PP] * spei6			0.07 ***	0.02								
Spp [AM] * dbh							0.51 *	0.24				
Spp [AM] * spei6							0.10 ***	0.03				

Table 4 (cont.)

Random Effects						
σ^2	0.09	0.10	0.10	0.14	0.15	0.11
τ_{00}	2.20 _{Tree}	1.15 _{Tree}	5.70 _{Tree}	2.11 _{Tree}	2.22 _{Tree}	3.68 _{Tree}
τ_{11}	0.01 _{Tree.dbh}	0.00 _{Tree.dbh}	0.09 _{Tree.dbh}	0.01 _{Tree.dbh}	0.03 _{Tree.dbh}	0.03 _{Tree.dbh}
ρ_{01}	-0.92 _{Tree}	-0.89 _{Tree}	-0.85 _{Tree}	-0.94 _{Tree}	-0.87 _{Tree}	-0.93 _{Tree}
ICC	0.96	0.92	0.98	0.94	0.94	0.97
Observations	869	820	843	780	835	867
R ² m / R ² c	0.14 / 0.96	0.42 / 0.95	0.28 / 0.98	0.12 / 0.94	0.23 / 0.95	0.24 / 0.97

3.8 Supporting Information

Table S1. Meteorological stations used to characterize local climate conditions including relative air humidity.

Site (code)	Meteorological station	Longitude E	Latitude N	Elevation (m a.s.l.)	Period
Accettura Palazzo (AP)	S. Mauro Forte	16° 15' 04''	40° 28' 54''	504	2006–2020
Grotta dell'Angelo (GA) Orto Siderio (OS)	Tito	15° 39' 25''	40° 34' 27''	729	2012–2020
Vietri di Potenza (VP)	Balvano	15° 30' 05''	40° 38' 58''	431	2012–2020
Pietrapertosa (PI) Castellmezzano (CA)	Albano di Lucania	16° 02' 07''	40° 34' 55''	809	2000–2020

Table S2. Resilience indices (means \pm SE) calculated using BAI data and 3-year intervals considering three droughts (2003, 2012 and 2017). Different letters indicate significant ($p < 0.05$) differences among years according to Mann-Whitney tests.

Site	Resistance			Recovery			Resilience		
	2003	2012	2017	2003	2012	2017	2003	2012	2017
APFO	1.42 \pm 0.10c	0.78 \pm 0.07a	1.15 \pm 0.06b	0.89 \pm 0.08a	1.28 \pm 0.14b	0.80 \pm 0.10a	1.18 \pm 0.08b	0.91 \pm 0.05a	0.89 \pm 0.10a
APQP	1.25 \pm 0.08b	0.99 \pm 0.06a	1.42 \pm 0.06c	1.26 \pm 0.09b	1.32 \pm 0.08b	0.69 \pm 0.04a	1.50 \pm 0.06c	1.25 \pm 0.05b	0.98 \pm 0.06a
GAFO	1.00 \pm 0.07b	0.80 \pm 0.06b	0.65 \pm 0.07a	1.43 \pm 0.11a	1.20 \pm 0.08a	2.54 \pm 0.45b	1.34 \pm 0.06b	0.92 \pm 0.07a	1.33 \pm 0.14b
GAPP	0.82 \pm 0.05b	0.87 \pm 0.05b	0.49 \pm 0.03a	1.08 \pm 0.04a	1.22 \pm 0.07a	1.53 \pm 0.10b	0.87 \pm 0.05b	1.06 \pm 0.08b	0.73 \pm 0.04a
OSFO	0.91 \pm 0.07a	0.89 \pm 0.08a	0.95 \pm 0.07a	1.67 \pm 0.35a	1.16 \pm 0.07a	3.21 \pm 0.65b	1.16 \pm 0.10a	0.99 \pm 0.08a	3.28 \pm 0.81b
OSQP	1.02 \pm 0.03b	0.84 \pm 0.03a	0.79 \pm 0.04a	1.02 \pm 0.04a	1.01 \pm 0.05a	1.29 \pm 0.12b	1.04 \pm 0.05b	0.85 \pm 0.05a	1.00 \pm 0.09b
VPAM	0.88 \pm 0.09b	0.87 \pm 0.07b	0.59 \pm 0.06a	1.77 \pm 0.24a	1.45 \pm 0.12a	1.26 \pm 0.13a	1.44 \pm 0.24b	1.21 \pm 0.12b	0.68 \pm 0.06a
VPQP	1.05 \pm 0.10b	0.66 \pm 0.04a	0.67 \pm 0.03a	1.86 \pm 0.21b	1.77 \pm 0.12b	1.33 \pm 0.10a	1.72 \pm 0.12c	1.12 \pm 0.07b	0.88 \pm 0.07a
PIFO	1.24 \pm 0.15b	0.76 \pm 0.07a	0.86 \pm 0.06a	1.70 \pm 0.14c	1.28 \pm 0.10b	0.99 \pm 0.06a	2.31 \pm 0.47b	0.92 \pm 0.06a	0.85 \pm 0.07a
PIQP	0.90 \pm 0.07b	0.97 \pm 0.06b	0.75 \pm 0.03a	1.58 \pm 0.20a	1.74 \pm 0.16a	1.09 \pm 0.08b	1.36 \pm 0.17b	1.63 \pm 0.14b	0.82 \pm 0.07a
CAFO	1.02 \pm 0.08a	0.82 \pm 0.09a	0.95 \pm 0.05a	1.08 \pm 0.09a	1.11 \pm 0.09a	1.17 \pm 0.06a	1.02 \pm 0.05b	0.82 \pm 0.05a	1.08 \pm 0.06b
CAQP	0.98 \pm 0.07a	1.27 \pm 0.06b	1.04 \pm 0.07a	1.28 \pm 0.08b	1.58 \pm 0.10c	0.87 \pm 0.04a	1.21 \pm 0.08b	2.00 \pm 0.17c	0.89 \pm 0.06a

Table S2 (cont.).

Site	Relative resilience			Impact		
	2003	2012	2017	2003	2012	2017
APFO	-0.24 ±0.13a	0.13±0.07b	-0.25 ±0.11a	-0.42 ±0.10a	0.22 ±0.07c	-0.15 ±0.06b
APQP	0.25 ±0.07b	0.27 ±0.07b	-0.44 ±0.06a	-0.25 ±0.08b	0.01 ±0.06c	-0.42 ±0.06a
GAFO	0.34 ±0.07b	0.12 ±0.05a	0.68 ±0.16c	0.00 ±0.07a	0.20 ±0.06b	0.35 ±0.07b
GAPP	0.05 ±0.03a	0.18 ±0.07b	0.24 ±0.03b	0.18 ±0.05b	0.13 ±0.05a	0.51 ±0.03c
OSFO	0.25 ±0.09a	0.10 ±0.05a	2.33 ±0.77b	0.09±0.07a	0.11 ±0.08a	0.05 ±0.07a
OSQP	0.02 ±0.04a	0.01 ±0.05a	0.21 ±0.09a	-0.02 ±0.03a	0.16 ±0.03b	0.21 ±0.04b
VPAM	0.56 ±0.21a	0.35 ±0.11a	0.09 ±0.09a	0.12 ±0.09a	0.13 ±0.07a	0.41 ±0.06b
VPQP	0.68 ±0.13c	0.46 ±0.06b	0.21 ±0.06a	-0.05 ±0.10a	0.34 ±0.04b	0.33 ±0.03b
PIFO	1.07 ±0.33b	0.16 ±0.07a	-0.01 ±0.05a	-0.24 ±0.15a	0.24 ±0.07b	0.14 ±0.06b
PIQP	0.47 ±0.17b	0.67 ±0.14b	0.07 ±0.06a	0.10 ±0.07a	0.03 ±0.06a	0.25 ±0.03b
CAFO	0.00 ±0.08a	0.00 ±0.07a	0.13 ±0.05a	-0.02 ±0.08a	0.18 ±0.09a	0.05 ±0.05a
CAQP	0.24±0.08b	0.73 ±0.14c	-0.14±0.04a	0.02 ±0.07b	-0.27 ±0.06a	-0.04 ±0.07b

Table S3. Comparisons of resilience indices calculated for three droughts (2003, 2012 and 2017) among coexisting tree species in the six study sites. Different letters indicate significant ($p < 0.05$) differences according to Mann-Whitney tests. Species' abbreviations: QP, *Quercus pubescens*; FO, *Fraxinus ornus*; PP, *Pinus pinaster*; AM, *Acer monspessulanum*.

Site	Tree species	Resistance			Recovery			Resilience			Relative resilience			Impact		
		2003	2012	2017	2003	2012	2017	2003	2012	2017	2003	2012	2017	2003	2012	2017
AP	FO-QP		ab	ab	ab			ab	ab		ab	ab			ba	ba
GA	FO-PP	ba			ba			ba		ba	ba		ba	ab		
OS	FO-QP				ba		ba			ab	ba		ba			
VP	AM-QP		ba	ab				ab							ab	ba
PI	FO-QP		ab			ab			ab			ab			ba	
CA	FO-QP		ab			ab	ba		ab	ba	ab	ab	ba		ba	

Table S4. Summary statistics of linear mixed models fitted to (log-transformed) resistance (Rt), recovery (Rc), resilience (Rs), and relative resilience (Rr) indices after the 2017 drought in response to the 2003 and 2012 droughts. Species-site is the random term. The last line shows the proportion of variance explained by fixed (R^2_m) and by fixed plus random terms (R^2_c). Significance levels: * $p < 0.05$, ** $p < 0.01$, *** $p < 0.001$.

Predictors	Resistance		Recovery		Resilience		Relative resilience	
	Factor	SE	Factor	SE	Factor	SE	Factor	SE
Intercept	-0.00	0.18	-0.00	0.22	0.01	0.18	0.00	0.22
Age	0.18 *	0.08	0.09	0.09	0.17	0.09	0.08	0.09
Dbh	-0.19 *	0.08	0.05	0.09	-0.13	0.09	0.02	0.09
Rt 2003	-0.04	0.05						
Rt 2012	0.09	0.06						
Rc 2003			0.06	0.06				
Rc 2012			0.07	0.06				
Rs 2003					0.06	0.07		
Rs 2012					-0.16 *	0.08		
Rr 2003							0.10	0.07
Rr 2012							0.04	0.07

Table S4 (cont.)

Random Effects				
σ^2	0.01	0.05	0.05	0.16
τ_{00}	0.01 _{SpeciesSite}	0.05 _{SpeciesSite}	0.03 _{SpeciesSite}	0.16 _{SpeciesSite}
ICC	0.47	0.50	0.39	0.50
N	12 _{SpeciesSite}	12 _{SpeciesSite}	12 _{SpeciesSite}	12 _{SpeciesSite}
Observations	178	179	178	177
R ² m / R ² c	0.08 / 0.52	0.02 / 0.51	0.07 / 0.43	0.02 / 0.51

Table S5. Summary statistics (SE, standard error) of linear mixed models of basal area increment (BAI) as a function of tree species, calendar year, BAI of the previous year (BAI_{t-1}), diameter at breast height (dbh), and SPEI-6 month (spei6). Species' abbreviations: QP, *Quercus pubescens*; FO, *Fraxinus ornus*; PP, *Pinus pinaster*; AM, *Acer monspessulanum*. Tree ID is the random term. The last line shows the proportion of variance explained by fixed (R^2_m) and by fixed plus random terms (R^2_c). Significance levels: * $p < 0.05$, ** $p < 0.01$, *** $p < 0.001$.

Predictors	AP		GA		OS		VP		PI		CM	
	factor	SE	factor	SE	factor	SE	factor	SE	factor	SE	factor	SE
Intercept	0.07	0.18	0.87 *	0.43	1.30 ***	0.35	0.05	0.16	0.48	0.35	0.34	0.30
Species [QP]	0.35	0.26			-1.57 ***	0.41	0.10	0.08	-0.35	0.42	-0.32	0.36
year	0.05	0.08	0.26 **	0.08	-0.00	0.03	0.09 *	0.04	0.21 **	0.08	-0.07 **	0.02
BAI_{t-1}	-0.17 ***	0.03	0.14 **	0.04	0.17 *	0.07	-0.10	0.23	-0.11 **	0.03	0.34 ***	0.08
Species [FO] * dbh	0.99 ***	0.18	1.54 ***	0.44	2.13 ***	0.41			1.31 **	0.41	1.05 **	0.33
Species [QP] * dbh	0.20	0.17			0.80 ***	0.16	0.70 ***	0.14	0.51 **	0.19	0.59 ***	0.17
Species [FO] * spei6	-0.15 *	0.06	0.19 ***	0.05	0.31 ***	0.05			0.01	0.05	0.03	0.03
Species [QP] * spei6	-0.11	0.06			0.13 **	0.05	-0.01	0.07	0.07	0.05	-0.01	0.03
Species [PP]			-0.59	0.54								
Species [PP] * dbh			0.28	0.26								
Species [PP] * spei6			0.03	0.05								
Species [AM] * dbh							0.64 ***	0.17				
Species [AM] * spei6							-0.06	0.07				

Table S5. (cont.)

Random Effects						
σ^2	0.04	0.09	0.07	0.08	0.08	0.04
τ_{00}	0.16 _{Tree}	0.16 _{Tree}	0.36 _{Tree}	0.24 _{Tree}	1.25 _{Tree}	0.24 _{Tree}
τ_{11}	0.01 _{Tree.spei6}	0.00 _{Tree.spei6}	0.01 _{Tree.spei6}	0.02 _{Tree.spei6}	0.00 _{Tree.dbh}	0.00 _{Tree.spei6}
ρ_{01}	0.47 _{Tree}	0.46 _{Tree}	0.91 _{Tree}	0.65 _{Tree}	-0.98 _{Tree}	-1.00 _{Tree}
ICC	0.80	0.65	0.84	0.74	0.94	0.74
N	30 _{Tree}	30 _{Tree}	30 _{Tree}	30 _{Tree}	30 _{Tree}	30 _{Tree}
Observations	119	119	119	119	119	119
R ² _m / R ² _c	0.64 / 0.93	0.66 / 0.88	0.59 / 0.93	0.46 / 0.86	0.21 / 0.95	0.43 / 0.94

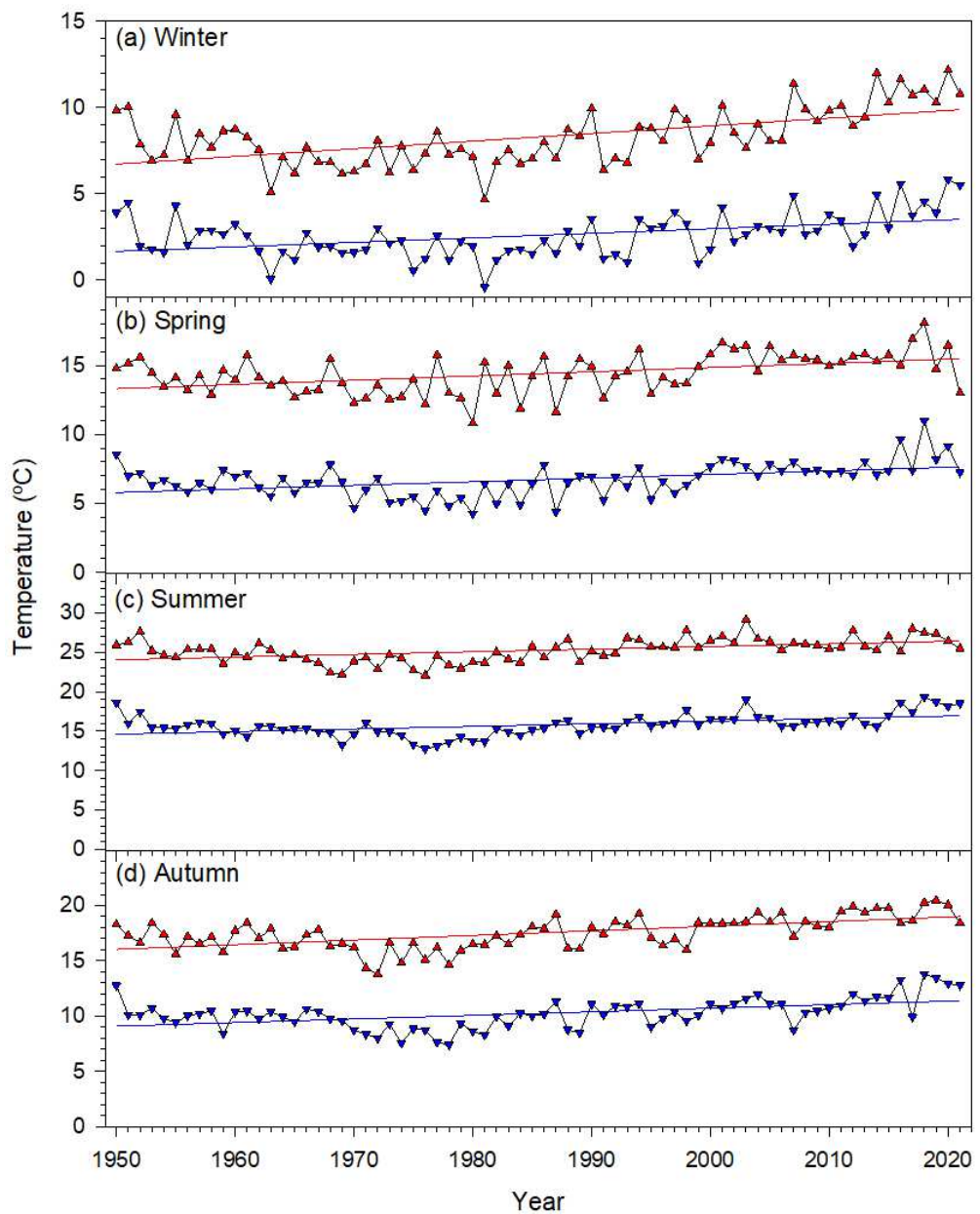


Figure S1. Variability and trends of seasonal maximum and minimum temperatures recorded in the study area. The fitted linear regressions indicate significant ($p < 0.05$, Mann-Kendall trend test) rising temperatures in all seasons.

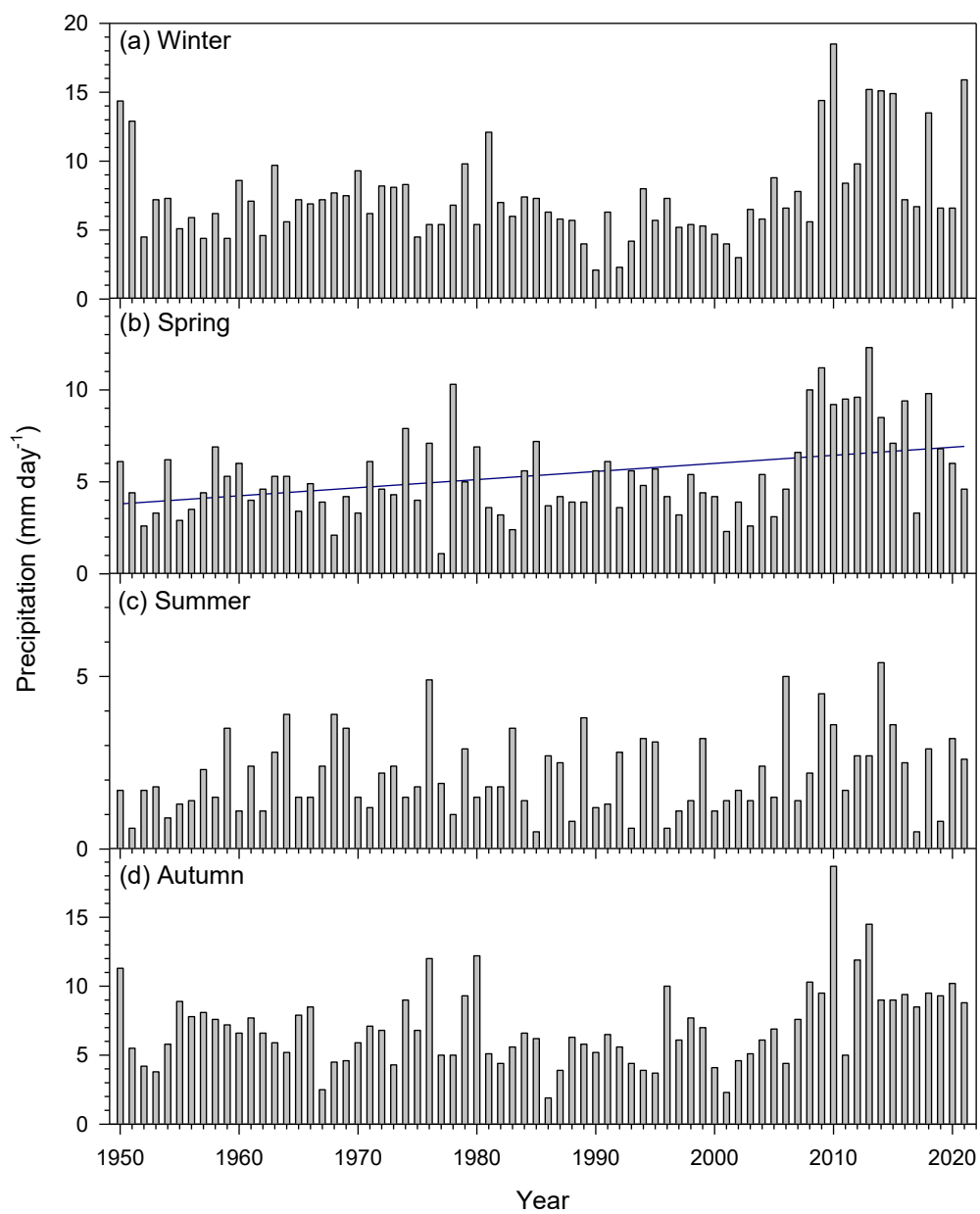


Figure S2. Variability and trends of seasonal precipitation recorded in the study area. The fitted linear regressions indicate significant ($p < 0.05$, Mann-Kendall trend test) rising precipitation in spring.

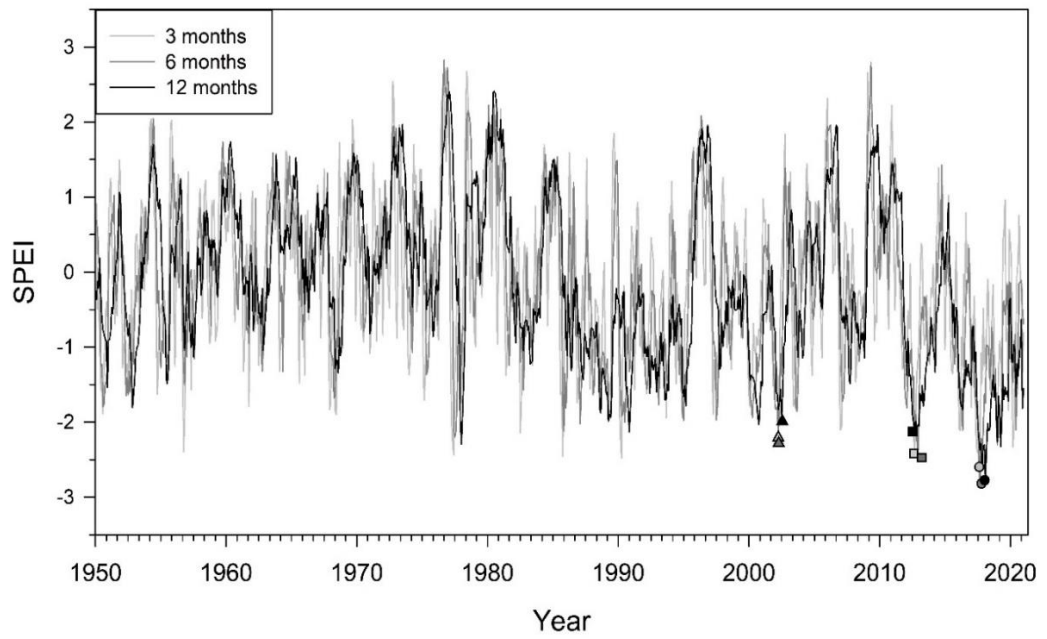


Figure S3. SPEI calculated at 3-, 6- and 12-month long scales. The dots show the minimum values reached of the series recorded in 2017, while the triangle and squares indicate the values from 2003 and 2012, respectively

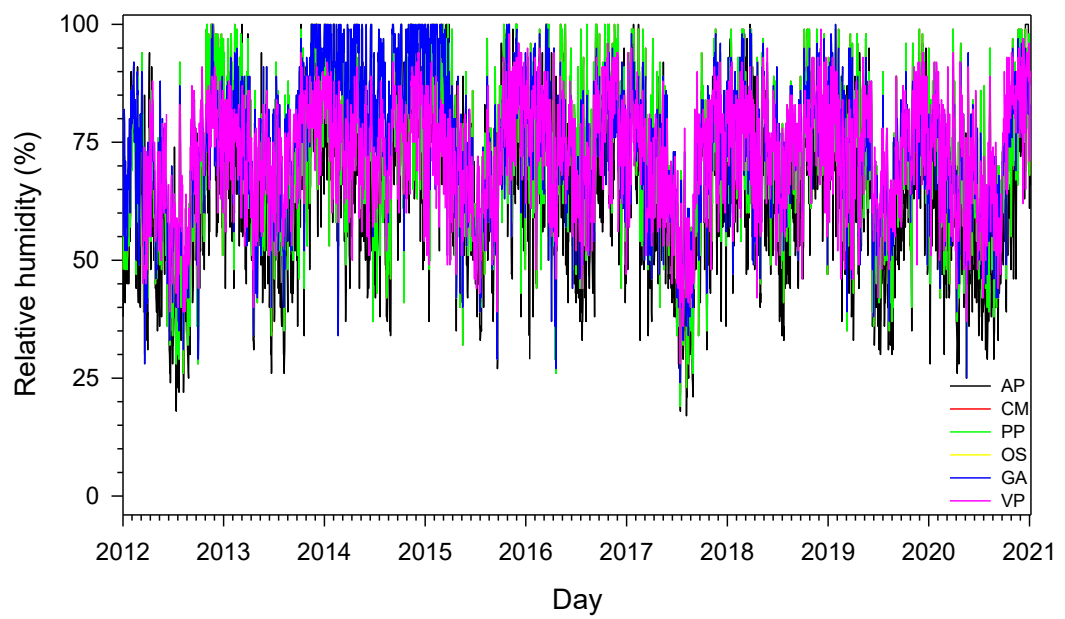


Figure S4. Daily data of relative air humidity measured from 2012 to 2021 in meteorological stations located near the six study sites. Note the drops of relative humidity in summer 2012 and 2017. See meteorological stations in Table S1.

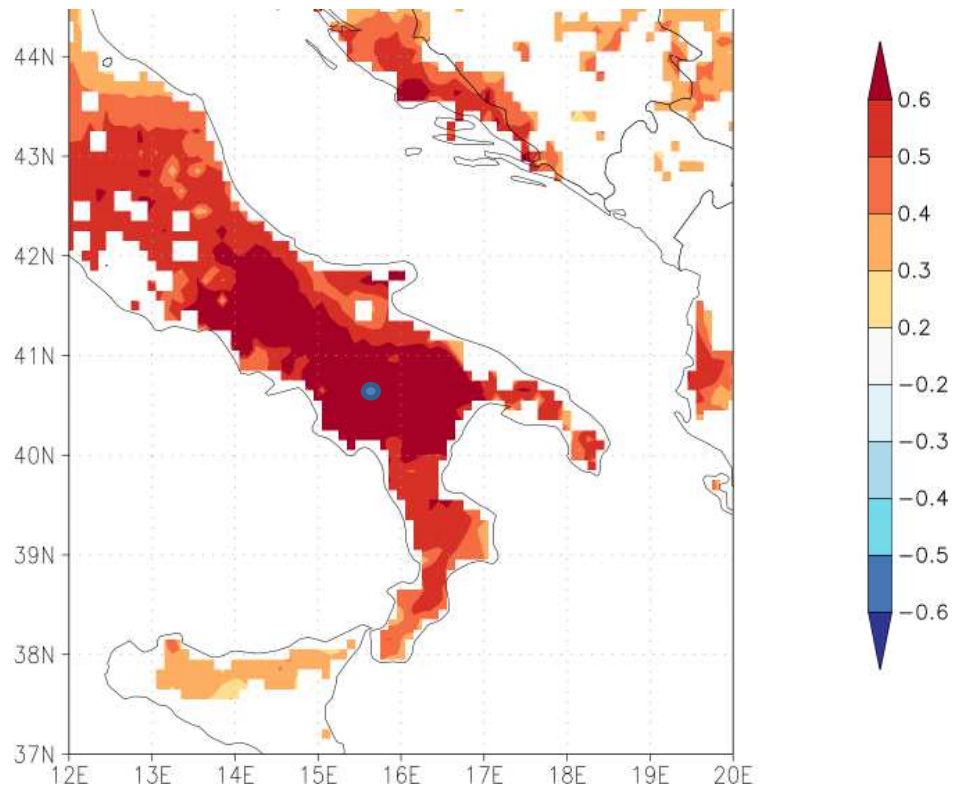


Figure S5. Spatial correlations between the *Q. pubescens* ring-width series (VP site) and the soil moisture estimated at 0-10 cm depth across southern Italy. The point shows the approximate location of the study stand and the color scale shows Pearson correlations.

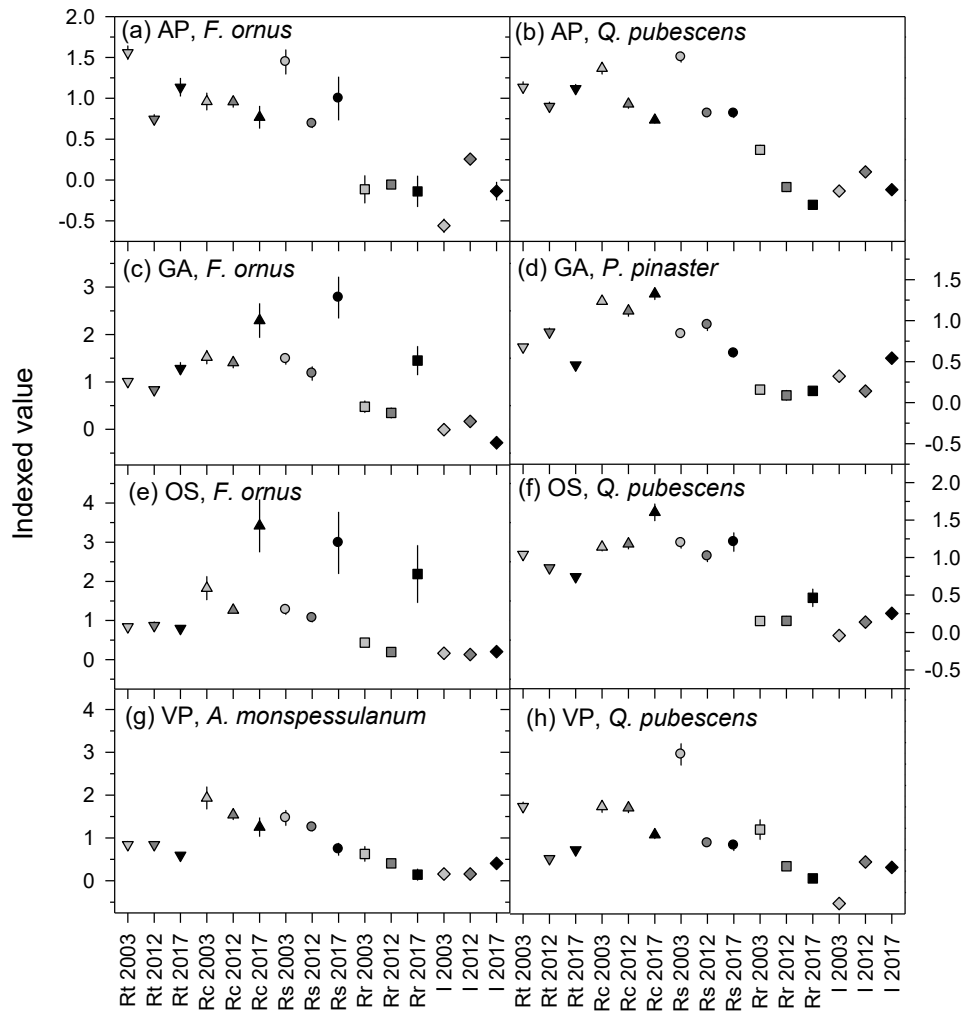


Figure S6. Basal area increment resilience indices based on 1-year periods in selected sites.

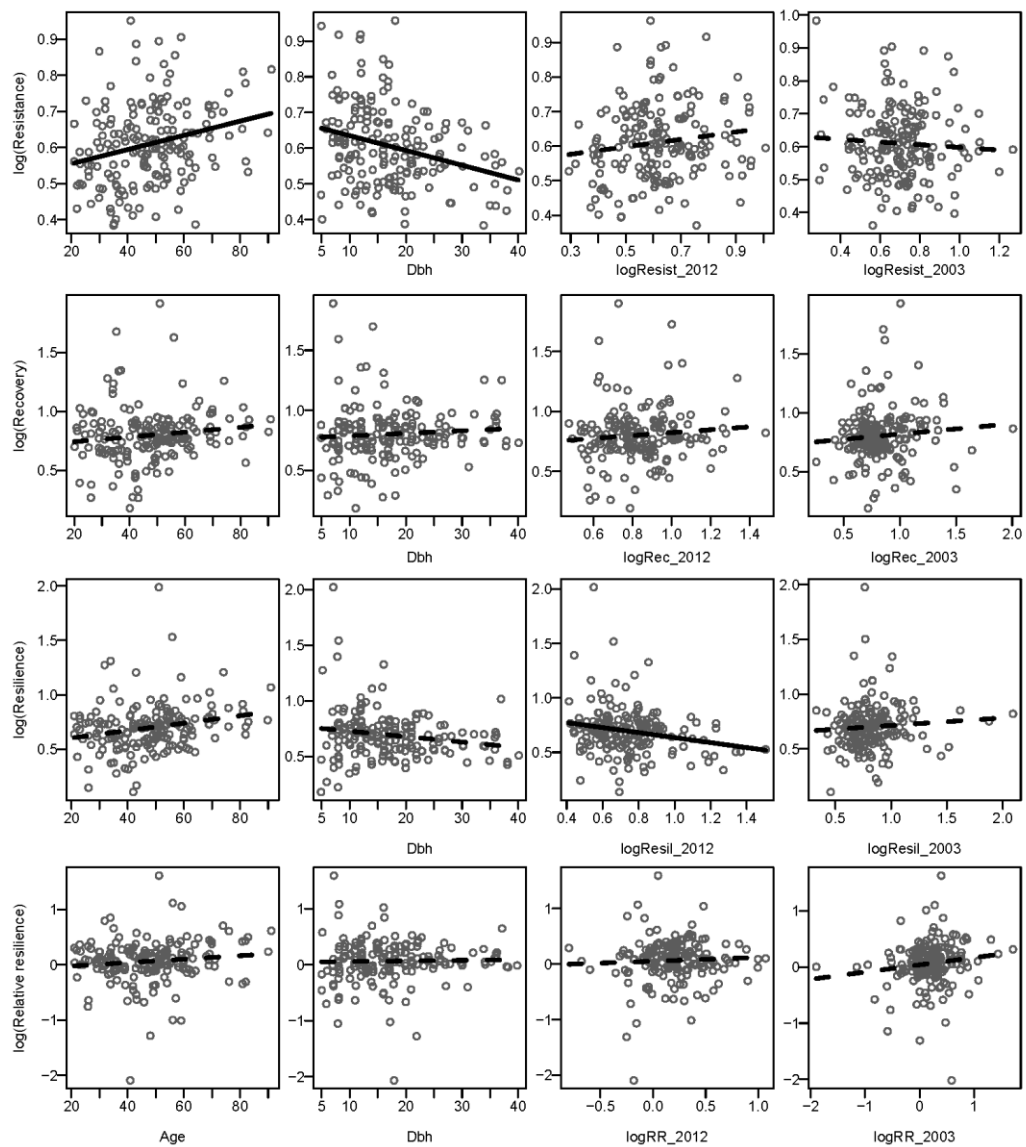


Figure S7. Relationships among resistance (Resist), recovery (Rec), resilience (Resil), and relative resilience (RR) indices (log-transformed values), tree age and tree diameter (dbh) considering the 2003 and 2012 droughts. Full lines represent significant ($p < 0.05$) estimated coefficients while dashed lines show non-significant relationships according to linear mixed models (see also Table S4).

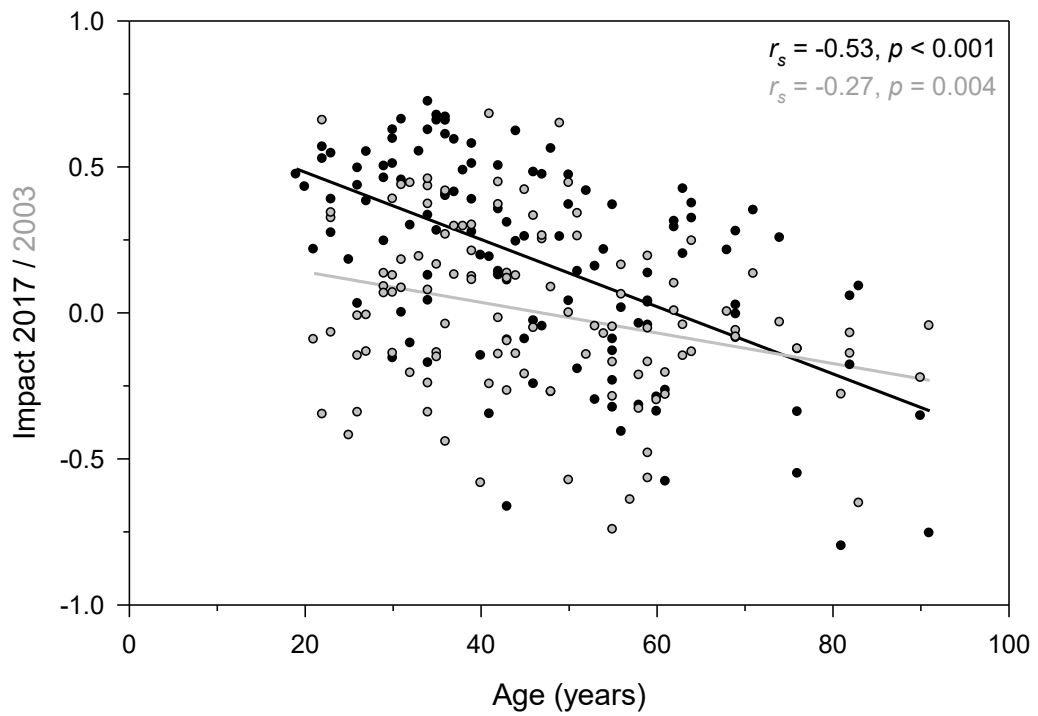


Figure S8. Negative association observed between tree age (calculated at 1.3 m) and the impact measured in 2017 (black symbols and lines) or 2003 (grey symbols and lines). Statistics correspond to Spearman correlation coefficients (r_s). The impact was measured using basal area increment and 3-year periods.

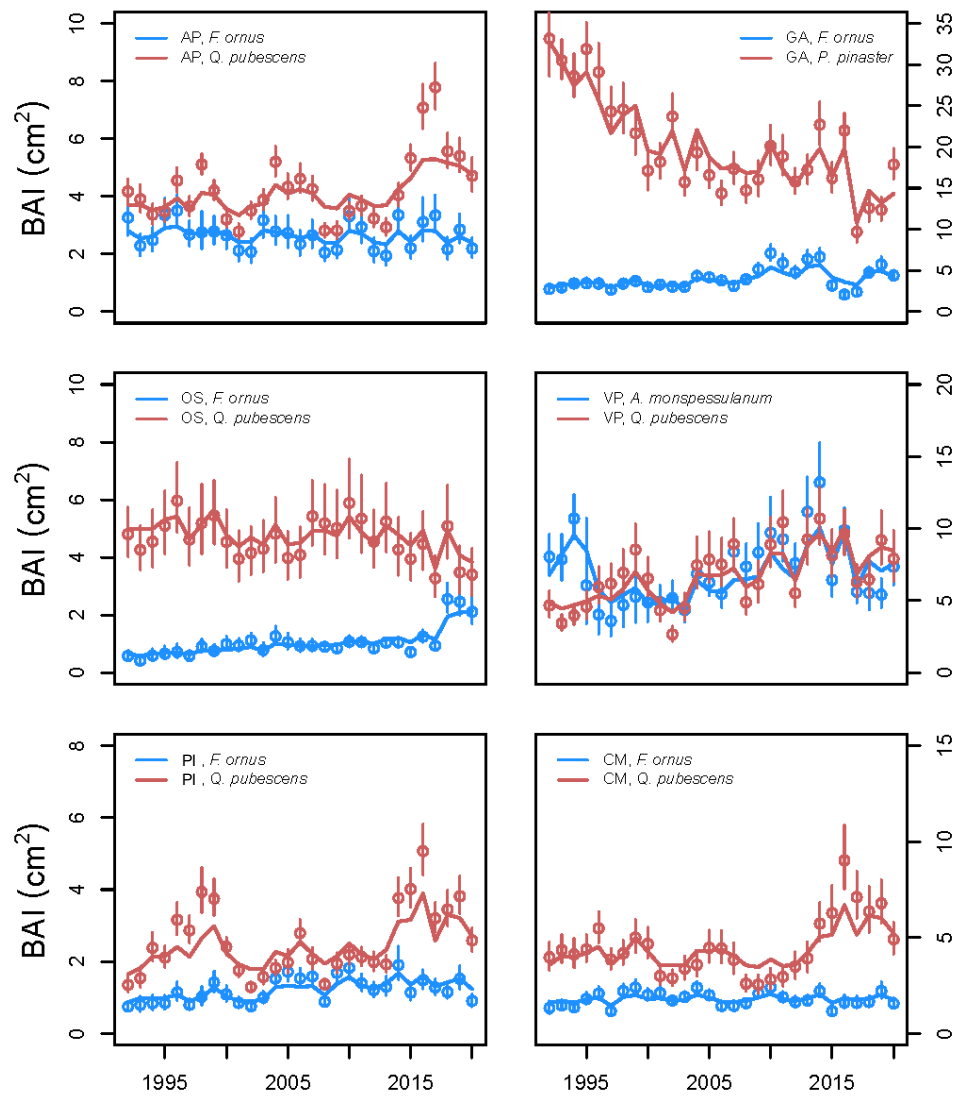


Figure S9. Basal area increment (BAI) measured (symbols, means \pm SE) and predicted (lines) based on linear mixed models and considering the period 1992–2020 (see also Tables 4 and S5).

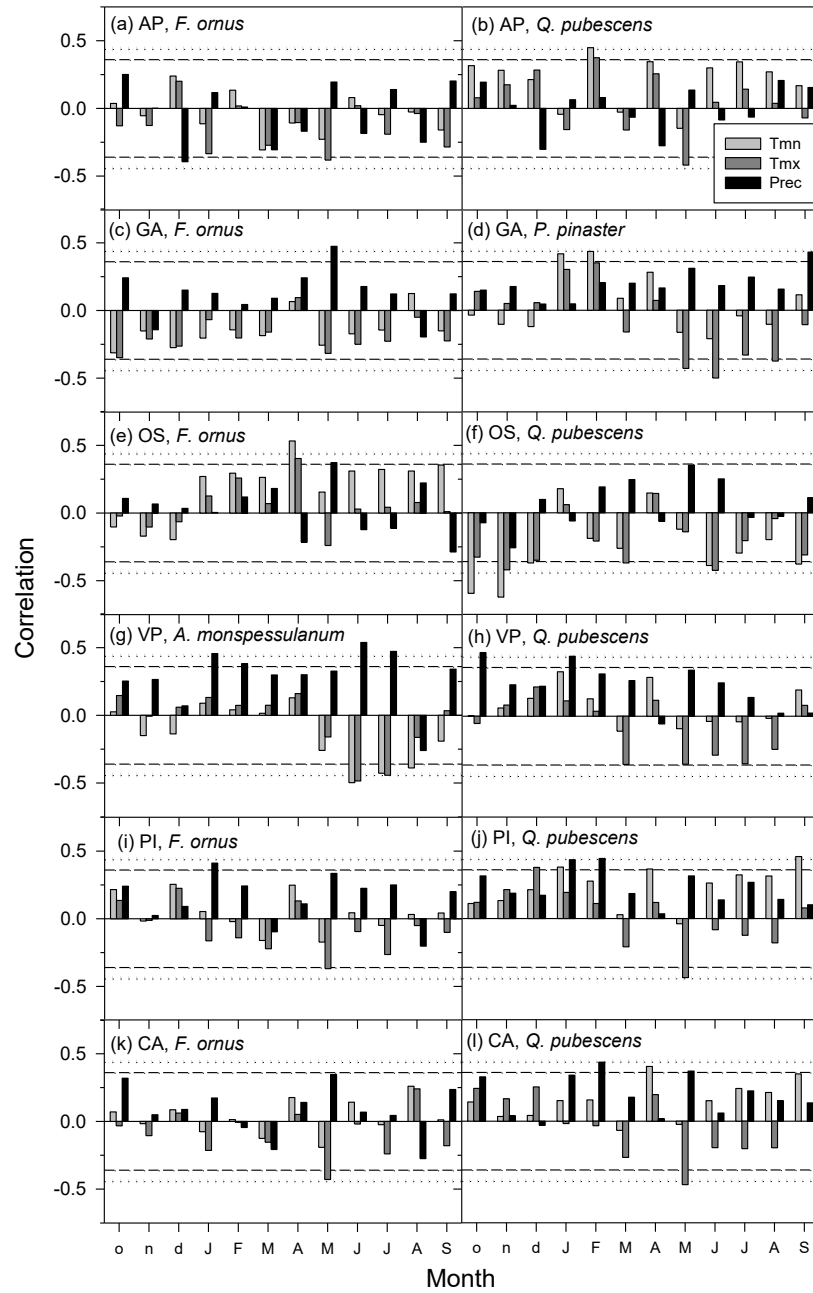


Figure S10. Climate-growth relationships based on Pearson correlations calculated for the study sites and species using monthly climate variables (Tmn, mean minimum temperature; Tmx, mean maximum temperature; Prec, precipitation). The window of analyses was from prior October to current September. Months of the previous year are abbreviated by lowercase letters. Dashed and dotted horizontal lines show the 0.05 and 0.01 significance levels, respectively.

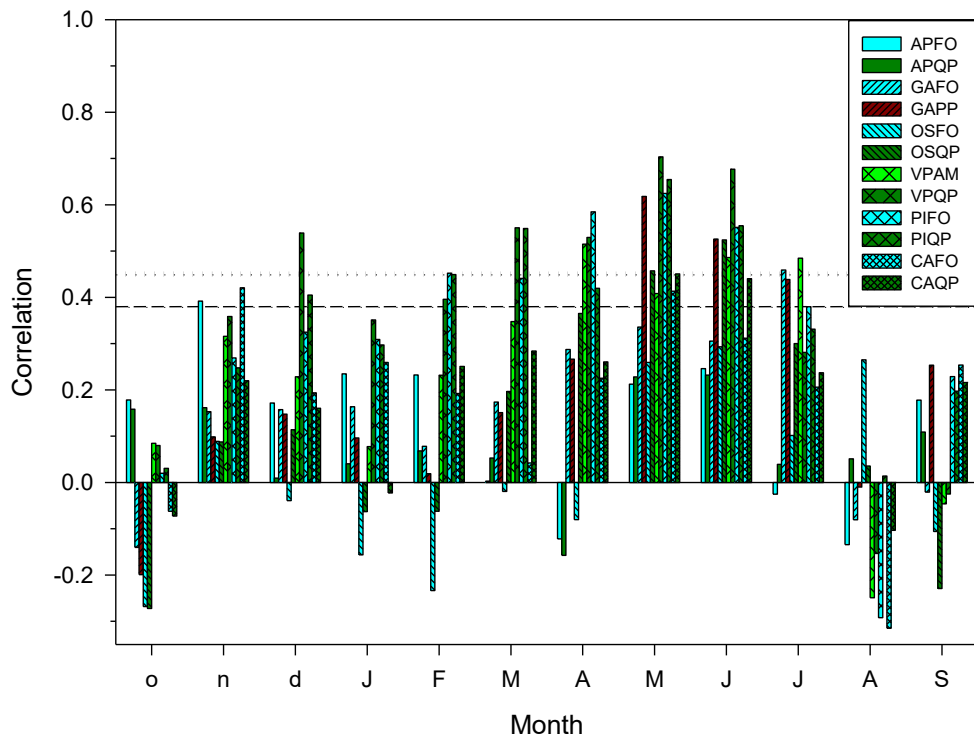


Figure S11. Soil moisture-growth correlations (Pearson coefficients) calculated for the study sites and species. Dashed and dotted lines indicate the 0.05 and 0.01 significance levels, respectively. See sites' codes in Table 1.

3.9 References

1. Allen C. D., Breshears D. D., McDowell N.G., 2015. On underestimation of global vulnerability to tree mortality and forest die off from hotter drought in the Anthropocene. *Ecosphere* 6: 1–55. <https://doi.org/10.1890/ES15-00203.1>
2. Anderegg W. R., Schwalm C., Biondi F., Camarero J. J., Koch G., Litvak M. et al. 2015. Pervasive drought legacies in forest ecosystems and their implications for carbon cycle models. *Science* 349: 528–532. DOI: 10.1126/science.aab1833
3. Backhaus S., Kreyling J., Grant K., Beierkuhnlein C., Walter J., Jentsch A., 2014. Recurrent mild drought events increase resistance toward extreme drought stress. *Ecosystems* 17: 1068–1081. DOI: 10.1007/s10021-014-9781-5
4. Barton K., 2022. MuMIn: Multi-Model Inference. Available online: <https://cran.r-project.org/web/packages/MuMIn/index.html> (accessed on 22 July 2022).
5. Bates D., Mächler M., Bolker B., Walker S., 2015. Fitting Linear Mixed-Effects Models Using lme4. *J. Stat. Soft.* 67: 1–48. <https://doi.org/10.48550/arXiv.1406.5823>
6. Batllori E., Lloret F., Aakala T., Anderegg W.R.L., Aynekulu E., et al., 2020. Forest and woodland replacement patterns following drought-related mortality. *Proc. Natl. Acad. Sci. U.S.A.* 117: 29720–29729. <https://doi.org/10.1073/pnas.2002314117>
7. Bochenek Z., Ziolkowski D., Bartold M., Orłowska K., Ochtyra A., 2018. Monitoring forest biodiversity and the impact of climate on forest environment using high-resolution satellite images. *Eur. J. Rem. Sens.* 51: 166–181. <https://doi.org/10.1080/22797254.2017.1414573>
8. Bréda N., Huc R., Granier A., Dreyer E., 2006. Temperate forest trees and stands under severe drought: A review of ecophysiological responses, adaptation processes and long-term consequences. *Ann. For. Sci.* 63: 625–644. <https://doi.org/10.1051/forest:2006042>
9. Camarero J.J., Franquesa M., Sangüesa-Barreda G., 2015. Timing of drought triggers distinct growth responses in holm oak: implications to predict

- warming-induced forest defoliation and growth decline. *Forests* 6: 1576–1597. <https://doi.org/10.3390/f6051576>
10. Camarero J.J., Sangüesa-Barreda G., Vergarechea M., 2016. Prior height, growth, and wood anatomy differently predispose to drought-induced dieback in two Mediterranean oak species. *Ann. For. Sci.* 73: 341–351. DOI: 10.1007/s13595-015-0523-4
 11. Camarero J.J., Gazol A., Sangüesa-Barreda G., Cantero A., Sánchez-Salguero R., Sánchez-Miranda A., Granda E., Serra-Maluquer X., Ibañez R., 2018. Forest growth responses to drought at short- and long-term scales in Spain: squeezing the stress memory from tree rings. *Front. Ecol. Evol.* 6: 9. <https://doi.org/10.3389/fevo.2018.00009>
 12. Camarero J.J., Gazol A., Linares J.C., Fajardo A., Colangelo M., Valeriano C., Sánchez-Salguero R., Sangüesa-Barreda G., Granda E., Gimeno T.E., 2021. Differences in temperature sensitivity and drought recovery between natural stands and plantations of conifers are species-specific. *Sci. Tot. Env.* 796: 148930. <https://doi.org/10.1016/j.scitotenv.2021.148930>
 13. Castagneri D., Vacchiano G., Hacket-Pain A., DeRose R.J., Klein T. and Bottero A., 2022. Meta-analysis reveals different competition Effects on tree growth resistance and resilience to drought. *Ecosystems* 25: 30–43. DOI: 10.1007/s10021-021-00638-4
 14. Caudullo G., & De Rigo D., 2016. *Fraxinus ornus* in Europe: distribution, habitat, usage and threats. *The European Atlas of Forest Tree Species: Modelling, Data and Information on Forest Tree Species*, Publ. Off. EU, Luxembourg 100-101.
 15. Cavender-Bares J., Holbrook N.M., 2001. Hydraulic properties and freezing-induced cavitation in sympatric evergreen and deciduous oaks with contrasting habitats. *Plant, Cell & Env.* 24: 1243–1256. <https://doi.org/10.1046/j.1365-3040.2001.00797.x>
 16. Choat B., Brodribb T.J., Brodersen C.R., Duursma R.A., López R., Medlyn B.E., 2018. Triggers of tree mortality under drought. *Nature* 558: 531–539. DOI: 10.1038/s41586-018-0240-x

17. Colangelo M., Camarero J.J., Battipaglia G., Borghetti M., De Micco V., Gentilesca T., Ripullone F., 2017. A multi-proxy assessment of dieback causes in a Mediterranean oak species. *Tree Physiol.* 37: 617–631. DOI: 10.1093/treephys/tpx002
18. Colangelo M., Camarero J.J., Borghetti M., Gentilesca T., Oliva J., Redondo M.A., Ripullone F., 2018. Drought and *Phytophthora* are associated with the decline of oak species in southern Italy. *Frontiers Plant Sci.* 9. <https://doi.org/10.3389/fpls.2018.01595>
19. Coluzzi R., Fascetti S., Imbrenda V., Italiano S.S.P., Ripullone F., Lanfredi M., 2020. Exploring the use of Sentinel-2 data to monitor heterogeneous effects of contextual drought and heatwaves on Mediterranean forests. *Land* 9: 325. <https://doi.org/10.3390/land9090325>
20. Cook E.R., Krusic P.J., Peters K., Holmes R.L., 2017. Program ARSTAN (version 49), Autoregressive tree-ring standardization program. Tree-Ring Laboratory of Lamont–Doherty Earth Observatory, Columbia University, USA.
21. Cornes R., van der Schrier G., van den Besselaar E.J.M., Jones P.D., 2018. An Ensemble Version of the E-OBS Temperature and Precipitation Datasets. *J. Geophys. Res. Atmos.* 123.
22. Damesin C., Rambal S., 1995. Field study of leaf photosynthetic performance by a Mediterranean deciduous oak tree (*Quercus pubescens*) during a severe summer drought. *New Phytol.* 131: 159–167. <https://doi.org/10.1111/j.1469-8137.1995.tb05717.x>
23. Dobbertin M., 2005. Tree growth as indicator of tree vitality and of tree reaction to environmental stress: a review. *Eur. J. For. Res.* 124, 319–333. <https://doi.org/10.1007/s10342-005-0085-3>
24. Fritts H.C., 1976. *Tree Rings and Climate*. Academic Press, London.
25. Gärtner H., Nievergelt D., 2010. The core-microtome: A new tool for surface preparation on cores and time series analysis of varying cell parameters. *Dendrochronologia* 28(2), 85–92. <https://doi.org/10.1016/j.dendro.2009.09.002>
26. Gazol A., Camarero J.J., Vicente-Serrano S.M., Sánchez-Salguero R. et al., 2018. Forest resilience to drought varies across biomes. *Glob Change Biol.* 24:2143–2158. <https://doi.org/10.1111/gcb.14082>

27. Gentilesca T., Camarero J.J., Colangelo M., Nolè A., Ripullone F., 2017. Drought-induced oak decline in the western Mediterranean region: An overview on current evidences, mechanisms and management options to improve forest resilience. *iForest Biogeosci. For.* 10: 796. <https://doi.org/10.3832/ifor2317-010>
28. Gessler A., Bottero A., Marshall J., Arend M., 2020. The way back: recovery of trees from drought and its implication for acclimation. *New Phytol.* 228: 1704–1709. <https://doi.org/10.1111/nph.16703>
29. Gonzalez de Andres E., Gazol A., Querejeta J.I., Igual J.M., Colangelo M., Sánchez-Salguero R., Camarero J.J., 2022. The role of nutritional impairment in carbon-water balance of silver fir drought-induced dieback. *Glob. Change Biol.* 28: 4439–4458. <https://doi.org/10.1111/gcb.16170>
30. Guada G., Camarero J. J., Sanchez-Salguero R. and Cerrillo R.M.N., 2016. Limited growth recovery after drought-induced forest dieback in very defoliated trees of two pine species. *Front. Plant Sci.* 7: 418. <https://doi.org/10.3389/fpls.2016.00418>
31. Holmes R.L., 1983. Computer-assisted quality control in tree-ring dating and measurement. *Tree-Ring Bull.* 43: 68–78.
32. Huang M., Wang X., Keenan T.F., Piao S., 2018. Drought timing influences the legacy of tree growth recovery. *Glob Change Biol.* 24: 3546–3559. <https://doi.org/10.1111/gcb.14294>
33. Ingrisch J., Bahn M., 2018. Towards a comparable quantification of resilience. *Trends Ecol. Evol.* 33: 251–259. <https://doi.org/10.1016/j.tree.2018.01.013>
34. Italiano S. S., Camarero J. J., Borghetti M., Colangelo M., Pizarro M., Ripullone F., 2023. Radial growth, wood anatomical traits and remote sensing indexes reflect different impacts of drought on Mediterranean forests. *For. Ecol. Manage.* 548: 121406. <https://doi.org/10.1016/j.foreco.2023.121406>
35. Jacquet J. S., Bosc A., O'Grady A., Jactel H., 2014. Combined effects of defoliation and water stress on pine growth and non-structural carbohydrates. *Tree Physiol.* 34: 367–376. <https://doi.org/10.1093/treephys/tpu018>
36. Jiang P., Liu H., Piao S., Ciais P., Wu X., Yin Y., Wang H., 2019. Enhanced growth after extreme wetness compensates for post-drought carbon

- loss in dry forests. Nat. Comm. 10: 195. <https://doi.org/10.1038/s41467-018-08229-z>
37. Johnstone J.F., Allen C.D., Franklin J.F., Frelich L.E., Harvey B.J., Higuera P.E., Mack M.C., Meentemeyer R.K., Metz M.R., Perry G.L.W., Schoennagel T., Turner M.G., 2016. Changing disturbance regimes, ecological memory, and forest resilience. *Front Ecol Environ* 14: 369–378. <https://doi.org/10.1002/fee.1311>
38. Jump A.S., Ruiz-Benito P., Greenwood S., Allen C.D., Kitzberger T., Fensham R., Martínez-Vilalta J., Lloret F., 2017. Structural overshoot of tree growth with climate variability and the global spectrum of drought-induced forest dieback. *Glob. Change Biol.* 23: 3742–3757. <https://doi.org/10.1111/gcb.13636>
39. van Kampen R., Fisichelli N., Zhang Y., Wason J., 2022. Drought timing and species growth phenology determine intra-annual recovery of tree height and diameter growth. *AoB Plants*, 14(3), plac012. <https://doi.org/10.1093/aobpla/plac012>
40. Kannenberg S. A., Schwalm C. R. and Anderegg W.R., 2020. Ghosts of the past: how drought legacy effects shape forest functioning and carbon cycling. *Ecol. Lett.* 23: 891–901. <https://doi.org/10.1111/ele.13485>
41. Kiorapostolou N., Petit G., Dannoura M., 2019. Similarities and differences in the balances between leaf, xylem and phloem structures in *Fraxinus ornus* along an environmental gradient. *Tree Physiol.* 39: 234–242. <https://doi.org/10.1093/treephys/tpy095>
42. Kowarik I., 2023. The Mediterranean tree *Acer monspessulanum* invades urban greenspaces in Berlin. *Dendrobiology*, 89: 20–26. <https://doi.org/10.12657/denbio.089.002>
43. Lemoine D., Peltier J., Marigo G., 2001. Comparative studies of the water relations and the hydraulic characteristics in *Fraxinus excelsior*, *Acer pseudoplatanus* and *A. opalus* trees under soil water contrasted conditions. *Ann. Sci. For.* 58: 723–731. <https://doi.org/10.1051/forest:2001159>

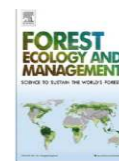
44. Lloret F., Keeling E.G., Sala A., 2011. Components of tree resilience: effects of successive low-growth episodes in old ponderosa pine forests. *Oikos* 120: 1909–1920. <https://doi.org/10.1111/j.1600-0706.2011.19372.x>
45. Lloret F., Lobo A., Estevan H., Maisongrande P., Vayreda J., Terradas J., 2007. Woody plant richness and NDVI response to drought events in Catalanian (northeastern Spain) forests. *Ecology* 88: 2270–2279. <https://doi.org/10.1890/06-1195.1>
46. Nakagawa S., Johnson P.C.D., Schielzeth H., 2017. The coefficient of determination R^2 and intra-class correlation coefficient from generalized linear mixed-effects models revisited and expanded. *J. R. Soc. Interface* 14. <https://doi.org/10.1098/rsif.2017.0213>
47. Ogle K., Barber J.J., Barron-Gafford G.A., Bentley L.P., Young J.M., Huxman T.E., Loik M.E., Tissue D.T., 2015. Quantifying ecological memory in plant and ecosystem processes. *Ecol. Lett.* 18. 221–235. <https://doi.org/10.1111/ele.12399>
48. Ouyang S. N., Gessler A., Saurer M., Hagedorn F., Gao D. C. et al., 2021. Root carbon and nutrient homeostasis determines downy oak sapling survival and recovery from drought. *Tree Physiology*, 41(8), 1400-1412. <https://doi.org/10.1093/treephys/tpab019>
49. Pardos M., Del Río M., Pretzsch H., Jactel H., Bielak et al., 2021. The greater resilience of mixed forests to drought mainly depends on their composition: Analysis along a climate gradient across Europe. *Forest Ecology and Management*, 481, 118687. <https://doi.org/10.1016/j.foreco.2020.118687>
50. Peltier D.M., Ogle K., 2019. Legacies of more frequent drought in ponderosa pine across the western United States. *Global Change Biol.* 25: 3803–3816. <https://doi.org/10.1111/gcb.14720>
51. Pignatti S., 1982. *Flora d'Italia*, Edagricole, Bologna, Italy.
52. Pinheiro J.C., Bates D.M., 2000. *Mixed-Effects Models in S and S-PLUS*. Springer, New York.
53. Portoghesi L., Chiocchini U., Dossi V., Alivernini A., 2008. Osservazioni geopedologiche e dendrometriche in popolamenti a dominanza di acero trilobo

- (*Acer monspessulanum* L.) sui Monti della Tolfa (Roma). *L'Italia Forestale e Montana* 63: 241-257. DOI: 10.4129/IFM.2008.3.03
54. Poyatos R., Llorens P., Piñol J., Rubio C., 2008. Response of Scots pine (*Pinus sylvestris* L.) and pubescent oak (*Quercus pubescens* Willd.) to soil and atmospheric water deficits under Mediterranean mountain climate. *Annals of Forest Science* 65: 306. DOI: 10.1051/forest:2008003
55. Pretzsch H., 2021. Trees grow modulated by the ecological memory of their past growth. Consequences for monitoring, modelling, and silvicultural treatment. *For. Ecol. Manage.* 487: 118982. <https://doi.org/10.1016/j.foreco.2021.118982>
56. Pretzsch H., Schütze G., & Uhl E., 2013. Resistance of European tree species to drought stress in mixed versus pure forests: evidence of stress release by inter-specific facilitation. *Plant Biology*, 15(3), 483-495. <https://doi.org/10.1111/j.1438-8677.2012.00670.x>
57. R Development Core Team. R., 2022. A Language and Environment for Statistical Computing; R Foundation for Statistical Computing: Vienna, Austria.
58. Rita A., Camarero J.J., Nolè A., Borghetti M., Brunetti M. et al., 2020. The impact of drought spells on forests depends on site conditions: The case of 2017 summer heat wave in southern Europe. *Glob Chang Biol.* 26: 851–863. <https://doi.org/10.1111/gcb.14825>
59. Rodell M., Houser P.R., Jambor U., Gottschalck J., Mitchell K., Meng C.J. et al., 2004. The global land data assimilation system. *Bull. Am. Meteor. Soc.* 85: 381–394. <https://doi.org/10.1175/BAMS-85-3-381>
60. Ruehr N.K., Grote R., Mayr S., Arneth A., 2019. Beyond the extreme: recovery of carbon and water relations in woody plants following heat and drought stress. *Tree Physiol.* 39: 1285–1299. <https://doi.org/10.1093/treephys/tpz032>
61. Schwalm C.R., Anderegg W.R.L., Mchalak A.M. et al., 2017. Global patterns of drought recovery. *Nature* 548: 202–205. DOI: 10.1038/nature23021
62. Schwarz J., Skiadaresis G., Kohler M. et al., 2020. Quantifying growth responses of trees to drought—a critique of commonly used resilience indices

- and recommendations for future studies. *Curr. For. Rep* 6: 185–200. DOI: 10.32942/osf.io/5ke4f
63. Sergent A.S., Rozenberg P., Bréda N., 2014. Douglas-fir is vulnerable to exceptional and recurrent drought episodes and recovers less well on less fertile sites. *Annals of Forest Science* 71: 697–708. DOI 10.1007/s13595-012-0220-5
64. Serra-Maluquer X., Granda E., Camarero J.J., Vilà-Cabrera A., Jump A.S. et al., 2021. Impacts of recurrent dry and wet years alter long-term tree growth trajectories. *J. Ecol.* 109: 1561–1574. <https://doi.org/10.1111/1365-2745.13579>
65. Shaw M., Rights J.D., Sterba S.K., Flake J.K., 2020. r2mlm: R-Squared Measures for Multilevel Models; 2020. Available online: <https://github.com/mkshaw/r2mlm> (accessed on 22 July 2022).
66. Tissier J., Lambs L., Peltier J. P., Marigo G., 2004. Relationships between hydraulic traits and habitat preference for six *Acer* species occurring in the French Alps. *Ann. For. Sci.* 61: 81–86. <https://doi.org/10.1051/forest:2003087>
67. Tomasella M., Casolo V., Aichner N., Petruzzellis F., Savi T., Trifilò P., Nardini A., 2019. Non-structural carbohydrate and hydraulic dynamics during drought and recovery in *Fraxinus ornus* and *Ostrya carpinifolia* saplings. *Plant Physiol. Biochem.* 145, 1–9. <https://doi.org/10.1016/j.plaphy.2019.10.024>
68. Tucker C.J., Sellers P., 1986. Satellite remote sensing of primary production. *International Journal of Remote Sensing* 7: 1395–1416. <https://doi.org/10.1080/01431168608948944>
69. Valeriano C., Gazol A., Colangelo M. & Camarero J. J., 2021. Drought drives growth and mortality rates in three pine species under Mediterranean conditions. *Forests*, 12: 1700. <https://doi.org/10.3390/f12121700>
70. Vicente-Serrano S.M., Beguería S., López-Moreno J.I., 2010. A multiscalar drought index sensitive to global warming: The standardized precipitation evapotranspiration index. *J. Clim.* 23: 1696–1718. <https://doi.org/10.1175/2009JCLI2909.1>
71. Yu X., Orth R., Reichstein M., Bahn M., Klosterhalfen A., Knohl A., Koebsch F., Migliavacca M., Mund M., Nelson J. A., Stocker B. D., Walther S., Bastos A., 2022. Contrasting drought legacy effects on gross primary

productivity in a mixed versus pure beech forest. *Biogeosciences* 19: 4315–4329. <https://doi.org/10.5194/bg-19-4315-2022>

72. Zhang Y., Keenan T.F. and Zhou S., 2021. Exacerbated drought impacts on global ecosystems due to structural overshoot. *Nat. Ecol. Evol.* 5: 1490–1498. <https://doi.org/10.1038/s41559-021-01551-8>



4. RADIAL GROWTH, WOOD ANATOMICAL TRAITS AND REMOTE SENSING INDEXES REFLECT DIFFERENT IMPACTS OF DROUGHT ON MEDITERRANEAN FORESTS

4.1 Abstract

Drought reduces canopy cover, productivity and tree growth in forests. However, there is still little knowledge on how drought affects coupling between canopy greenness assessed by remote sensing and hydraulic conductivity detected by wood anatomy. This combination could improve the understanding of forest response to climate change. Thus, we investigated the impacts of a hot drought, which occurred in summer 2017, on radial growth, earlywood hydraulic diameter (Dh), a proxy of conductivity, and several remote-sensing indices in mixed Mediterranean hardwood forests (*Quercus pubescens* Willd. – *Fraxinus ornus* L.). In general, growth showed a higher coherence among trees and a higher responsiveness to climate. Growth decreased during the drought year, particularly for *Q. pubescens*, which showed high defoliation and dieback intensity. Both species showed a decline of Dh in 2018 after the drought and subsequent warm winter conditions. We found positive relationships between Dh and remote-sensing data for *Q. pubescens* in some of these vulnerable sites, where (i) growth was constrained by dry spring-summer conditions and (ii) Dh and growth covaried. These findings indicate a high variability among sites and tree species in their responses to drought considering earlywood anatomy, growth canopy cover and water content. However, some common patterns emerge such as links between potential hydraulic conductivity (Dh), tree cover and Dh-growth covariation in the most impacted sites. Further, *F. ornus* seem to perform better in terms of growth under drought conditions, showing less mortality and dieback than *Q. pubescens*. Future studies

could explore how water transport and changes in canopy cover respond to dry and warm conditions and if that covariation indicates vulnerability to drought.

Keywords: EVI; *Fraxinus ornus*; hydraulic diameter; NDVI; NDWI; *Quercus pubescens*.

4.2 Introduction

Worldwide climate extremes such as droughts and heat waves are affecting forest ecosystems by reducing their productivity, cover and modifying their composition and structure, often triggering dieback episodes (Allen et al. 2015). Several tree-ring studies have evidenced a drought-related reduction of radial growth and resilience associated with a higher mortality risk (Gazol et al. 2018, DeSoto et al. 2020). Furthermore, droughts can cause changes in the wood anatomy by reducing the vessel lumen area and the hydraulic conductivity as has been observed in several ring-porous oak species (Corcuera et al. 2004, Colangelo et al. 2017). Thus, wood anatomical variables can record environmental signals including climate extremes (Fonti et al. 2010). Furthermore, wood anatomical variables such as the number and area (lumen) of vessels could be more meaningful and functional measures of post-drought resilience than tree-ring width (Schwarz et al. 2020). Using wood-anatomical variables such as lumen area or vessel density can allow overcoming some critical issues encountered when using tree-ring width to assess drought impacts such as different responses to spring or summer droughts between co-occurring species due to different xylem phenology or dynamics of use of stored carbon (Michelot et al. 2012).

However, several studies have noted that forests responses to climate events such as droughts depend on local factors such as site latitude, elevation, aspect, soil type and forest composition (Lloret et al. 2007, Rita et al. 2020). These studies have often assessed the impacts of droughts at continental to local scales using satellite-derived vegetation indices which are proxies of forest health, cover or greenness. Among these indices, one of the most widely used is the Normalized Different Vegetation Index (NDVI) (Rouse et al. 1973), which is very sensitive to

photosynthetic activity and has been widely used to assess the health and productivity of drought-prone oak forests (e.g., Coluzzi et al. 2020, Khoury and Coomes 2020, Vicente-Serrano et al. 2020). The NDVI was subsequently improved by developing the Enhanced Vegetation Index (EVI) (Huete et al. 1997), which reduces soil noise, atmospheric aerosols and the saturation of the reflectance signal at high levels of green biomass (Matsushita et al. 2007). The EVI has been widely used for investigating forest dieback allowing for an improved signal in thinned areas (Dionisio et al. 2012, Huang and Xia 2019). It has been observed that forest growth and dieback are captured by the NDVI and EVI variability, at least in seasonally dry Mediterranean forests (Ogaya et al. 2015). To get information about water stress of vegetation the Normalized Difference Water Index (NDWI) was developed and used to estimate the water content of canopies and determining drought stress (Gao 1996, Cheng et al. 2006, Sturm et al. 2022).

In addition to spatial variability, allocation shifts in stressed trees could lead to decoupled responses of canopy cover, growth and wood anatomy to climate (Mašek et al. 2023). Thus, the potential of remote sensing information to assess drought impacts on forests is evident, but it should be complemented by growth and wood anatomy data which may be more responsive proxies of drought stress (Gazol et al. 2018). Some studies have used tree ring and remote sensing series to better analyze the response of forests to extreme climate events such as droughts or frosts with variable results (Gazol et al. 2018, Moreno-Fernández et al. 2022, Tonelli et al. 2023, Vicente-Serrano et al. 2013, Wang et al. 2021); but few studies have yet compared remote sensing with wood anatomical variables such as earlywood vessel lumen area which provide sub-annual information (Fonti et al. 2010, Prendin et al. 2020).

This study aimed to analyze the responses of mixed hardwood forests to a severe drought by using radial growth, earlywood anatomy and remote-sensing indices (NDVI, EVI and NDWI). We assessed if these variables covary as a function of climatic variations in two coexisting porous-ring species (*Quercus pubescens*, *Fraxinus ornus*) vegetating in four sites characterized by different environmental conditions.). By comparing the responses of these species, we sought to determine which of the proxies used (anatomical variables, vegetation indices) best highlight

the impact of the drought event and thus which sites or species were most affected by the drought.

We expect that: (i) cover (e.g., NDVI, EVI) and growth (tree-ring width and area) variables would be positively related; and (ii) canopy water content (e.g., NDWI) and wood-anatomical variables related to hydraulic conductivity (e.g., earlywood hydraulic diameter) would be also positively related.

Given that *Q. pubescens* adopts a water-spending (anisohydric) strategy (Damesin and Rambal 1995, Poyatos et al. 2008, Rosner 2012), severe drought events could expose this species more to hydraulic collapse and dieback. *Fraxinus ornus*, on the other hand, seems to have a relatively isohydric strategy and shows a good control of reserves useful for rapid post-drought recovery (Tomasella et al. 2019). Indeed, *F. ornus* under conditions of reduced soil water availability, manages to allocate relatively more to leaf biomass and conductive phloem (Kiorapostolou and Petit 2018) trying to counteract the impact of drought. Therefore, we expect the oak species (*Q. pubescens*) to be more sensitive and responsive to climatic stresses and changes in tree cover and greenery, in terms of growth and wood anatomy, than the ash species (*F. ornus*). Further, we expect to find the strongest associations between climate, cover-greenness variables (e.g., NDVI), growth (ring area) and wood anatomical variables in the most drought-stressed, least productive site. However, in colder sites we expect that the 2017 warm conditions would improve growth. Lastly, we also expect that comparing the response of *Q. pubescens* and *F. ornus* may provide useful insights into future trajectories of the Mediterranean forest community under climate change, with relevant management implications.

4.3 Material and methods

4.3.1 Study area

The study sites are mixed Mediterranean hardwood forests located in the Basilicata region, southern Italy (Fig. 1). Sites were selected because they showed damage after the 2017 extreme summer drought event (Fig. S1) with symptoms such as: leaf browning, premature leaf shedding, canopy dieback and elevated tree mortality (Coluzzi et al. 2020). Four sites with different productivity and environmental conditions where *Quercus pubescens* and *Fraxinus ornus* coexisted were selected.

The sites presented different elevations, slopes and aspects (Table 1). They are located on sandstone substrates and clay soils.

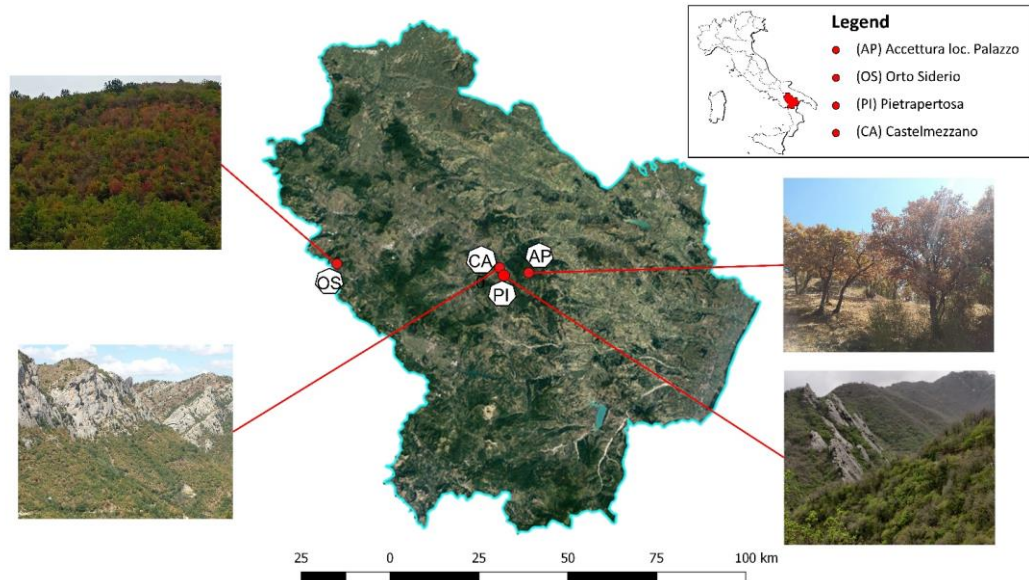


Figure 1. Sites studied (OS, CA, PI and CA) located in the Basilicata region, southern Italy. The images show the impacts of the 2017 summer drought on the studied forests. See site codes in Table 1.

Data from local meteorological stations close to the experimental sites were used to characterize the climatic conditions and variability (Table 1 and Table S1). The study area is subjected to Mediterranean climate conditions with warm and dry summers, cold winters and rainfall peaks in spring (March) and autumn (November). The Palazzo site (hereafter AP) located within the Accettura municipality territory is characterized by an average annual rainfall of 734 mm and an average annual temperature of 16 °C. The forest is a mixed oak-ash stand. The Orto Siderio site (hereafter OS), located within the Savoia di Lucania municipality territory, is also dominated by oak and ash with other minor hardwood species (*Crataegus orientalis* M. Bieb., *Quercus cerris* L. and *Ostrya carpinifolia* Scop). Here, the average annual rainfall is 889 mm and the average annual temperature is 13.0 °C. In this site, oak dieback was very evident with the highest mortality rate (61%) (Table 2). In the Pietrapertosa site (hereafter PI) *O. carpinifolia*, *C. orientalis* and *Pistacia terebinthus* L. are also found. The average annual rainfall is 671 mm

and the average annual temperature is 12.7 °C. Lastly, in the Castelmezzano site (hereinafter CA), oak and ash co-occur with *Acer monspessulanum* L., *Cornus mas* L. and *P. terebinthus* and the climatic conditions are similar to those of the PI site. All experimental sites are generally even aged and high forests, with the exception of the AP site where high forest and coppice coexist, with this latter being converted to high forest thanks to cessation of low coppice cuttings in the last decades. Indeed all these sites have been little or non exploited in the recent past because of difficulties to reach these locations.

4.3.2 Climate data and drought index

To calculate relationships between climate, growth, wood anatomy and remote sensing indices, as data from neighboring weather stations were too short and with heterogeneous time series (from 10 to 20 years), we used homogeneous, gap-filled climate series from the 0.1°-gridded EOBS climate dataset (v25.0e; Cornes et al. 2018). We obtained monthly data from April to September of mean maximum and minimum temperatures and total precipitation for the 2001–2021 period. Although they have coarse spatial resolutions which do not allow for a detailed site-specific climate distinction, we selected this dataset because it provides long and homogeneous regional climate records. In addition, we also calculated the annual averages of temperature (MAT) and precipitation (MAP) for each site, using data records from local meteorological stations (Table 1 and Table S1).

Soil moisture was estimated for a 0-10 cm depth from the 0.1°-gridded NASA Land Data Assimilation Systems (LDAS, <https://ldas.gsfc.nasa.gov/FLDAS/FLDASgoals.php>). Lastly, we calculated the 0.1°-gridded Standardized Precipitation Evapotranspiration Index (SPEI), which is a multi-scalar drought index computed from monthly rainfall, temperature and potential evapotranspiration showing cumulative water surplus or deficit (Vicente-Serrano et al. 2010). We considered 12-month long SPEI values from April to September.

4.3.3 Field sampling

At each of the four study sites, a series of structural surveys were carried out in 2021. At each site, an area of 5000 m² (circular shape) was identified that was representative of the entire forest stand in terms of structure, composition and soil conditions. In each plot, all tree diameters at breast height (1.30 m), heights, plant status (living/dead) and the percentage of defoliation for each plant (crown transparency >50% or <50%) were measured (Dobbertin 2005, Camarero et al. 2016). These measurements allowed to estimate for each stand tree density and basal area. Two transects of 50 m each were also carried out within each plot, along which it was possible to assess the projection of the crowns on the ground and thus the degree of canopy cover of each species. The assessment of the percentage cover was carried out not only to characterize each stand, but also to observe the canopy cover in the field and confirm the absence of clearings, rock formations or other types of cover other than tree crowns, which could have influenced or altered the remotely sensed vegetation indices.

4.3.4 Tree-ring width data

At each site, within each plot (5000 m²), 15 dominant trees of each of the two representative species (oak, ash) were randomly sampled. Dominant trees have been selected as they form forest cover predominantly detected by satellite images and also because they are less affected on growth rings than submissive trees by competition for light, nutrients and water. Then 30 trees per site were sampled, for each of which two wood cores were taken at 1.3 m using a Pressler increment borer. Cores were air-dried, and their surfaces were cut using a sledge core microtome to clearly distinguish ring boundaries (Gärtner and Nievergelt 2010). Tree rings were visually cross-dated under the binocular microscope by assigning characteristic rings (Fritts 1976). Then, tree-ring widths were measured to the nearest 0.01 mm using the LINTAB package (Rinntech, Heidelberg, Germany). The COFECHA program (Holmes 1983) was used to evaluate the visual cross-dating of the tree-ring series by calculating moving correlations between individual series and the mean series of each species in each site.

4.3.5 Quantitative earlywood anatomy

We selected six trees per site and one radius per tree to perform anatomical analyses of ash and oak earlywood (hereafter EW). Selected trees were those showing the highest correlation between their indexed ring-width series and the mean site series. Wood anatomy was analyzed for the common 2001–2021 period.

Following Fonti et al. (2010) the surface of the cores was cleaned with high-pressure water blasting to remove both tyloses and wood dust from the vessel lumina. To improve the contrast, the vessel lumens were filled with white chalk powder. High resolution images of the rings (see Fig. S2) were captured at 20–40 magnification using a binocular and a camera (Zeiss Axiocam 208 color). The EW vessels were considered those with lumen diameters $>50 \mu\text{m}$ and located in the first third section of the ring along the radial direction (Camarero et al. 2021). The EW lumen areas were measured in a tangential window of 2.5 mm using the ImageJ software (Schneider et al. 2012).

We quantified the following wood-anatomical traits following Scholz et al. (2013): ring area (mm^2), EW and latewood (LW) areas (mm^2), absolute and relative (%) areas occupied by vessels in the EW, EW vessel lumen area (μm^2) and vessel density. We also calculated two additional variables (Dh (μm), hydraulic diameter; Kh ($\text{kg m}^{-1} \text{s}^{-1} \text{MPa}^{-1}$), potential hydraulic conductivity) by considering the Hagen–Poiseuille lumen theoretical hydraulic conductivity for a vessel size (Tyree and Zimmermann 2002).

The hydraulic diameter (Dh) for all EW vessels measured in each ring was the average of $\sum d^5 / \sum d^4$, where d is the diameter of each EW vessel assuming a circular shape (Sperry et al. 1994). Lastly, the Kh of the EW was estimated as

$$Kh = (\rho \times \pi \times \sum d^4) / (128 \times \mu \times Ar) \quad (1)$$

where ρ is the density of water at 20 °C (998.2 kg m^{-3} at 20 °C), d is the vessel lumen diameter, μ is the viscosity of water ($1.002 \times 10^{-9} \text{ MPa s}$ at 20 °C) and Ar is the EW area imaged. We focused on EW vessels because they account for most of

the ring hydraulic conductivity, particularly in the outermost ring in the case of ring-porous species (Ellmore and Eweres 1985).

4.3.6 Remote sensing data

Analyses were performed using the Google Earth Engine platform (Gorelick et al. 2017) (<https://earthengine.google.com>, accessed 15 January 2023), for the 2001–2021 period, using Landsat scene collections for Top of the Atmosphere (TOA) reflectivity. A preliminary conversion from TOA scene reflectivity to surface reflectivity was performed, followed by atmospheric corrections and a cloudiness threshold of 40%. In addition, the data obtained from the different sensors (TM, ETM+ and OLI) of the Landsat satellites (L5, L7, L8 and L9) were harmonised to obtain as much data as possible over the reference period (i.e. about 2880 spectral index values analyzed). The analysis for each study site was conducted on a representative forest stand area of 5000 m², i.e. the area involved in the field sampling. Using these data, three indices (NDVI, EVI, NDWI) were obtained (see the formulas in Table S2) with a spatial resolution of 30 m. The NDVI and EVI indices are used to characterize the canopy cover and photosynthetic activity, while the NDWI is used to examine the water content of the canopy. The indices were calculated at annual resolution or considering the seasons (prior winter, from December to February; spring, March to May; summer, June to August; autumn, September to November) or only the growing season (April to September). Furthermore, using the Landsat image collections, we obtained the summer land surface temperature for each site (Ermida et al. 2020). To achieve this, we considered the wavelength of the thermal infrared bands (TIRS 1 and TIRS 2) with a spatial resolution of 100 m. In this way, we assessed the thermal emissivity of the soil to evaluate the impact of the 2017 drought on vegetation (Fig. S3).

4.3.7 Statistical analyses

Since the growth (ring area) and EW anatomy variables (Dh) used did not show any significant trend (Kendall τ tests, $p > 0.05$), we did not detrend their series which were averaged for each site and species. However, all annual or seasonal remote sensing indices showed significant positive trends ($p < 0.05$) due to the growth of

tree cover and greenness over time. We removed these trends by fitting linear regression to the indices series and then subtracting observed minus fitted values so as to obtain residuals. To assess the changes in EW Dh between consecutive years we calculated ratios between the Dh of the current (year t) and previous (year t-1) years in each site. Comparisons between sites or species were assessed using non-parametric Mann-Whitney tests.

Finally, to assess relationships between variables such climate, the SPEI drought index, Dh and remote-sensing indices we calculated Pearson correlations considering seasonal climatic values (mean temperatures and soil moisture; total precipitation) of the prior winter (December to February) and the growing season (April to September). Statistical analyses were done using the PAST software (Hammer et al. 2001).

4.4 Results

4.4.1 *The 2017 drought and stand structure*

Both the local climate data and the satellite-derived summer land surface temperature showed very dry and warm conditions in 2017, followed by warm conditions in 2018 (Figs. S1 and S3).

The lowest growing-season NDVI (0.67) and NDWI (0.20) values were found in site CA, whilst site AP showed the highest EVI (0.48) value (Table 2). Overall, the mortality rate was higher ($p = 0.03$) in oak (24%), particularly in site OS, than in ash (1%), but the basal area was also higher in the case of oak (19.2 vs 3.9 m² ha⁻¹; $p = 0.03$).

4.4.2 *Growth and EW anatomy responses to the 2017 drought*

The annual ring area was similar between *Q. pubescens* (2.4 mm²) and *F. ornus* (2.2 mm²) (Table 3). A similar result was found for the EW (1.1 vs. 0.8 mm²) and LW areas (1.3 vs. 1.4 mm²). Both the EW Dh and Kh were higher ($p = 0.02$) in *Q. pubescens* (286 μm, 12.2 10⁻¹⁰ Kg m⁻¹ s⁻¹ MPa⁻¹) than in *F. ornus* (146 μm, 1.9 10⁻¹⁰ Kg m⁻¹ s⁻¹ MPa⁻¹). The highest Dh and Kh values were found for *Q. pubescens* in sites AP and OS, and the lowest Dh and Kh values for *F. ornus* from OS site (Table 3).

The mean Dh series of *Q. pubescens* and *F. ornus* were positively correlated in three out of the four study sites (AP, $r = 0.60$, $p = 0.004$; PI, $r = 0.65$, $p = 0.001$; CA, $r = 0.56$, $p = 0.008$), whereas the ring-area series were not significantly correlated in any study site.

In 2017, the ring area of both tree species dropped in OS and PI sites (Fig. 2). In OS, both species recovered ring area values in 2018. Regarding the EW Dh, it decreases in 2018 in all sites, particularly in the case of *Q. pubescens* (Fig. 3). The Dh reduction in 2018 was the strongest in site PI and the weakest in site CA (Fig. S4). There were positive and significant relations between ring area and EW Dh in the case of *Q. pubescens* in sites AP, OS and CA and in the case of *F. ornus* in site OS (Fig. 4).

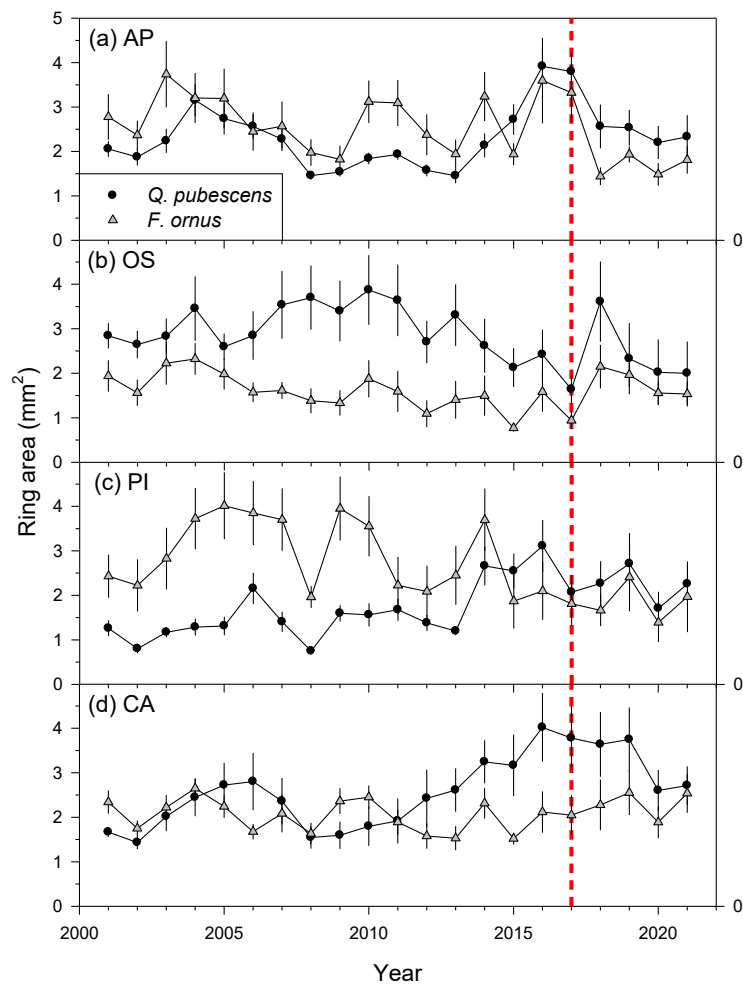


Figure 2. Ring area values measured for *Q. pubescens* and *F. ornus* in the four study sites (AP, OS, PI and CA). The dashed vertical line shows the 2017 drought. Values are means \pm SE.

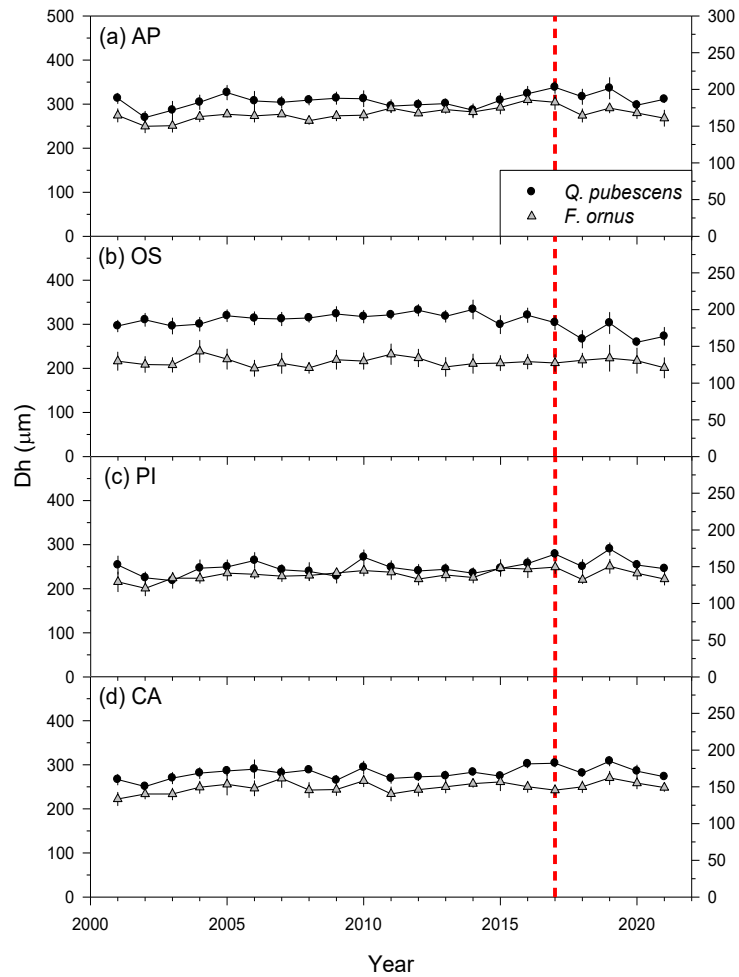


Figure 3. Earlywood hydraulic diameters (D_h) for *Q. pubescens* and *F. ornus* in the four study sites. The dashed vertical line shows the 2017 drought. Values are means \pm SE.

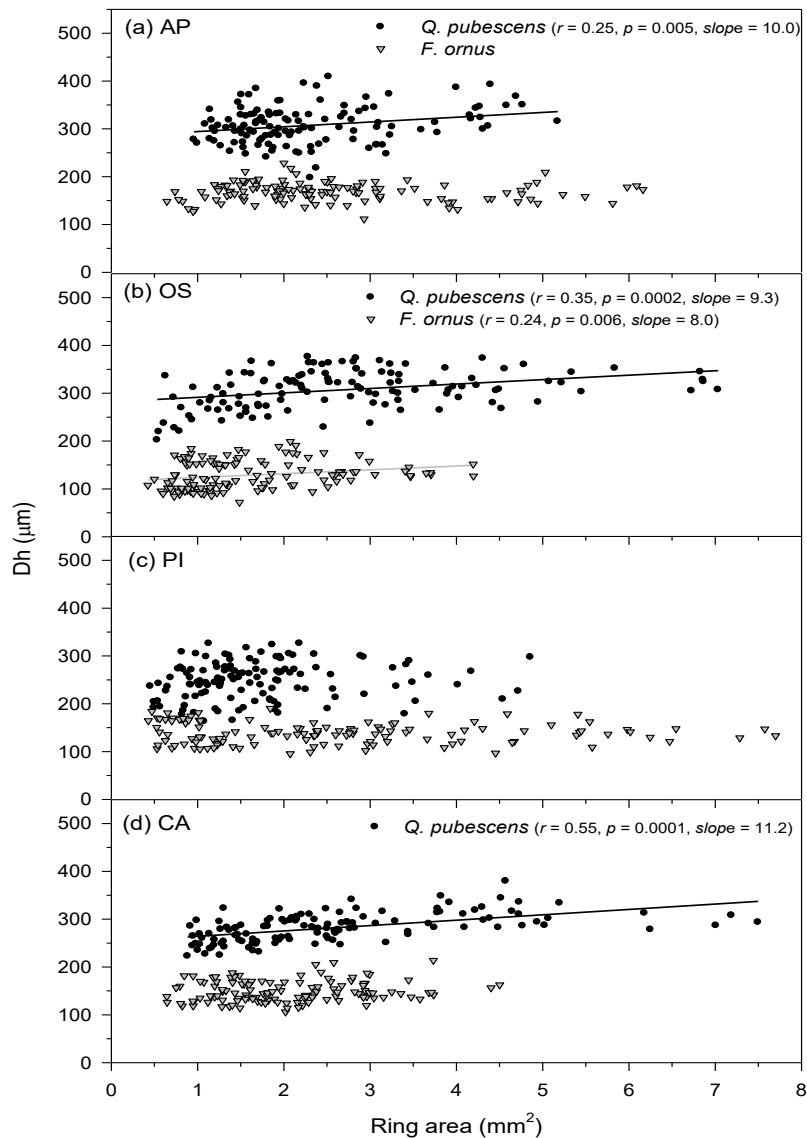


Figure 4. Relationships between ring area and the earlywood hydraulic diameter (Dh) in the four study sites. Lines show significant ($p < 0.05$) linear regressions between both variables. Statistics show the correlation coefficients (r), its significance level (p) and the slopes of regressions.

Lastly, the within-site coherence (Pearson correlations) among individual series of ring-area was higher than that among individual series of EW Dh in the case of *Q. pubescens* (0.61 mm^2 vs. $0.27 \text{ } \mu\text{m}$, $p = 0.02$) and also in the case of *F. ornus* (0.45 mm^2 vs. $0.15 \text{ } \mu\text{m}$, $p = 0.03$) (Table S3). The mean coherence of Dh series was high (0.41) only in site PI and in the case of *Q. pubescens*, whereas in the case of ring area it peaked in site AP and also for *Q. pubescens* (0.74).

4.4.3 Relationships between growth, wood anatomy and remote-sensing indices

We detected drops of the prior-winter and the growing-season NDVI in 2017-2018 in site OS, but the growing-season NDWI increased in site AP (Fig. 5). In site AP, the growing-season NDWI and the *Q. pubescens* ring area were positively related (Fig. 5a). In site OS, the *Q. pubescens* EW Dh was positively correlated with the prior-winter NDVI (Fig. 5b) and the growing-season EVI (Fig. 5c).

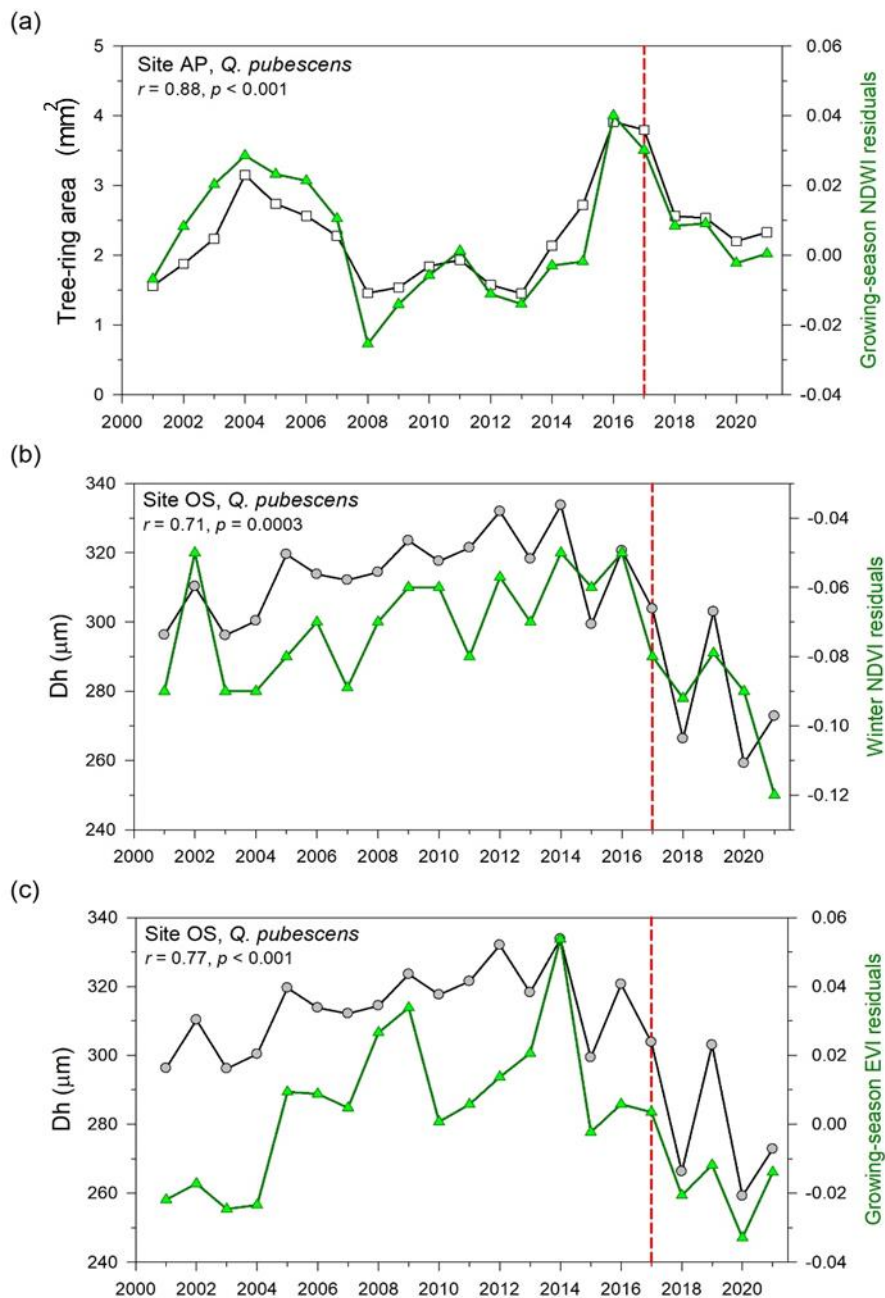


Figure 5. Main relationships found between remote-sensing variables and ring area (a) or hydraulic diameter (*Dh*) (b and c). The dashed vertical line indicates the 2017 drought.

4.4.4 Relationships between climate, growth, earlywood anatomy and remote-sensing indices

Radial growth was enhanced by wet-cool conditions in spring and summer in *Q. pubescens* from sites OS and CA and *F. ornus* from site PI (Table 4). Warm prior autumn to winter conditions also improved *Q. pubescens* growth. In sites OS and PI, a high spring-summer SPEI was positively related to *F. ornus* growth. The EW Dh of both species was enhanced by cool prior December conditions (Table 4). In sites CA, PI and OS, the EW Dh of *F. ornus* increased in response to wet conditions from February to May.

Few significant correlations, and only in some sites, were found when relating climate variables, including the SPEI, and the remote-sensing indices. In site OS, the NDVI and the EVI showed positive relationship with the April-September precipitation ($r = 0.52, p = 0.02$ and $r = 0.55, p = 0.009$, respectively). Only in this site we found a positive association between prior-winter precipitation and the NDVI ($r = 0.42, p = 0.04$). In the same site, the May and June soil moisture were positively related to the NDWI ($r = 0.46, p = 0.05$) and NDVI ($r = 0.52, p = 0.02$) series, respectively. Again in site OS, the June maximum temperature negatively correlated with the NDVI ($r = -0.54, p = 0.01$) and the NDWI ($r = -0.66, p = 0.002$). In site AP, the growing season NDVI ($r = -0.46, p = 0.05$) and the EVI ($r = -0.69, p = 0.001$) were negatively related to the 12-month SPEI, whereas in site PI the April NVWI was negatively correlated with the SPEI ($r = -0.50, p = 0.04$).

4.5 Discussion

Overall, the associations observed between climate, growth, earlywood anatomy and remote-sensing indices were contingent on site conditions and species' characteristics. Similar results have been found in a previous paper at larger scale in Mediterranean environment (Rita et al. 2020). Indeed, the impact of summer drought greatly depended on site conditions since elevation, exposure and vegetation type influence this response. These diverse relationships indicate that the impact of the 2017 drought on forest growth and productivity was heterogeneous. For instance, the growth drop due to the 2017 drought was evident in some sites (e.g., site OS) but not in others (e.g., site AP). The fact that in AP growth declined

in 2018 could be likely related to a delayed response to the summer 2017 drought. Furthermore, in this site, wet winter-spring conditions improved *Q. pubescens* growth, allowing trees to grow abundantly before the summer drought arrives. This was also shown by the positive relationship to the growing-season NDWI, that can be explained by the high oak cover of this site, which was dominated by *Q. pubescens*. This finding emphasizes the need of a reliable description of stand structure and composition when analyzing mixed forests using remote-sensing information.

Interestingly, the most impacted site OS also presented: (i) the highest percentage of dead *Q. pubescens* trees, (ii) a strong covariation between growth and earlywood hydraulic diameter (EW Dh) of both species, and (iii) positive associations between the EW Dh of *Q. pubescens* and remote-sensing indices (EVI, NDVI). Indeed, this site with relatively high slope and clay soils was probably the most vulnerable to the negative impacts of the 2017 summer hot drought. Nevertheless, although more sensitive, site OS was not the least productive site, as expected, according to remote-sensing data. This is most likely due to the fact that the remotely sensed data returns an average value of the entire mixed stand. Thus, the ash tree, which was already present with a developed canopy in the dominated strip of the forest, as a result of the death or desiccation of the oak tree canopies, still maintained the green cover (as an underlying green layer) by exploiting the available light gaps. This could be the reason why the remote sensing indices did not perceive significant reductions in greenness compared to the other sites.

We found a reduction of the 2018 EW Dh in three out of the four study sites (AP, OS and PI). In the most vulnerable site OS, this post-drought reduction was also observed in the NDVI and EVI. Such carry-over could have been caused by the warm conditions during the 2017-2018 winter leading to smaller earlywood vessels in 2018. In previous studies on Mediterranean oaks, both a low coherence among trees and a negative association between winter temperatures and EW Dh were also found (Alla and Camarero 2012). Such decrease in Dh led to a reduced potential hydraulic conductivity in 2018 which was not translated into reduced radial growth, therefore confirming a high recovery capacity of the study stands.

This recovery capacity has been observed in other drought-prone Mediterranean stands (Gazol et al. 2018) and could be due to post-drought thinning to alterations in stand structure and composition due to the death or defoliation of the canopy of the most affected sites (e.g. the OS site) (Coluzzi et al. 2020).

The results presented suggest a probable reorganisation and improved response of *F. ornus* at sites such as OS and CA, where *Q. pubescens* showed greater defoliation, but surviving oak trees also showed a high resumption of growth after drought. At these more affected sites, the increased dieback and death of *Q. pubescens* may have reduced competition for water and soil nutrients in favour of surviving conspecifics and *F. ornus*. Furthermore, the reduction in competitors may not only favour the availability of resources for the individuals that have tolerated the disturbance, but also allow for an increase in the drought resistance of forest stands.

These responses depend not only on site characteristics (Rita et al. 2020), but also on forest structure and stand composition (Lloret et al. 2007). As expected, *Q. pubescens* was more responsive to climate and changes in tree cover and greenness (higher growth-Dh covariation, higher correlations with NDVI, EVI and NDWI than *F. ornus*, excepting the high growth-SPEI correlations found in site PI.). A similar growth-Dh covariation has also been observed in other ring-porous tree species (Camarero et al. 2021), and it has been hypothesised that significant deviations of the growth-anatomy covariation could indicate stress conditions.

In less impacted sites such as AP, *Q. pubescens* could have formed most of their ring before the 2017 drought onset or it may have relied more on stored non-structural carbohydrates than *F. ornus* to grow (Colangelo et al. 2017). The temporal mismatch between growth phenology (xylogenesis) and drought timing influences growth legacies and could explain these different responses (Camarero et al. 2015, 2018, Huang et al. 2018). Such carry-over effects and/or the occurrence of compound climate events (in our case, drought followed by a warm winter) would also explain the reduction in the 2018 vessel lumen area. In addition, different carbon allocation patterns could explain differences between coexisting species. For example, *F. ornus* allocates more carbon to leaf biomass and phloem to compensate for the negative impacts of reduced soil water availability on

stomatal conductance (Kiorapostolou and Petit 2018). In addition, embolism phenomena leading to tree desiccation and dieback should also be investigated. Not only drought but also the increase in CO₂ would seem to influence xylem embolism phenomena in different forest species (Tognetti et al. 1999), e.g. significant effects of high CO₂ concentrations on the loss of hydraulic conductivity were observed in *Q. pubescens*, while the response was less pronounced in *F. ornus*.

4.5.1 Management implications

Adaptive forest management could be used for managing dieback stands through targeted and flexible interventions on the stand structure, composition and regeneration (Gentilesca et al. 2017). By reducing competition and structural homogeneity and by promoting biodiversity, forests could be less vulnerable to drought (Borghetti 2012). Useful actions, at the early stages of dieback with widespread defoliation, would be interventions on understory vegetation to increase the available soil moisture. This attempts to retain water in the soil and promote the degradation of organic matter and nutrient availability. Selective thinning could be performed to increase resilience by reducing intra- and inter-specific competition (Gentilesca et al. 2017), favouring selected trees which better recover after drought. Thus, in our case, action should be taken to reduce stand density but also to favour *Q. pubescens* (with greater defoliation and mortality rates than *F. ornus*) in order to maintain the composition of the mixed forest and to improve forest resilience. Furthermore, for highly degraded sites, regeneration should be encouraged, and the production of viable seed should be enhanced. Therefore, regeneration cuts should be anticipated in order to replace declining trees with young trees that are more resistant to stress events and with higher viable seed production.

4.6 Conclusions

We analyzed the impacts of a hot summer drought on growth, earlywood anatomy (hydraulic diameter) and remote-sensing indices (NDVI, EVI and NDWI) in mixed hardwood forests. We found disparate responses depending on site conditions and the considered species. At all sites, the species analysed showed a reduction in ring area as a consequence of the 2017 drought extreme event. This reduction in growth

was less evident at the AP site, which is located at a higher altitude and therefore probably experienced the heat wave later than the other stands. At this site, the trees probably took advantage of the non-structural carbohydrates for radial growth during the drought and then suffered the disturbance in the following year, unlike all the other sites.

Furthermore, looking at the local climatic data (Table 1), we see that the AP site, despite being located at a higher altitude, is the warmest site, with higher average temperatures than the other sites and higher maximum temperatures reached in 2017. It is probably also for this reason that in 2017 the plants at the AP site did not show sharp drops in performance (reduction in ring area) as at other sites, because the stand may have already adapted over time to warmer thermal conditions.

While a year after the drought a general decline in Dh was observed, probably as a consequence of dry summer conditions followed by a warm winter more evident for *Q. pubescens*. Overall, the data obtained seem to indicate a better condition of *F. ornus* than *Q. pubescens* even in the most impacted sites. Indeed drought resistant ash species may progressively outcompete more mesic oak species in the mixed Mediterranean forest under a drought-prone climate, with relevant effects for forest management and ecosystem services at the landscape scale. The information obtained from our study will be useful in improving our understanding of the relationships between growth, wood anatomy and remote sensing and will allow us to supplement our knowledge of the understudied *F. ornus*. Further research could consider investigating how changes in stand composition or structural diversity influence tree growth, wood anatomy and forest productivity and how these changes determine forest vulnerability to drought.

4.7 Tables

Table 1. Characteristics of the four study sites where *Q. pubescens* and *F. ornus* coexist and were sampled. MAT and MAP are the annual averages of temperature and precipitation for each site, obtained using data records from local meteorological stations (Table S1).

Site (code)	Longitude E	Latitude N	Elevation (m a.s.l.)	Slope (%)	Aspect	Substrate	MAT (°C)	MAP (mm)	Average temperature hottest month (July) (°C)	Average temperature coldest month (January) (°C)	Maximum temperature hottest month (July2017) (°C)	Annual rainfall 2017 (mm)
Accettura Palazzo (AP)	16.148	40.516	790	15	W	Sandstone	16	734	26	7	39,6	548
Orto Siderio (OS)	15.546	40.573	600	35	N-NW	Clay	13	889	23	5	35,5	628
Pietrapertosa (PI)	16.058	40.533	625	35	N-NW	Sandstone	12,7	671	22	4	35	548
Castellmezzano (CA)	16.054	40.534	665	50	S-SE	Sandstone	12,7	671	22	4	35	548

Table 2. Structural and vegetation characteristics of the four stands analysed. Breast diameter values (dbh) are the mean \pm SD of each species. Remote sensing indices are calculated for the growing season (April to September) and for the period 2001-2021.

Site	Sampled species	Stem density (Ind ha ⁻¹)	Dbh (cm)	Basal area (m ² ha ⁻¹)	Dead trees in each species (%)	Crown defoliation 51-100% (%)	Canopy cover (%)	NDVI	EVI	NDWI
AP	<i>F. ornus</i>	220	16.0 \pm 3.8	4.87	0	0	25	0.73	0.48	0.25
	<i>Q. pubescens</i>	580	19.0 \pm 6.6	18.06	0	45	72			
OS	<i>F. ornus</i>	560	9.0 \pm 3.2	3.96	0	7	60	0.74	0.45	0.29
	<i>Q. pubescens</i>	720	18.0 \pm 6.8	20.88	61	89	35			
PI	<i>F. ornus</i>	300	7.0 \pm 0.7	0.82	0	0	40	0.74	0.45	0.26
	<i>Q. pubescens</i>	1300	14.0 \pm 5.1	23.39	11	45	62			
CA	<i>F. ornus</i>	1260	8.0 \pm 2.4	5.97	3	10	66	0.67	0.45	0.20
	<i>Q. pubescens</i>	640	16.0 \pm 6.5	14.56	19	84	45			

Table 3. Mean growth and anatomical variables calculated for each species and study site. The dbh values are means \pm SD of the six trees sampled per site of each species. Values of ring area, earlywood (EW) and latewood (LW) area, hydraulic diameter (Dh) and hydraulic conductivity (Ks) are also means \pm SD calculated for the common period 2001-2021.

Site	Species	Dbh (cm)	Ring area (mm ²)	EW area (mm ²)	LW area (mm ²)	Dh (μ m)	Kh * 10 ⁻¹⁰ (Kg m ⁻¹ s ⁻¹ MPa ⁻¹)
AP	<i>F. ornus</i>	17.0 \pm 3.3	2.54 \pm 0.71	0.96 \pm 0.14	1.58 \pm 0.59	167.0 \pm 8.8	2.81 \pm 0.41
	<i>Q. pubescens</i>	19.0 \pm 4.2	2.30 \pm 0.70	1.30 \pm 0.25	1.01 \pm 0.52	307.5 \pm 16.2	16.74 \pm 4.97
OS	<i>F. ornus</i>	8.0 \pm 2.3	1.61 \pm 0.40	0.63 \pm 0.10	0.98 \pm 0.32	128.9 \pm 5.9	1.15 \pm 0.31
	<i>Q. pubescens</i>	26.0 \pm 8.2	2.88 \pm 0.67	1.22 \pm 0.16	1.46 \pm 0.50	306.4 \pm 20.0	16.28 \pm 3.90
PI	<i>F. ornus</i>	10.0 \pm 1.6	2.72 \pm 1.00	0.91 \pm 0.19	1.80 \pm 0.83	138.7 \pm 7.3	1.76 \pm 0.34
	<i>Q. pubescens</i>	17.0 \pm 4.4	1.76 \pm 0.65	0.80 \pm 0.15	0.96 \pm 0.53	249.1 \pm 17.0	5.92 \pm 1.88
CA	<i>F. ornus</i>	11.0 \pm 2.5	2.06 \pm 0.39	0.85 \pm 0.07	1.21 \pm 0.34	149.4 \pm 7.3	1.75 \pm 0.33
	<i>Q. pubescens</i>	21.0 \pm 4.9	2.66 \pm 0.93	1.01 \pm 0.17	1.65 \pm 0.77	281.1 \pm 14.0	9.78 \pm 2.68

Table 4. Pearson correlations between ring area or hydraulic diameter (Dh) and climate variables (period 2001-2021). Months abbreviated by lower- and upper-case letters correspond to the prior and current years, respectively. Only significant ($p < 0.05$) coefficients are presented.

Site AP, Ring area												
	o	n	d	J	F	M	A	M	J	J	A	S
Maximum temperature												
<i>Q. pubescens</i>		0.50										
<i>F. ornus</i>												
<hr/>												
Minimum temperature												
<i>Q. pubescens</i>		0.46										
<i>F. ornus</i>												
<hr/>												
Precipitation												
<i>Q. pubescens</i>					0.49			0.47				
<i>F. ornus</i>					0.58							
<hr/>												
Soil moisture												
<i>Q. pubescens</i>												
<i>F. ornus</i>												
<hr/>												
SPEI6												
<i>Q. pubescens</i>												
<i>F. ornus</i>		0.57										
<hr/>												
Site AP, Dh												
	o	n	d	J	F	M	A	M	J	J	A	S
Maximum temperature												
<i>Q. pubescens</i>					-0.58							
<i>F. ornus</i>					0.68							
<hr/>												
Minimum temperature												
<i>Q. pubescens</i>					-0.51							
<i>F. ornus</i>					-0.56							
<hr/>												
Precipitation												
<i>Q. pubescens</i>												
<i>F. ornus</i>												
<hr/>												
Soil moisture												
<i>Q. pubescens</i>												
<i>F. ornus</i>		0.52										
<hr/>												
SPEI6												
<i>Q. pubescens</i>												
<i>F. ornus</i>												
<hr/>												
Site OS, Ring area												
	o	n	d	J	F	M	A	M	J	J	A	S
Maximum temperature												
<i>Q. pubescens</i>		0.46										
<i>F. ornus</i>												
<hr/>												
Minimum temperature												
<i>Q. pubescens</i>		0.66	0.62									
<i>F. ornus</i>												
<hr/>												
Precipitation												
<i>Q. pubescens</i>									0.55	0.46		
<i>F. ornus</i>												
<hr/>												
Soil moisture												
<i>Q. pubescens</i>									0.50	0.49	0.55	
<i>F. ornus</i>												
<hr/>												
SPEI6												
<i>Q. pubescens</i>									0.47	0.57		
<i>F. ornus</i>											0.52	0.51
<hr/>												
Site OS, Dh												
	o	n	d	J	F	M	A	M	J	J	A	S
Maximum temperature												
<i>Q. pubescens</i>											-0.48	
<i>F. ornus</i>											-0.46	
<hr/>												
Minimum temperature												
<i>Q. pubescens</i>												
<i>F. ornus</i>												
<hr/>												
Precipitation												
<i>Q. pubescens</i>												
<i>F. ornus</i>										0.47		
<hr/>												
Soil moisture												
<i>Q. pubescens</i>												
<i>F. ornus</i>											0.48	
<hr/>												
SPEI6												
<i>Q. pubescens</i>												
<i>F. ornus</i>												
<hr/>												

Table 4. (cont.)

Site CA, Ring area												
Maximum temperature	o	n	d	J	F	M	A	M	J	J	A	S
<i>Q. pubescens</i>			0.60									
<i>F. ornus</i>												
Minimum temperature												
<i>Q. pubescens</i>						0.50						
<i>F. ornus</i>												
Precipitation												
<i>Q. pubescens</i>												
<i>F. ornus</i>												
Soil moisture												
<i>Q. pubescens</i>												
<i>F. ornus</i>												
SPEI6												
<i>Q. pubescens</i>												
<i>F. ornus</i>												
Site CA, Dh												
Maximum temperature	o	n	d	J	F	M	A	M	J	J	A	S
<i>Q. pubescens</i>			-0.58									
<i>F. ornus</i>			-0.47									
Minimum temperature												
<i>Q. pubescens</i>			-0.46									
<i>F. ornus</i>												
Precipitation												
<i>Q. pubescens</i>												
<i>F. ornus</i>					0.47							
Soil moisture												
<i>Q. pubescens</i>												
<i>F. ornus</i>						0.48						
SPEI6												
<i>Q. pubescens</i>												
<i>F. ornus</i>												

Site PI, Ring area												
Maximum temperature	o	n	d	J	F	M	A	M	J	J	A	S
<i>Q. pubescens</i>		0.46	0.62									
<i>F. ornus</i>												
Minimum temperature												
<i>Q. pubescens</i>					0.49							
<i>F. ornus</i>						0.51					-0.55	
Precipitation												
<i>Q. pubescens</i>												
<i>F. ornus</i>												
Soil moisture												
<i>Q. pubescens</i>												
<i>F. ornus</i>							0.64			0.48		
SPEI6												
<i>Q. pubescens</i>												
<i>F. ornus</i>							0.73	0.80	0.72	0.67	0.56	
Site PI, Dh												
Maximum temperature	o	n	d	J	F	M	A	M	J	J	A	S
<i>Q. pubescens</i>			-0.58									
<i>F. ornus</i>			-0.62									
Minimum temperature												
<i>Q. pubescens</i>			-0.46									
<i>F. ornus</i>			-0.49									
Precipitation												
<i>Q. pubescens</i>												
<i>F. ornus</i>												
Soil moisture												
<i>Q. pubescens</i>												
<i>F. ornus</i>									0.55			
SPEI6												
<i>Q. pubescens</i>												
<i>F. ornus</i>												

4.8 Supporting Information

Table S1. Local meteorological stations used to characterize climate conditions.

Site (code)	Meteorological station	Longitude E	Latitude N	Elevation (m a.s.l.)	Period
Accettura Palazzo (AP)	S. Mauro Forte	16° 15' 04''	40° 28' 54''	504	2006–2020
Orto-Siderio (OS)	Tito	15° 39' 25''	40° 34' 27''	729	2012–2020
Pietrapertosa (PI) Castellmezzano (CA)	Albano di Lucania	16° 02' 07''	40° 34' 55''	809	2000–2020

Table S2. Formulas of the remote-sensing indices (NDVI, EVI and NDWI). Abbreviations: where ρ_{NIR} , ρ_{Red} , ρ_{Blue} and ρ_{SWIR} represent the reflectance in the near-infrared, red, blue and short-wave infrared wavelengths, while (6) and (7.5) are the atmospheric correction coefficients, (2.5) is the gain factor and (1) is the ground correction factor.

Vegetation Index	Reference
$\text{NDVI} = (\rho_{\text{NIR}} - \rho_{\text{Red}}) / (\rho_{\text{NIR}} + \rho_{\text{Red}})$	Rouse et al., (1973)
$\text{EVI} = 2.5 (\rho_{\text{NIR}} - \rho_{\text{Red}}) / (\rho_{\text{NIR}} + 6\rho_{\text{Red}} - 7.5 \rho_{\text{Blue}} + 1)$	Huete et al., (1997)
$\text{NDWI} = (\rho_{\text{NIR}} - \rho_{\text{SWIR}}) / (\rho_{\text{NIR}} + \rho_{\text{SWIR}})$	Gao, (1996)

Table S3. Mean (\pm SD) Pearson correlation values among individual series of growth (ring area) and anatomical (Dh, earlywood hydraulic diameter) variables calculated for the common period 2001–2021.

Site	Species	Ring area	Dh
AP	<i>F. ornus</i>	0.40 \pm 0.16	0.15 \pm 0.21
	<i>Q. pubescens</i>	0.74 \pm 0.10	0.21 \pm 0.17
OS	<i>F. ornus</i>	0.39 \pm 0.23	0.14 \pm 0.20
	<i>Q. pubescens</i>	0.48 \pm 0.30	0.25 \pm 0.22
PI	<i>F. ornus</i>	0.61 \pm 0.13	0.12 \pm 0.27
	<i>Q. pubescens</i>	0.62 \pm 0.11	0.41 \pm 0.14
CA	<i>F. ornus</i>	0.44 \pm 0.21	0.17 \pm 0.20
	<i>Q. pubescens</i>	0.65 \pm 0.17	0.23 \pm 0.24

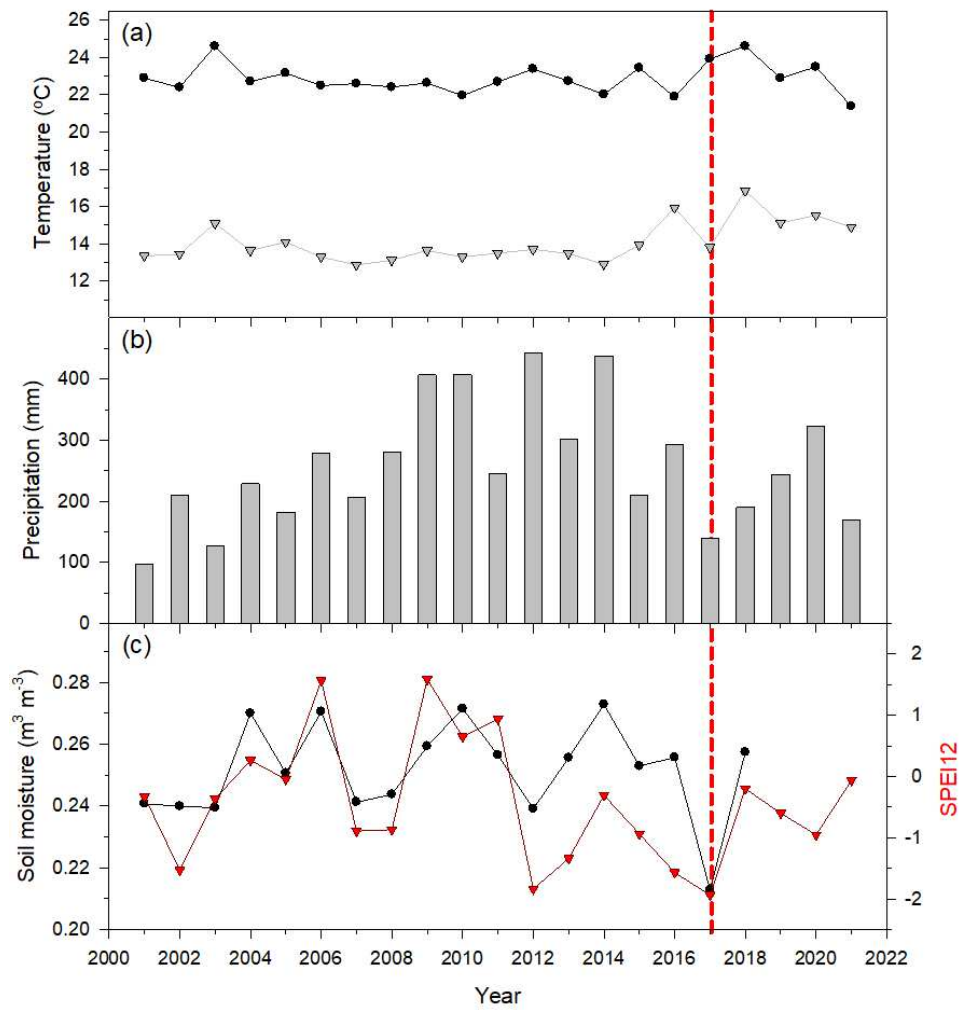
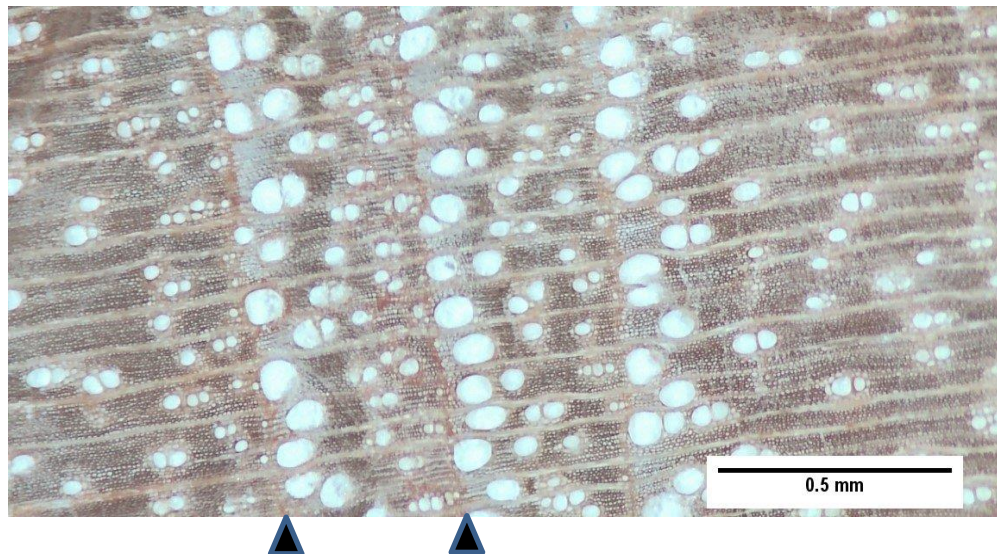


Figure S1. Annual climate data of the reference period, calculated considering only the growing season (April to September): (a) mean maximum and minimum temperatures; (b) precipitation; and (c), soil moisture (black line) and the 12-month September SPEI (SPEI12, red line). The dashed vertical line indicates the 2017 drought.

(a)



(b)

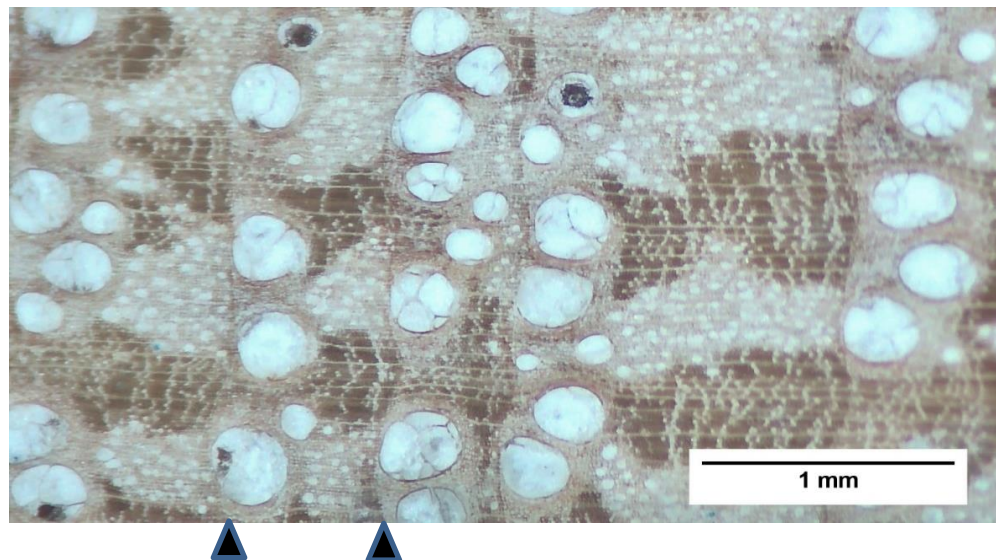


Figure S2. Wood cross-sections of (a) *Fraxinus ornus* and (b) *Quercus pubescens*. The black arrows delimit a typical narrow annual ring.

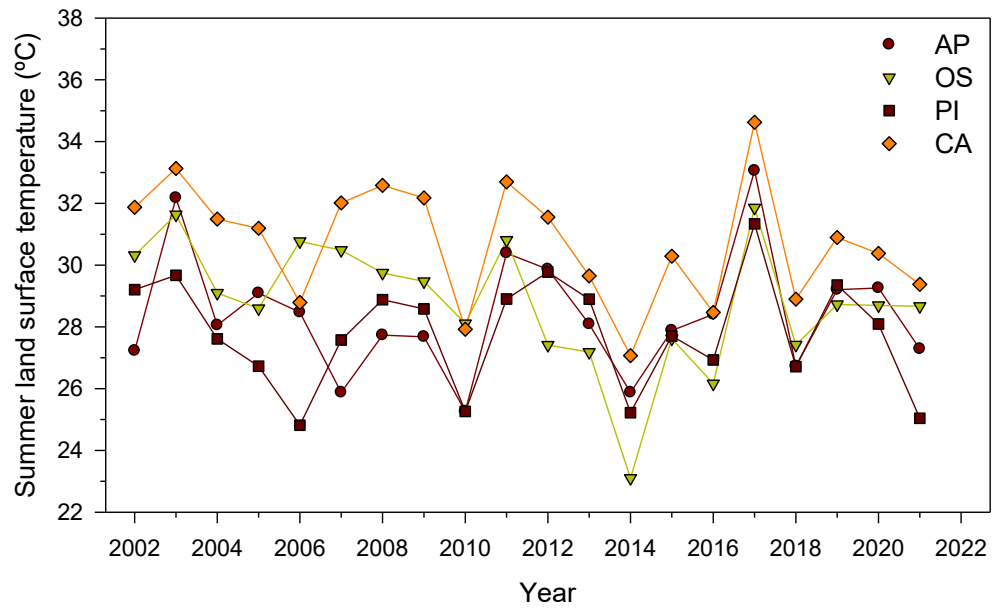


Figure S3. Summer land surface temperature in the four study sites during the period 2002-2021.

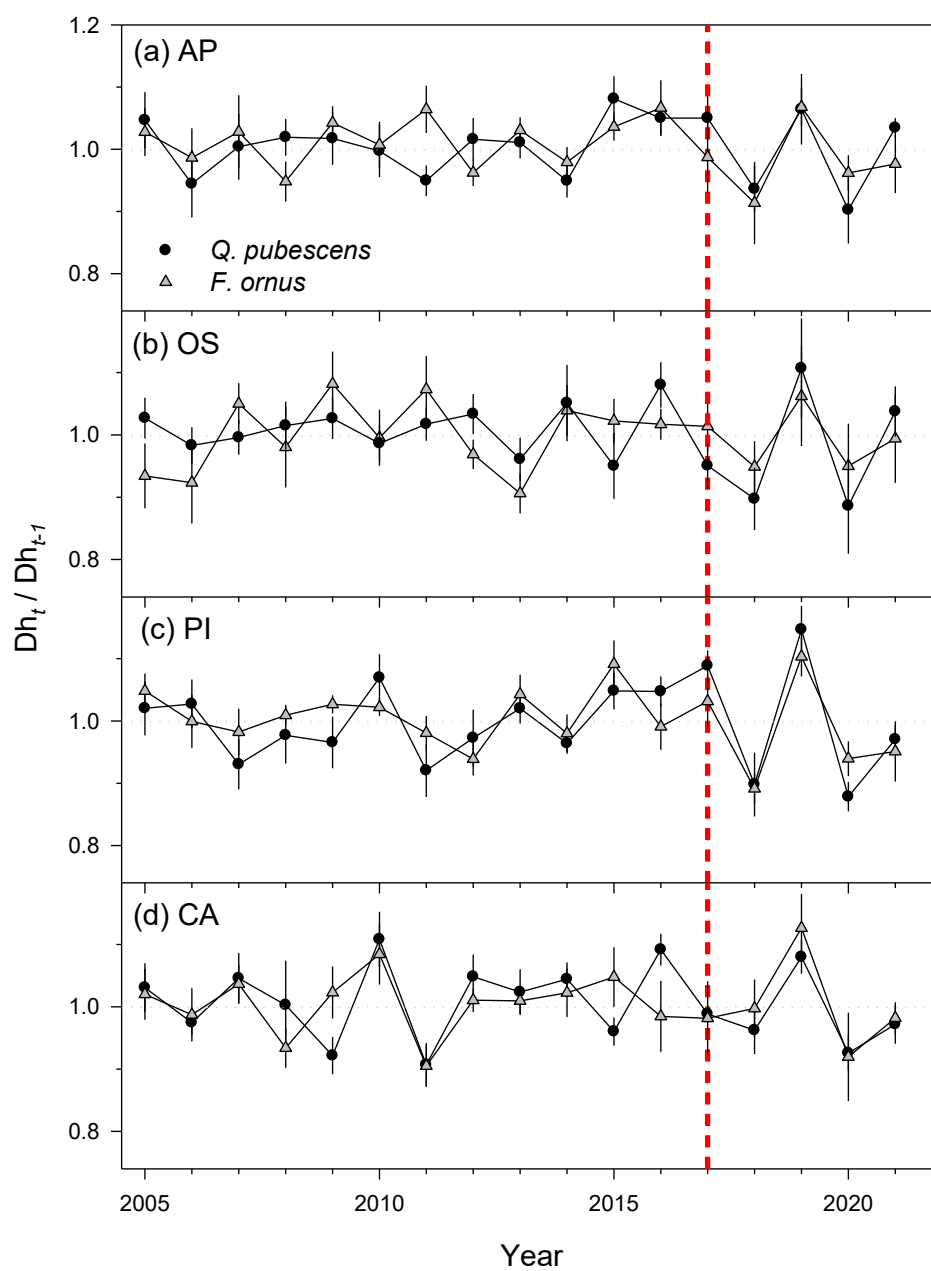


Figure S4. Ratios between the earlywood hydraulic diameter (Dh) of the current (year t) and previous (year $t-1$) years in the four study sites. The dashed vertical line indicates the 2017 drought. Values are means \pm SE.

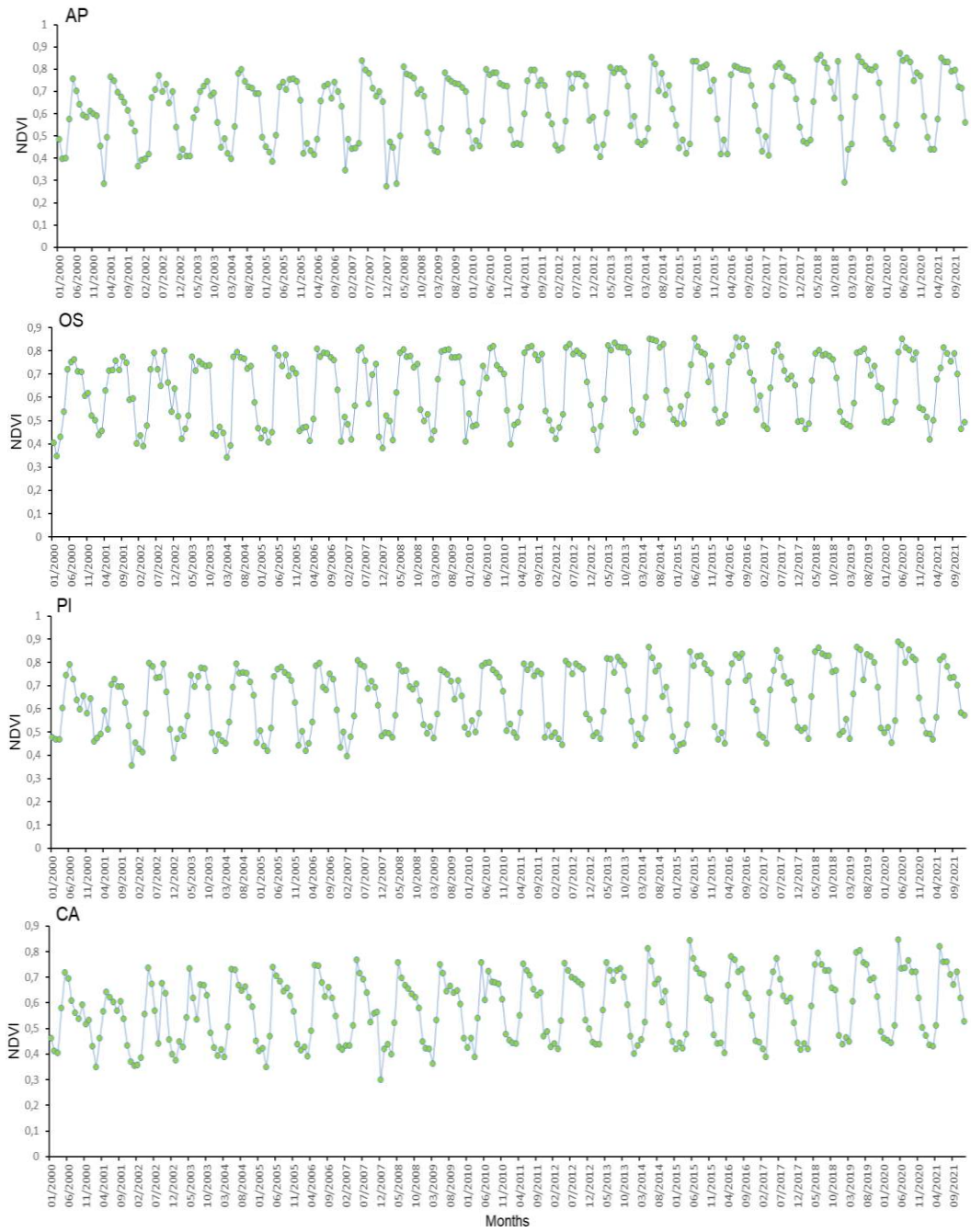


Figure S5. Monthly NDVI index trends over the last 20 years, at the 4 sites AP, OS, PI and CA.

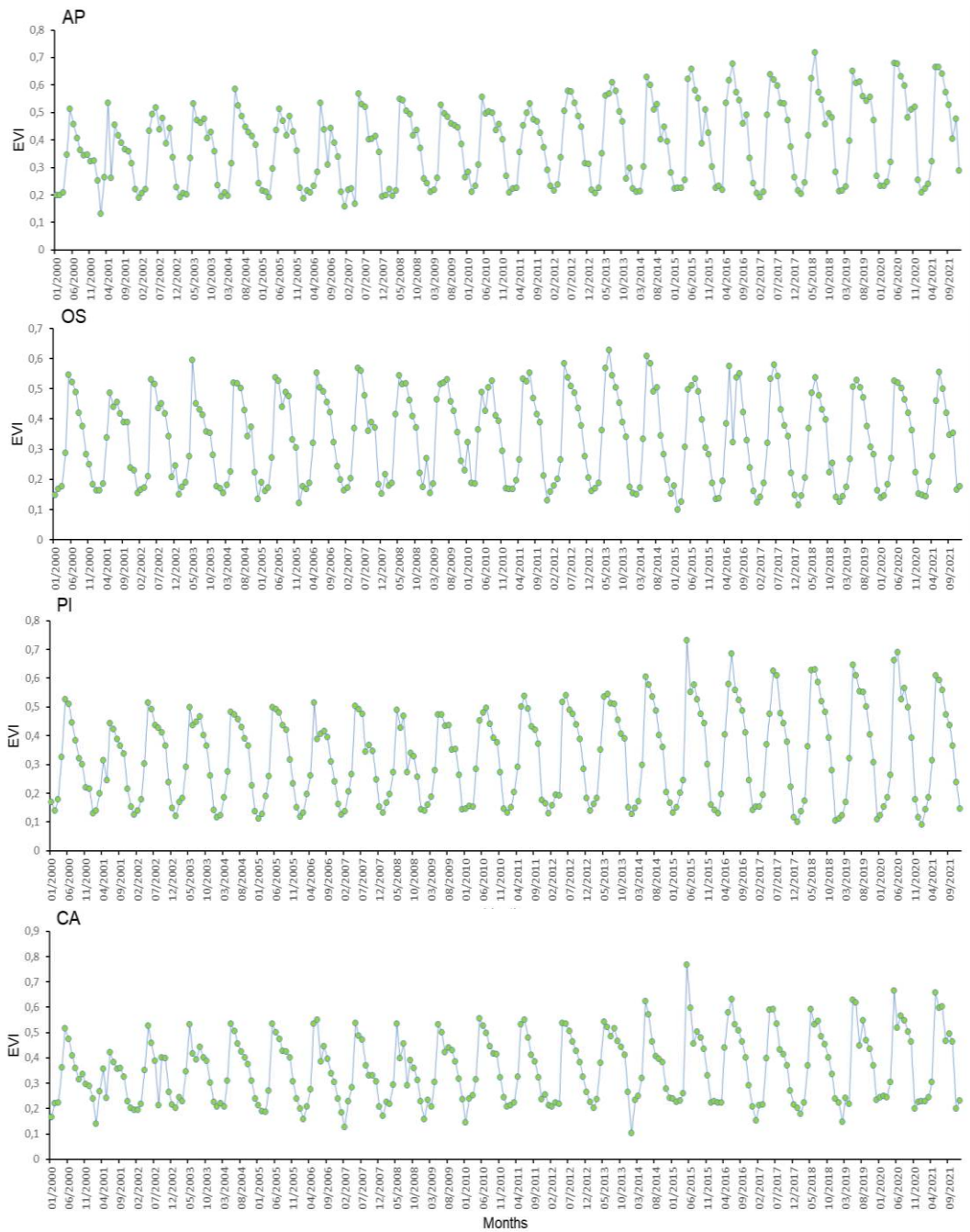


Figure S6. Monthly EVI index trends over the last 20 years, at the 4 sites AP, OS, PI and CA

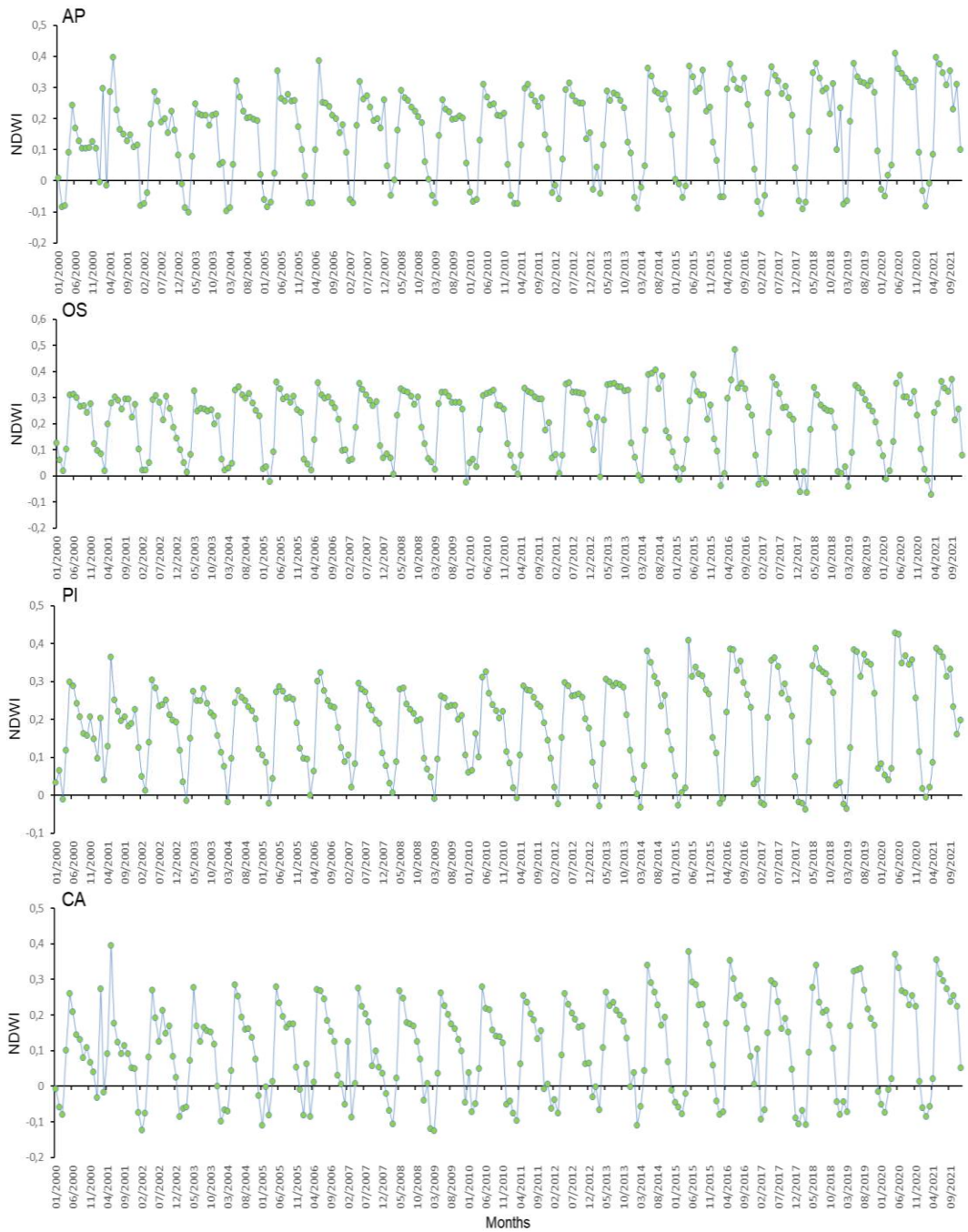


Figure S7. Monthly NDWI index trends over the last 20 years, at the 4 sites AP, OS, PI and CA.

4.9 References

1. Alla A.Q. and Camarero J.J., 2012. *Contrasting responses of radial growth and wood anatomy to climate in a Mediterranean ring-porous oak: implications for its future persistence or why the variance matters more than the mean*. Eur. J. Forest Res. 131: 1537–1550. DOI: 10.1007/s10342-012-0621-x .
2. Allen C.D., Breshears D.D., McDowell N.G., 2015. *On underestimation of global vulnerability to tree mortality and forest die-off from hotter drought in the Anthropocene*. Ecosphere 6:129. <http://dx.doi.org/10.1890/ES15-00203.1>
3. Borghetti M., 2012. *Principi fondanti, mosaico delle conoscenze e selvicoltura adattativa*. Forest@-Journal of Silviculture and Forest Ecology, 9(4), 166. <https://doi.org/10.3832/efor0699-009>
4. Camarero J.J., Franquesa M. and Sangüesa-Barreda G., 2015. *Timing of drought triggers distinct growth responses in holm oak: implications to predict warming-induced forest defoliation and growth decline*. Forests 6: 1576–1597. <https://doi.org/10.3390/f6051576>
5. Camarero J.J., Sangüesa-Barreda G., Vergarechea M., 2016. *Prior height, growth, and wood anatomy differently predispose to drought-induced dieback in two Mediterranean oak species*. Annals of Forest Science 73: 341–351. DOI:10.1007/s13595-015-0523-4.
6. Camarero J.J., Gazol A., Sangüesa-Barreda G., Cantero A., Sánchez-Salguero R., Sánchez-Miranda A., ...& Ibañez R., 2018. *Forest growth responses to drought at short- and long-term scales in Spain: squeezing the stress memory from tree rings*. Front. Ecol. Evol. 6: 9. DOI: 10.3389/fevo.2018.00009.
7. Camarero J.J., Colangelo M., Rodríguez-González P.M., Sánchez-Miranda A., Sánchez-Salguero R., Campelo F., Rita A., Ripullone F., 2021. *Wood anatomy and tree growth covary in riparian ash forests along climatic and ecological gradients*. Dendrochronologia 70, 125891.

<https://doi.org/10.1016/j.dendro.2021.125891>

8. Cheng Y. B., Zarco-Tejada P. J., Riaño D., Rueda C. A., Ustin S.L., 2006. *Estimating vegetation water content with hyperspectral data for different canopy scenarios: Relationships between AVIRIS and MODIS indexes*. Remote Sensing of Environment 105: 354–366. DOI:10.1016/j.rse.2006.07.005.
9. Colangelo M., Camarero J.J., Battipaglia G., Borghetti M., De Micco V., Gentilesca T. and Ripullone F., 2017. *A multi-proxy assessment of dieback causes in a Mediterranean oak species*. Tree Physiology 37: 617–631. DOI:10.1093/treephys/tpx002
10. Coluzzi R., Fascetti S., Imbrenda V., Italiano S.S.P., Ripullone F., Lanfredi M., 2020. *Exploring the Use of Sentinel-2 Data to Monitor Heterogeneous Effects of Contextual Drought and Heatwaves on Mediterranean Forests*. Land 9: 325. DOI:10.3390/land9090325
11. Corcuera L., Camarero J.J. and Gil-Pelegrín E., 2004. *Effects of a severe drought on growth and wood-anatomical properties of Quercus faginea*. IAWA J. 25: 185-204
12. Cornes R.C., van der Schrier G., van den Besselaar E.J.M., Jones P.D., 2018. *An ensemble version of the E-OBS temperature and precipitation data sets*. J. Geophys. Res. Atm. 123, 9391–9409. <https://doi.org/10.1029/2017JD028200>
13. Damesin C., & Rambal, S., 1995. *Field study of leaf photosynthetic performance by a Mediterranean deciduous oak tree (Quercus pubescens) during a severe summer drought*. New Phytol., 131(2), 159-167. <https://doi.org/10.1111/j.1469-8137.1995.tb05717.x>
14. DeSoto L., Cailleret M., Sterck F., Jansen S., Kramer K., Robert E.M.R., ... & Martínez-Vilalta, J., 2020. *Low growth resilience to drought is related to future mortality risk in trees*. Nat. Commun. 11: 545. <https://doi.org/10.1038/s41467-020-14300-5>

15. Dionisio M. A., Alcaraz-Segura D., Cabello J., 2012. *Satellite-based monitoring of ecosystem functioning in protected areas: recent trends in the oak forests (Quercus pyrenaica Willd.) of Sierra Nevada (Spain)*. International Perspectives on Global Environmental Change 355, 37.
16. Dobbertin M., 2005. *Tree growth as indicator of tree vitality and of tree reaction to environmental stress: a review*. Eur. J. Forest Res. 124: 319–333. <https://doi.org/10.1007/s10342-005-0085-3>
17. Ellmore G.S., Ewers F.W., 1985. *Hydraulic conductivity in trunk xylem of elm, Ulmus americana*. IAWA journal Bull. 6: 303–307.
18. Ermida S. L., Soares P., Mantas V., Götsche F. M., Trigo I. F., 2020. *Google Earth Engine open-source code for land surface temperature estimation from the Landsat series*. Remote Sens. 12, 1471. DOI:10.3390/rs12091471 .
19. Fonti P., von Arx G., García-González I., Eilmann B., Sass-Klaassen U., Gärtner H. and Eckstein, D., 2010. *Studying global change through investigation of the plastic responses of xylem anatomy in tree rings*. New Phytol. 185: 42–53. <https://doi.org/10.1111/j.1469-8137.2009.03030.x>
20. Fritts HC., 1976. *Tree Rings and Climate*. Academic Press, London.
21. Gao B.C., 1996. *NDWI-A normalized difference water index for remote sensing of vegetation liquid water from space*. Remote Sens. Environ. 58: 257–266. [https://doi.org/10.1016/S0034-4257\(96\)00067-3](https://doi.org/10.1016/S0034-4257(96)00067-3)
22. Gärtner H, Nievergelt D., 2010. *The core-microtome: a new tool for surface preparation on cores and time series analysis of varying cell parameters*. Dendrochronologia 28:85–92. DOI:10.1016/j.dendro.2009.09.002
23. Gazol A., Camarero J.J., Vicente-Serrano S.M., Sánchez-Salguero R., Gutiérrez E., de Luis M., ...& Galván J.D., 2018. *Forest resilience to drought varies across biomes*. Glob. Change Biol., 24: 2143–2158. DOI: 10.1111/gcb.14082 .

24. Gentilesca T., Camarero J.J., Colangelo M., Nolè A., Ripullone F., 2017. *Drought induced oak decline in the western Mediterranean region: an overview on current evidences, mechanisms and management options to improve forest resilience*. *IForest*, 10(5), 796-806. DOI: 10.3832/ifor2317-010 .
25. Gorelick N., Hancher M., Dixon M., Ilyushchenko S., Thau D., Moore, R., 2017. *Google Earth Engine: Planetary-scale geospatial analysis for everyone*. *Remote Sens. Environ.* 202, 18-27. <https://doi.org/10.1016/j.rse.2017.06.031>
26. Hammer Ø., Harper D.A.T., Ryan P.D., 2001. *PAST: Paleontological statistics software package for education and data analysis*. *Palaeontologia Electronica* 4: 9.
27. Holmes R., 1983. *Computer-assisted quality control in tree-ring dating and measurement*. *Tree Ring Bull.* 43, 69–78.
28. Huang M., Wang X., Keenan T.F. Piao S., 2018. *Drought timing influences the legacy of tree growth recovery*. *Glob. Change Biol.* 24: 3546–3559. DOI: 10.1111/gcb.14294 .
29. Huang K., Xia J., 2019. *High ecosystem stability of evergreen broadleaf forests under severe droughts*. *Glob. Change Biol.*, 25: 3494–3503. DOI: 10.1111/gcb.14748 .
30. Huete A.R., Liu H.Q., Batchily K.V., Van Leeuwen W.J., 1997. *A comparison of vegetation indices over a global set of TM images for EOS-MODIS*. *Remote Sens. Environ.* 59: 440–451. [https://doi.org/10.1016/S0034-4257\(96\)00112-5](https://doi.org/10.1016/S0034-4257(96)00112-5)
31. Khoury S., Coomes D.A., 2020. *Resilience of Spanish forests to recent droughts and climate change*. *Glob. Change Biol.* 26: 7079–7098. DOI: 10.1111/gcb.15268
32. Kiorapostolou N., Petit G., 2018. *Similarities and differences in the balances between leaf, xylem and phloem structures in *Fraxinus ornus* along an*

- environmental gradient*. *Tree Physiol.* 29: 234–242. DOI:10.1093/treephys/tpy095 .
33. Lloret F., Lobo A., Estevan H., Maisongrande P., Vayreda J. and Terradas J., 2007. *Woody plant richness and NDVI response to drought events in Catalanian (Northeastern Spain) forests*. *Ecology* 88: 2270–2279. <https://doi.org/10.1890/06-1195.1>
34. Mašek J., Tumajer J., Lange J., Kaczka R., Fišer P., Tremel V., 2023. *Variability in tree-ring width and NDVI responses to climate at a landscape level*. *Ecosystems*, 1–14. <https://doi.org/10.1007/s10021-023-00822-8>
35. Matsushita B., Yang W., Chen J., Onda Y. & Qiu G., 2007. *Sensitivity of the enhanced vegetation index (EVI) and normalized difference vegetation index (NDVI) to topographic effects: a case study in high-density cypress forest*. *Sensors* 7: 2636–2651. <https://doi.org/10.3390/s7112636>
36. Michelot A., Simard S., Rathgeber C., Dufrêne E., Damesin C., 2012. *Comparing the intra-annual wood formation of three European species (Fagus sylvatica, Quercus petraea and Pinus sylvestris) as related to leaf phenology and non-structural carbohydrate dynamics*. *Tree Physiol.* 32, 1033–1043. DOI:10.1093/treephys/tps052 .
37. Moreno-Fernández D., Camarero J.J., García M., Lines E. R., Sánchez-Dávila J., Tijerín J., ... & Ruiz-Benito P., 2022. *The Interplay of the Tree and Stand-Level Processes Mediate Drought-Induced Forest Dieback: Evidence from Complementary Remote Sensing and Tree-Ring Approaches*. *Ecosystems* 25, 1738-1753. <https://doi.org/10.1007/s10021-022-00793-2>
38. Ogaya R., Barbeta A., Basnou C., Peñuelas J., 2015. *Satellite data as indicators of tree biomass growth and forest dieback in a Mediterranean holm oak forest*. *Ann. For. Sci.* 72: 135–144. DOI:10.1007/s13595-014-0408-y .
39. Poyatos R., Llorens P., Piñol J. & Rubio C., 2008. *Response of Scots pine (Pinus sylvestris L.) and pubescent oak (Quercus pubescens Willd.) to soil and*

- atmospheric water deficits under Mediterranean mountain climate*. Ann. For. Sci., 65(3), 1. DOI: 10.1051/forest:2008003
40. Prendin A. L., Carrer M., Karami M., Hollesen J., Bjerregaard Pedersen N., Pividori M., ... & Normand S., 2020. *Immediate and carry-over effects of insect outbreaks on vegetation growth in West Greenland assessed from cells to satellite*. J. Biogeogr. 47, 87-100. DOI: 10.1111/jbi.13644 .
41. Rita A., Camarero J.J., Nolè A., Borghetti M., Brunetti M., Pergola N., Serio C., Vicente-Serrano S. M., Tramutoli V., Ripullone F., 2020. *The impact of drought spells on forests depends on site conditions: The case of 2017 summer heat wave in southern Europe*. Glob. Change Biol. 26: 851-863. DOI: 10.1111/gcb.14825
42. Rosner S., 2012. *Acoustic emission related to stomatal closure of four deciduous broad-leaved woody species*. In *30th European Conference on Acoustic Emission Testing (EWGAE)*. EWGAE, Granada. J. Acoustic Emission, 30: 11-20.
43. Rouse J., Haas R., Schell J., Deering D., 1973. *Monitoring Vegetation Systems in the Great Plains with ERTS*. Third ERTS Symposium, NASA 1, 309–317.
44. Schneider C.A., Rasband W.S., Eliceiri K.W., 2012. *NIH Image to ImageJ, 25 years of image analysis*. Nat. Methods 9, 671–675. <https://doi.org/10.1038/nmeth.2089>
45. Scholz A., Klepsch M., Karimi Z., Jansen S., 2013. *How to quantify conduits in wood?* Front. Plant Sci. 4, 1–11. <https://doi.org/10.3389/fpls.2013.00056>
46. Schwarz J., Skiadaresis G., Kohler M., Kunz J., Schnabel F., Vitali V., Bauhus J., 2020. *Quantifying Growth Responses of Trees to Drought-a Critique of Commonly Used Resilience Indices and Recommendations for Future Studies*. Curr. For. Rep. 6, 185-200. DOI:10.1007/s40725-020-00119-2.

47. Sperry J.S., Nichols K.L., Sullivan J.E.M., Eastlack S.E., 1994. *Xylem embolism in ring-porous, diffuse-porous, and coniferous trees of northern Utah and interior Alaska*. Ecology 75, 1736–1752. <https://doi.org/10.2307/1939633>
48. Sturm J., Santos M. J., Schmid B. & Damm A., 2022. *Satellite data reveal differential responses of Swiss forests to unprecedented 2018 drought*. Glob. Change Biol. 28: 2956-2978. DOI: 10.1111/gcb.16136 .
49. Tomasella M., Casolo V., Aichner N., Petruzzellis F., Savi T., Trifilò P. & Nardini A., 2019. *Non-structural carbohydrate and hydraulic dynamics during drought and recovery in Fraxinus ornus and Ostrya carpinifolia saplings*. Plant Physiol. Biochem., 145, 1-9. <https://doi.org/10.1016/j.plaphy.2019.10.024>
50. Tognetti R., Longobucco A. & Raschi A., 1999. *Seasonal embolism and xylem vulnerability in deciduous and evergreen Mediterranean trees influenced by proximity to a carbon dioxide spring*. Tree physiol., 19(4-5), 271-277. <https://doi.org/10.1093/treephys/19.4-5.271>
51. Tonelli E., Vitali A., Malandra F., Camarero J.J., Colangelo M., Nolè A., ... & Urbinati C., 2023. *Tree-ring and remote sensing analyses uncover the role played by elevation on European beech sensitivity to late spring frost*. Sci. Total Environ., 857, 159239. <https://doi.org/10.1016/j.scitotenv.2022.159239>
52. Tyree M.T., Zimmermann, M.H., 2002. *Xylem structure and the ascent of sap*. Springer, Berlin, Germany.
53. Vicente-Serrano S.M., Beguería S., López-Moreno J.I., 2010. *A multiscalar drought index sensitive to global warming: The Standardized Precipitation Evapotranspiration Index*. J. Clim. 23, 1696–1718. <https://doi.org/10.1175/2009JCLI2909.1>
54. Vicente-Serrano S.M., Gouveia C., Camarero J.J., Beguería S., Trigo R., López-Moreno J.I., ...& Sanchez-Lorenzo A., 2013. *Response of vegetation to drought time-scales across global land biomes*. PNAS 110, 52-57. <https://doi.org/10.1073/pnas.1207068110>

55. Vicente-Serrano S.M., Martin-Hernandez N., Camarero J.J., Gazol A., Sanchez-Salguero R., Pena-Gallardo M., ...& Galván J. D., 2020. *Linking tree-ring growth and satellite-derived gross primary growth in multiple forest biomes. Temporal-scale matters.* Ecol. Indic. 108: 105753. <https://doi.org/10.1016/j.ecolind.2019.105753>
56. Wang Z., Lyu L., Liu L., Liang H., Huang J., Zhang Q.B., 2021. *Topographic patterns of forest decline as detected from tree rings and NDVI.* Catena 198: 105011. <https://doi.org/10.1016/j.catena.2020.105011>

5. Conclusion

Dendrochronological and dendro-anatomical analyses are useful tools to study forest dieback and if combined to remote sensing they can successfully be applied at a large scale. Therefore, the integration of field and satellite data seems to be promising also for studying the response and vulnerability of forests to climate change. However, the complexity of forest ecosystems requires further refinement of existing methods. The response of forest stands to drought varies in relation to climate zone, site characteristics, species composition, etc. The research methodologies adopted so far are mainly calibrated on the single hypothesis, that increased forest stress and dieback are caused by drought and rising temperatures. Therefore, in order to obtain adequate information on forest dynamics in view of climate change, a multi-proxy analysis is necessary and, capable of assessing the state of forests employing different approaches, both qualitative and quantitative (visual field analysis, dendrochronological study, wood anatomy and remote sensing). This is especially true in the Mediterranean forests, which are particularly complex and heterogeneous in terms of site characteristics and species composition. With this aim, this work attempted to integrate field and remote sensing data to examine the response of Mediterranean mixed forests.

Using dendrochronological data, we observed, depending on the site, a more or less severe reduction of tree-ring growth of the species analysed during the 2017 drought. We also found evidence of structural overshoot phenomena on some stands (VP site and GA site) that showed high growth increases before the drought in response to favourable climatic conditions. Among the analysed species, *F. ornus* showed a better recovery after drought, while in general *Q. pubescens* showed greater resistance. *A. monspessulanum* behaved similarly to oak, while broadleaf trees generally responded better in terms of resilience than *P. pinaster*.

The remote sensing indices (NDVI, EVI and NDWI), used to examine the 4 sites (AP, OS, CA and PI) hosting the same forest species (*Q. pubescens* and *F. ornus*),

also showed site-specific responses, confirming the importance of site characteristics in relation to the response of stands to climatic disturbances. While the anatomical study showed in all four sites a variable reduction of the ring area in response to the extreme drought event of 2017. This reduction in growth was less evident at site AP, a site located at higher elevation and also the warmest one, confirming that site conditions influence stand response. However it is likely that either the higher site was affected later by the heatwave or, being a very warm site, the forest stand is already adapted and was less affected by the heatwave. The year following the drought there was a general decrease in Dh at all sites and all species: an anatomical alteration in response to the previous drought conditions. *Q. pubescens* was the most reactive and sensitive species to climatic dynamics, while *F. ornus* seems to show less dieback and less sensitivity to water stress even in the most affected sites.

The present work provided information on the dynamics of Mediterranean mixed forests through a multidisciplinary and multiscale study detecting also legacy effects and structural overshoot phenomena, topics not widely studied so far. We also provide dendrochronological and dendroclimatic information on minor Mediterranean tree species, *A. monspessulanum* and *F. ornus*, but which could play a fundamental role in the composition of drought-resistant forest stands.

In particular *F. ornus* showed lower defoliation and mortality, higher recovery and lower negative legacy effect, in general a good response to the 2017 drought event. Thus, the ash tree may have an extra advantage over other species, contributing form to more resilient communities.

To further improve the information obtained and clearly identify the future dynamics that will drive the response of forests to climate change, it will be necessary to implement long-term monitoring to reconstruct over time how forests, species and entire communities will respond to new climate scenarios.

More specific information on post-drought stand dynamics would also require physiological analyses of non-structural carbohydrate concentrations to understand how carbon allocation dynamics may influence forest response. Nonetheless, this work attempts to make a step further in documenting possible alterations in the specific composition of Mediterranean mixed forests, towards communities dominated by species better adapted to increasingly frequent drought events. It would be necessary to study how changes in stand composition or structural diversity affect forest productivity and how these changes may influence the vulnerability of forests to drought. While, using the indices of resistance, recovery and resilience of forest stands to extreme climatic events, management and design methods could be developed to achieve more resistant and resilient forest systems in view of extreme climatic events.

We can therefore conclude by saying that this work allows us to expand on the current state of the art, addressing little-studied topics and providing additional information on the vulnerability of forests, which will certainly be useful for future research aimed at further clarifying the response of forests to ongoing climate change.

6. Funding and Acknowledgments

6.1 Funding

Assessing Forest Vulnerability to Climate Change Combining Remote Sensing and Tree-Ring Data: Issues, Needs and Avenues

The Italian Ministry of University has supported this research in the framework of the project ARS01_00405, “OT4CLIMA” (D.D. 2261 del 6.9.2018, PON Ramp; I 2014–2020 and FSC). This study was also supported within the Agritech National Research Center and partially financed by the European Union Next-Generation EU (Piano Nazionale di Ripresa e Resilienza (PNRR)–Missione 4 Componente 2, Investimento 1. 4–D.D. 1032 17 /06 /2022, CN00000022).

Drought legacies in mixed Mediterranean forests: effects of overshoot droughts, species characteristics and site conditions

The Italian Ministry of University has supported this research in the framework of the project ARS01_00405, “OT4CLIMA, Advanced EO technologies for studying Climate Change impacts on the environment” (D.D. 2261 del 6.9.2018, PON R & I 2014-2020 and FSC). This study was also supported within the Agritech National Research Center and partially financed by the European Union Next-Generation funds (Piano Nazionale di Ripresa e Resilienza (PNRR) – Missione 4 Componente 2, Investimento 1. 4 – D.D. 1032 dopo 17 /06 /2022 CN00000022).

Radial Growth, Wood Anatomical Traits And Remote Sensing Indexes Reflect Different Impacts Of Drought On Mediterranean Forests

The Italian Ministry of University has supported this research in the framework of the project ARS01_00405, “OT4CLIMA, Advanced EO technologies for studying Climate Change impacts on the environment” (D.D. 2261 del 6.9.2018, PON R & I 2014-2020 and FSC). This study was also supported within the Agritech National Research Center and partially financed by the European Union Next Generation EU

(Piano Nazionale di Ripresa e Resilienza (PNRR) – Missione 4 Componente 2, Investimento 1.4 – D.D. 1032/17/06/2022/CN00000022).

6.2 Acknowledgments

Drought legacies in mixed Mediterranean forests: effects of overshoot droughts, species characteristics and site conditions

JJC acknowledges support of the project CGL2015-69186-C2-1-R (Spanish Ministry of Science). We acknowledge the E-OBS dataset from the EU-FP6 project UERRA (<http://www.uerra.eu>) and the Copernicus Climate Change Service, and the data providers in the ECA&D project (<https://www.ecad.eu>).

Radial Growth, Wood Anatomical Traits And Remote Sensing Indexes Reflect Different Impacts Of Drought On Mediterranean Forests

JJC acknowledges support of the project CGL2015-69186-C2-1-R (Spanish Ministry of Science). We acknowledge the E-OBS dataset from the EU-FP6 project UERRA (<http://www.uerra.eu>) and the Copernicus Climate Change Service, and the data providers in the ECA&D project (<https://www.ecad.eu>).